

LAPPEENRANTA UNIVERSITY OF TECHNOLOGY
Faculty of Technology
LUT Energy

HEAT EXCHANGER DIMENSIONING

Jussi Saari

TABLE OF CONTENTS

1	INTRODUCTION	7
2	GENERAL BACKGROUND	8
2.1	BASIC ISSUES OF HEAT EXCHANGER DESIGN.....	8
2.2	HEAT EXCHANGER DESIGN PROCESS.....	9
3	TYPES OF HEAT EXCHANGERS	12
3.1	FLOW ARRANGEMENTS.....	12
3.1.1	<i>Basic single-pass arrangements</i>	12
3.1.2	<i>Multipass arrangements</i>	14
3.2	COMMON TYPES OF PHYSICAL CONSTRUCTION.....	16
3.2.1	<i>Tubular – double-pipe</i>	17
3.2.2	<i>Tubular – shell and tube</i>	17
3.2.3	<i>Plate heat exchangers</i>	21
3.2.4	<i>Spiral heat exchanger</i>	25
3.2.5	<i>Compact heat exchangers</i>	25
3.3	SELECTION OF APPROPRIATE HEAT EXCHANGER TYPE.....	27
3.3.1	<i>Fluid pressures and temperatures</i>	27
3.3.2	<i>Fouling</i>	28
3.3.3	<i>Material choices</i>	29
3.3.4	<i>Cost</i>	30
4	METHODS OF HEAT EXCHANGER CALCULATION	31
4.1	QUICK ESTIMATES.....	34
4.2	LOGARITHMIC MEAN TEMPERATURE DIFFERENCE (LMTD) METHOD.....	35
4.2.1	<i>Definition of LMTD</i>	35
4.2.2	<i>Complex flow arrangements</i>	38
4.2.3	<i>Special Cases</i>	41
4.2.4	<i>Summary</i>	41
4.3	ϵ -NTU -METHOD.....	42
4.3.1	<i>Dimensionless parameters: ϵ, C^* and NTU</i>	42
4.3.2	<i>Effectiveness – NTU relationships</i>	44
4.3.3	<i>Summary</i>	50
4.4	P -NTU -METHOD.....	53
5	OVERALL HEAT TRANSFER COEFFICIENT	55
5.1	DEFINITION.....	55
5.2	U-VALUE OF EXTENDED-SURFACE HEAT EXCHANGERS.....	57
6	HEAT TRANSFER AND PRESSURE DROP CORRELATIONS	60
6.1	A BRIEF INTRODUCTION ON CONVECTION HEAT TRANSFER.....	60
6.1.1	<i>Dimensionless parameters</i>	61
6.1.2	<i>Analogy of friction and heat transfer: practical consequences</i>	63
6.2	SOLVING CONVECTION HEAT TRANSFER COEFFICIENT FROM EMPIRICAL CORRELATIONS.....	64
6.3	INTERNAL FLOW IN A PIPE.....	66
6.3.1	<i>Fully developed turbulent flow</i>	68
6.3.2	<i>Fully developed laminar flow</i>	70
6.3.3	<i>Entry length</i>	71
6.4	FLOW ACROSS TUBE BUNDLES.....	72
6.4.1	<i>Plain tubes</i>	73
6.4.2	<i>Finned tube banks</i>	75
6.4.3	<i>Shell-side flow in a shell-and-tube exchanger</i>	77
6.5	PLATE HEAT EXCHANGER SURFACES.....	80
6.5.1	<i>Gasketed plate heat exchangers</i>	80

6.5.2	<i>Spiral heat exchangers</i>	81
6.6	COMPACT HEAT EXCHANGER SURFACES	81
7	PRESSURE DROP	83
7.1	PRESSURE DROP CALCULATION – GENERAL PRINCIPLE	84
7.1.1	<i>Core entrance pressure drop</i>	84
7.1.2	<i>Core pressure drop</i>	85
7.1.3	<i>Core exit pressure drop</i>	87
7.1.4	<i>Total pressure drop</i>	87
7.2	PRESSURE DROP IN SPECIFIC TYPES OF HEAT EXCHANGER	88
7.2.1	<i>Tubular heat exchangers, outside flow</i>	88
7.2.2	<i>Gasketed plate heat exchangers</i>	92
8	FOULING	94
8.1	FOULING PROCESS	94
8.1.1	<i>Rate of fouling</i>	95
8.1.2	<i>Effects of operating parameters on fouling</i>	96
8.2	ACCOUNTING FOR THE EFFECTS OF FOULING	97

NOMENCLATURE

SYMBOLS

Roman

A	area [m ²]
B	width [m]
c	specific heat [J / kgK]
C	heat capacity rate [W / K]
C^*	ratio of heat capacity rates in ε -NTU method. [-]
C_f	Fanning friction factor (coefficient of friction) [-]
d	diameter [m]
d_h	hydraulic diameter [m]
e	surface roughness [m]
f	Darcy (Moody) friction factor [-]
F	correction factor in logarithmic mean temperature difference method [-]
G	1. mass velocity [kg / m ² s] 2. conductance [W / K]
h	convection heat transfer coefficient [W / m ² K]
j_H	Colburn j -factor, $St Pr^{2/3}$ [-]
k	thermal conductivity [W / mK]
K	unit resistance [-]
L	length [m]
m	mass [kg]
\dot{m}	mass flow rate [kg / s]
NTU	Number of Transfer Units, (dimensionless conductance), [-]
Nu	Nusselt number [-]
p	pressure [Pa]
P	1. temperature effectiveness [-] 2. power [W]
Pr	Prandtl number [-]
q	heat transfer rate [W]
q''	heat flux [W / m ²]
q_v	volume flow rate [m ³ / s]
r	radius [m]
R	1. (thermal) resistance [K / W] 2. ratio of heat capacity rates in logarithmic mean temperature difference method or P -NTU method. [-]
R''	(thermal) resistance per area [m ² K / W] 1. R''_{tc} contact resistance per area [m ² K / W] 2. R''_f fouling resistance per area [m ² K / W]
Re	Reynolds number [-]
s	1. wall thickness [m] 2. fin spacing [m]
S	spacing [m]
St	Stanton number [-]
t	thickness [m]

T	temperature [K]
U	overall heat transfer coefficient [W / m ² K]
v	specific volume [m ³ / kg]
w	flow velocity [m / s]

Greek

α	thermal diffusivity, $\alpha = k / \rho c_p$ [m ² / s]
β	heat transfer area per volume [m ² / m ³]
δ	gap between the plates of a plate or spiral heat exchanger [m]
ε	heat exchanger effectiveness [-]
ρ	density [kg / m ³]
η_f	fin efficiency [-]
η_o	overall surface efficiency [-]
η_p	pump/fan efficiency [-]
μ	dynamic viscosity [Pa s]
ν	kinematic viscosity [m ² / s]
τ	shear stress [N / m ²]

SUPERSCRIPTS

'	per length
''	per area
'''	per volume
*	dimensionless

SUBSCRIPTS

avg	average
c	1. cold side of heat exchanger 2. core of the heat exchanger
D	diagonal
e	entry to heat exchanger core
f	1. fouling 2. fin 3. fluid
ff	free-flow
fr	frontal
h	hot side of heat exchanger
i	1. inlet 2. inside
L	longitudinal
lm	logarithmic mean
m	1. mass 2. mean 3. modified

max	maximum
min	minimum
o	1. outlet 2. outside
p	isobaric
rad	radiation
s	surface
t	total
T	transverse
tb	tube-to-baffle
w	wall

ABBREVIATIONS

BC	Baffle Cut
CC	Cross-Corrugated
CW	Cross-Wavy
HVAC	Heating, Ventilating and Air Conditioning
HX	Heat Exchanger
LMTD	Logarithmic Mean Temperature Difference
MTD	Mean Temperature Difference
NTU	Number of Transfer Units
PHE	Plate Heat Exchanger
TEMA	Tubular Exchanger Manufacturer's Association

1 INTRODUCTION

The purpose of this design guide is to give the reader a general idea of the problem field of heat exchanger design, sizing and optimizing. Emphasis is on thermo-hydraulic design of the heat exchanger; mechanical design and system optimization are beyond the scope of this guide.

Only recuperators, or heat exchangers where two fluids are separated by the heat transfer surface that normally has no moving parts, are covered. This restriction of scope leaves out regenerators – heat exchangers where the heat transfer is performed through a material that is alternately brought to contact with hot and cold streams, storing energy from the hot stream and releasing it into the cold one. Boilers and condensers are also left outside of the scope of the guide.

2 GENERAL BACKGROUND

An overview of heat exchanger design problems, a summary of key issues to cover in the design process, and a design methodology of heat exchangers is presented in this chapter.

2.1 BASIC ISSUES OF HEAT EXCHANGER DESIGN

Applications of heat exchangers present two distinct categories of design problems (Sarkomaa 1994):

1. Design and optimization of mass-produced heat exchangers, e.g. automobile radiators, heat exchangers of HVAC equipment, oil cooling heat exchangers for machinery, etc.
2. Design and optimization of heat exchangers manufactured as one-off, or at most in small series, for a specific application.

As the production runs of first group of heat exchangers are often measured in thousands or more, a very careful and detailed optimization of their technical and economical characteristics can be worthwhile if even only very small improvements can be achieved. Heat exchangers in the second problem category, on the other hand, must often be designed to be functional and economical in their intended use on the basis of sometimes rough or incomplete data, which makes overly detailed and careful optimization procedures impractical.

The following chapters are written mostly with the second types of design and optimization problems in mind. Typical characteristics for these cases include poor knowledge of the exact types of fluid flows and their properties and fouling characteristics, and that those characteristics as well as the mass flow rates may fluctuate depending on changes in the production and process environment.

At least the following issues should usually be considered when designing a heat exchanger (Sarkomaa 1994):

1. **Fouling:** The heat exchanger must fulfil process requirements after fouling. If possible, the heat exchanger should be designed to be self-cleaning, in other words so that the growth rate of fouling layer will slow down and eventually stop at a certain level. Whether this is possible or not, fouling must be considered so that at the end of a period of use when maintenance is performed, the heat exchanger still achieves the required heat duty. Sometimes determining sufficient excess heat transfer area or additional heat exchangers to take into account the effects of rapid fouling processes can make up a significant part of the whole heat exchanger design problem.

2. **Environment of use:** The heat exchanger must be designed in accordance to the environment where it will be used, so that in addition to the mechanical and thermal stresses of normal use, the heat exchanger is also designed against damage that could result from issues related to transportation, installation, process start-up and run-down as well as likely misuse or accident scenarios.
3. **Maintenance:** The heat exchanger should be easily maintainable. In practical terms this means ease of cleaning, easy removal of especially those parts likely subjected to significant fouling, erosion, corrosion, vibrations, creep, or other forms of damage or decay. Maintainability is also connected to the environment of use, for example in space requirements around the heat exchanger for maintenance and possibly accessibility for and proximity of lifting and moving equipment at the site.
4. **Flexibility:** Sometimes, for example if the mass flow rates of the fluids can vary greatly, it may be necessary to allow for considerable adjustments in use of the heat exchanger,. This can sometimes require the heat transfer area to be divided between parallel heat exchangers separated with valves.
5. **Limitations of mass and dimensions:** The dimensions and mass of the heat exchanger may be limited not only by the usage environment, but also equipment and locations related to manufacture, transportation, moving, lifting or maintenance.
6. **Minimizing the cost:** The goal of heat exchanger selection and design is always to minimize the cost. The main cost-related parameter is often the total heat transfer area. To minimize the heat transfer area typically means maximizing the fluid velocities within the limitations set by pressure drop, erosion and vibrations. Additional cost-related issues include pumping cost to counter the pressure drops, maintenance costs, and production losses due to maintenance or unreliability.

2.2 HEAT EXCHANGER DESIGN PROCESS

The process of heat exchanger design is in most sources (Taborek 1983a, Sarkomaa 1994, Sekulić 2003) described to follow through roughly the following steps:

1. Problem definition: design specifications
2. Selection of heat exchanger type
3. Thermo-hydraulic design
4. Mechanical design
5. Manufacturing, cost and process optimization considerations.

The steps are rarely entirely sequential; results from various steps frequently have influence on choices made previously, and typically several iterations must be made before a final acceptable design is completed. The influences and feedbacks between

different steps are clearly seen in Figure 2.1 (adapted and simplified from Sarkomaa 1994 and Sekulić 2003).

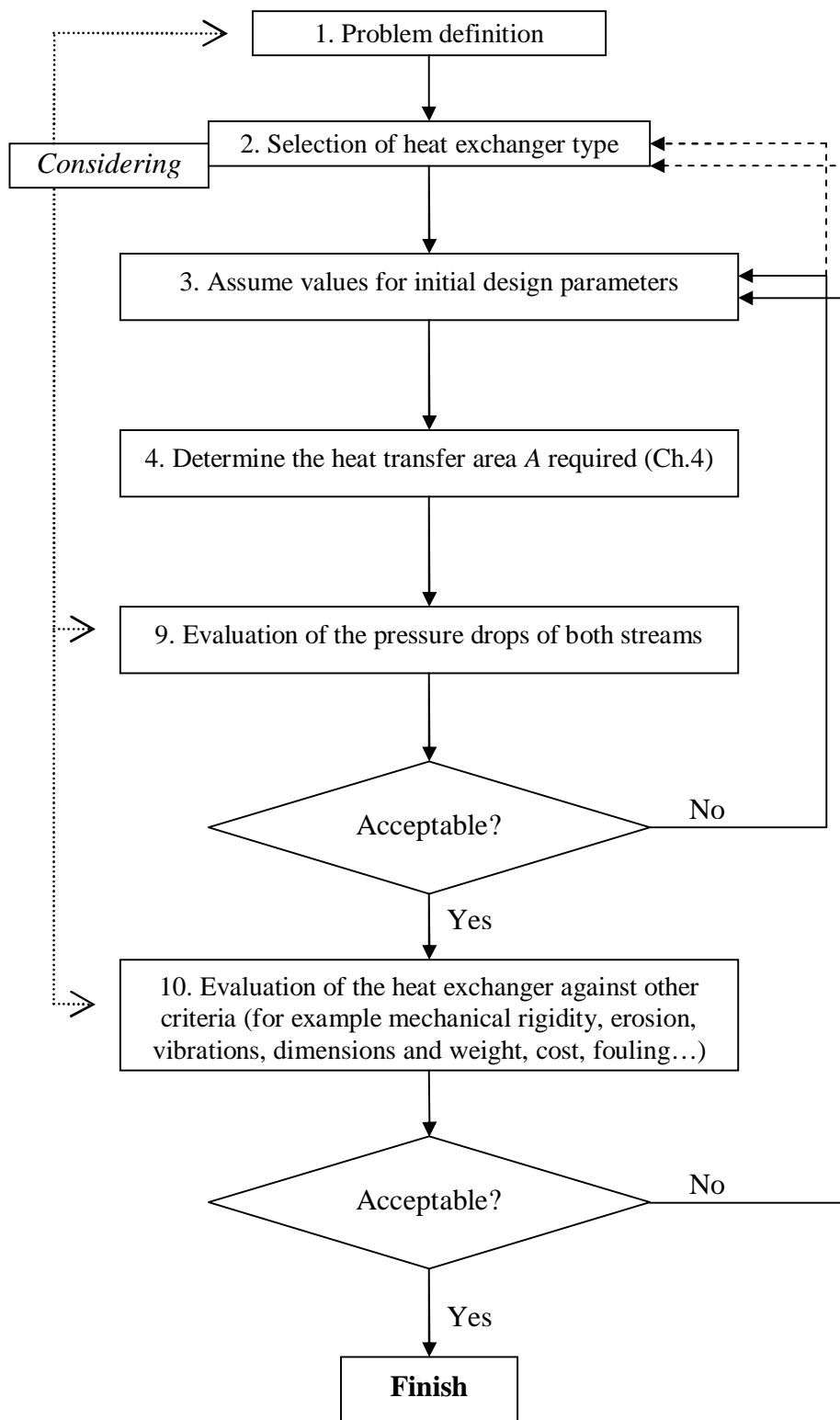


Figure 2.1 Process of heat exchanger design, adapted and simplified from (Sarkomaa 1994) and (Shah 2003).

The emphasis in the following chapters will be on the second and particularly the third steps. Issues related to heat exchanger type selection will be discussed in chapter 3.3, after the basic heat exchanger types have been covered.

Similar stages must usually be considered even if the requirement for a heat exchanger can be fulfilled by simply finding a suitable mass-produced heat exchanger from vendors' catalogues. This is often the case if the requirement is for a small heat exchanger manufactured of stainless or carbon steel. These are typically mass produced in very large quantities, and due to mass produced quantities costs are typically low and delivery times short.

From the purchasers point of view the relevant thermo-hydraulic design problem is then that of *rating problem*, that is, where from input data of exact flow arrangements, dimensions, geometry, surface and material properties, and fluid flow data (inlet temperatures, mass flow rates and property and fouling data) one calculates the fluid outlet temperatures, total heat transfer rate, and pressure drop characteristics of the heat exchanger in the expected situations where the heat exchanger may be needed.

If the heat exchanger requirement is for a larger heat exchanger of 10...20 m² or more heat transfer area, and particularly if the requirement includes special characteristics, a heat exchanger may need to be designed specifically for such requirements. In such cases one faces a *sizing problem*, described in Fig. 2.2.

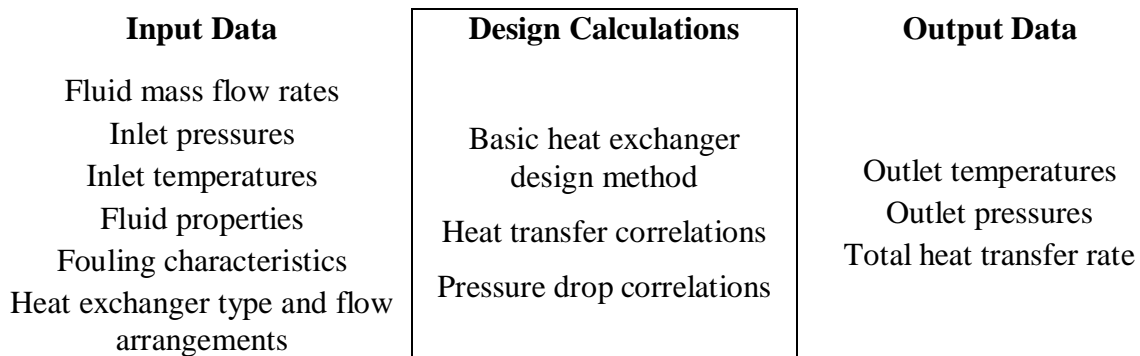


Figure 2.2. *Input and output data for heat exchanger thermo-hydraulic sizing problem; adapted from (Sarkomaa 1994).*

Sizing can be performed in various levels of detail, typically starting from a rough estimation for the magnitude of required heat transfer area, and followed by either a sizing calculation with some of the more detailed design methods for thermo-hydraulic calculation of heat transfer performance, and/or or with numerical computational fluid dynamic (CFD) software.

The emphasis in the following chapters is in presenting methods for reasonably accurate design of heat exchangers that can be applied either by hand or utilized in computer programs.

3 TYPES OF HEAT EXCHANGERS

Heat exchangers can be designed to accomplish numerous flow arrangements and with countless construction methods and geometries. A few basic types make up the overwhelming majority of heat exchanger market, however, and only the most commonly used configurations will be covered in the following chapters.

Chapter 3.1 explains the basic flow arrangements and the concept of multi-passing. Chapter 3.2 deals with the most common types of heat exchanger construction, and also cover the specific details and peculiarities of flow arrangement pertinent to each type of heat exchanger. Finally Chapter 3.3 will give a set of very general guidelines on selecting an appropriate type of heat exchanger and suitable material given the specifics of the application.

3.1 FLOW ARRANGEMENTS

The arrangement of hot and cold fluid flows relative to each is important for how efficiently the heat transfer area of the heat exchanger can be used to transfer the required heat load. Besides the efficient usage of heat transfer area, other considerations in the selection of flow arrangement include for example pressure drop considerations, header design, allowable thermal stresses on the heat exchanger materials, and issues related to the end use location and plumbing.

3.1.1 Basic single-pass arrangements

The two simplest flow arrangements possible in heat exchangers are counter-flow, and parallel-flow. These and the resulting hot- and cold-fluid temperature profiles in a simple double-tube heat exchanger with tube length L are demonstrated in Figure 3.1.

As is evident from the temperature profiles, the counter-flow arrangement will enable more heat transfer with given inlet temperatures, and also enables moderate heat transfer rates to be achieved at smaller area due to avoiding the problem of diminishing temperature difference in the parallel-flow arrangement. Besides problem of diminishing temperature difference at the outlet end, an additional disadvantage of the parallel-flow arrangement is the very large temperature difference at the inlet end, which may create problematically high thermal stresses in some situations.

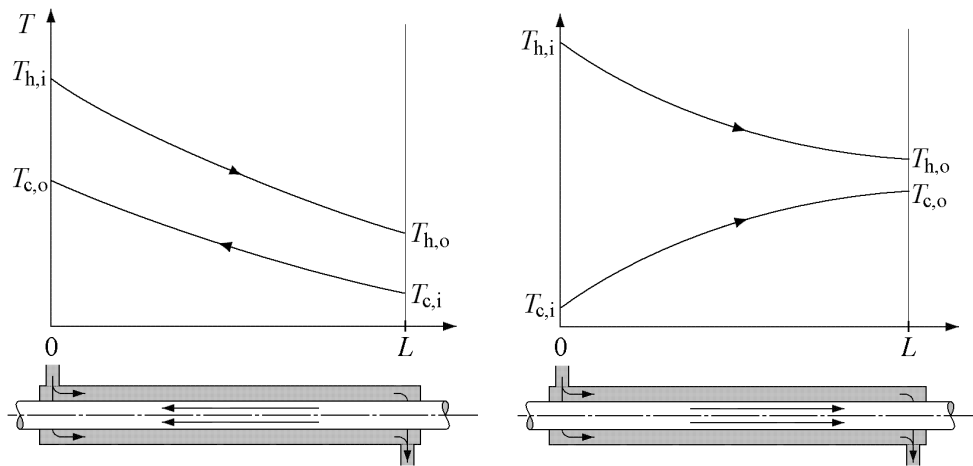


Figure 3.1. Basic double-tube heat exchanger in counter-flow (left) and parallel-flow (right) configurations.

The advantages of parallel-flow arrangement are few, but in some cases important. The main advantage is the typically more uniform heat transfer surface temperature distribution. This can be advantageous if both fluids are fairly hot, where parallel-flow arrangement provides lower maximum temperature of heat transfer surface. If this allows a cheaper material to be used, it may outweigh the disadvantage of needing more heat transfer area than other flow arrangements would.

The higher minimum temperature may also sometimes be advantageous, for example to prevent the freezing of the warmer fluid if it is a liquid near its freezing point, or to prevent the condensation of acid vapours at the surface if the warmer fluid is a gas that contains acids. Issues such as convenient plumbing of inlet and outlet flows at the installation site may also sometimes outweigh the importance of efficient heat transfer area usage. Particularly if the required heat transfer rate is much less than maximum possible rate allowed by the fluid flow rates and temperatures, this disadvantage of parallel-flow arrangement becomes small.

The third basic flow arrangement possibility is cross flow. In a cross-flow arrangement it is also significant whether the flows are mixed or unmixed; that is, if the fluid is able to mix freely in direction transverse to the flow direction, or if its movement is channelled by the heat exchanger design in a way that prevents such mixing. This is demonstrated in Figure 3.2.

In the left-side example of Figure 3.2 the fluid flowing across the tube bundle is considered mixed, but the fluid in the tubes is prevented from mixing because of the tubes. Usually if there are at least four or five rows of tubes in the flow direction of the fluid moving across the tube bundle, the tube-side fluid can be considered completely unmixed (Shah 2003, pp.61). On the other hand, if there were only one row of tubes, then clearly the fluid in tubes should be considered mixed, and cases in between (from two up to four or five rows) the tube-side fluid should be considered to be partially mixed.

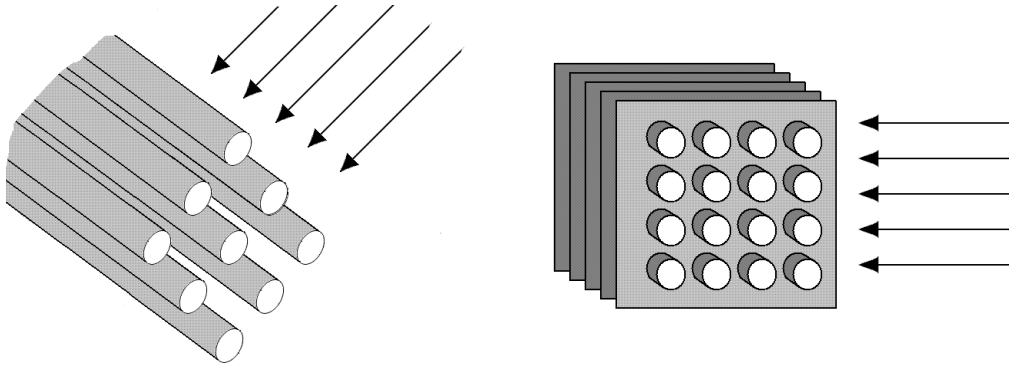


Figure 3.2. Cross-flow arrangements: one fluid mixed, one unmixed (left) and with both fluids unmixed (right).

Temperature distributions of inlet and outlet fluid flows for mixed-unmixed and unmixed-unmixed cross-flow heat exchangers are demonstrated in Fig. 3.3. The cold flow is assumed unmixed in both cases; hot fluid is unmixed in the left, mixed in the right-side example.

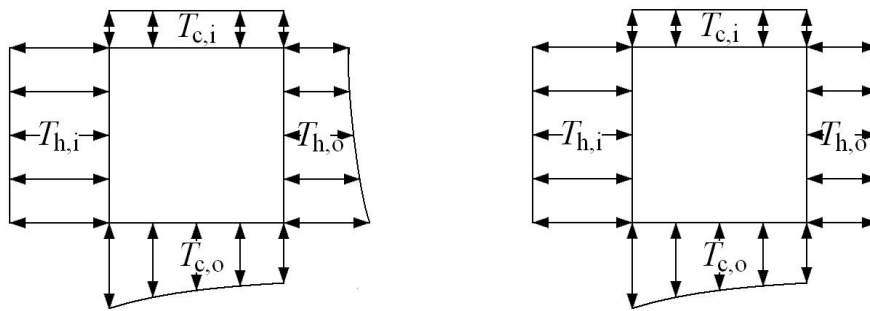


Figure 3.3. Temperature profiles at inlet and outlet of unmixed-unmixed and mixed-unmixed cross-flow heat exchangers.

Cross-flow arrangement does not provide quite as efficient use of heat transfer area as counter-flow does, but unless a very high heat transfer rate (near the maximum possible within the boundaries of 2nd law of thermodynamics) is required, it's performance is not much worse. It is frequently much easier to design uncomplicated headers that produce an even flow distribution for a cross-flow than for a counter-flow arrangement. Due to header design issues plate-type counter-flow heat exchangers frequently have sections of cross-flow pattern at the inlet and outlet headers.

3.1.2 Multipass arrangements

Sometimes it is useful to arrange one or both fluids to pass through the heat exchanger more than once. From thermal performance point of view, one of the fluid flows passing through the exchanger more than once doesn't yet necessarily mean that the heat exchanger should be considered a multi-pass one, however: a true multi-pass configuration exists only if it is not possible to "fold" the heat exchanger into a single-

pass one. This is demonstrated in Figure 3.4, where the left-side example is a true multi-pass heat exchanger (two-pass cross-counterflow), but the one on the right side is in fact a one-pass cross-flow heat exchanger.

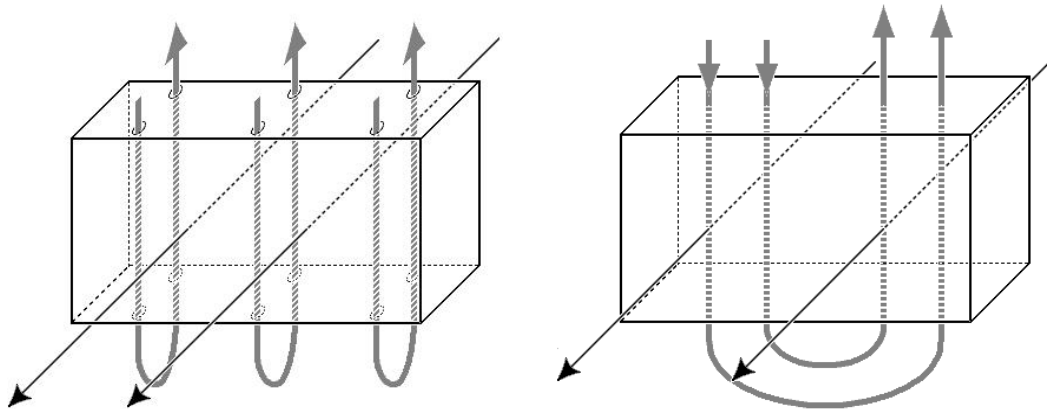


Figure 3.4. *Multipassing: a two-pass cross-counterflow heat exchanger (left), and one-pass cross-flow heat exchanger.*

The reason why the right-side example cannot be considered a true multi-pass heat exchanger is obvious, if one imagines what would happen if the heat exchanger was cut in half between the downwards- and upwards-going flows demonstrated by the thick gray arrows. If the right-side half would be swung down and to the left along an imaginary hinge in the bottom, it is clear that the flow patterns of the two fluids relative to each other would not change, but the geometry would become a clear one-pass arrangement. With the left-side example no such cut-and-swing that would make the heat exchanger into a single-pass one is possible; therefore it represents a true multi-pass heat exchanger.

It is also evident from the figure that when the fluid represented by thick gray arrows re-enters the heat exchanger on the left side example, the fluid flow across it will be at a different temperature than it was in the first pass, which is not the case in the right-side example – another sign that shows that only the left-side example can be considered a multi-pass unit.

Arranging a one-pass heat exchanger as in the right-side example of Fig 3.4 can sometimes be necessary for example in order to fit the heat exchanger to the space and shape requirements of an installation site. With true multipassing on the other hand it is possible to change the nature of a single-pass cross-flow heat exchanger a towards counter-flow or parallel-flow arrangements.

Particularly if a very high heat transfer rate (relative to the maximum possible with the available temperature differences and flow rates) is required, a choice of cross-flow instead of counter-flow may demand a significant increase of heat transfer area, but at the same time pure counter-flow heat exchanger is sometimes problematic to design headers for; in such a case a multi-pass cross-counterflow arrangement will provide a lower heat transfer area requirement than a single-pass crossflow would, but still allows

the designer to take advantage of the easy header design of crossflow exchangers. Likewise cross-parallelflow may allow a convenient balance of the more efficient usage of heat transfer area of cross-flow geometry with the advantages that sometimes may make a parallel-flow design desirable.

If the flow arrangement corresponds to a cross-counterflow or cross-parallelflow arrangement, then the heat exchanger will need to be analyzed in stages; a two-pass cross-counterflow arrangement of Figure 3.4 for example could be presented as a combination of two heat exchangers in series (Figure 3.5 a). If the number of passes n is greater than two (Fig 3.5 b), the performance of the series of cross-flow exchangers approaches that of a single counterflow exchanger as n approaches infinity.

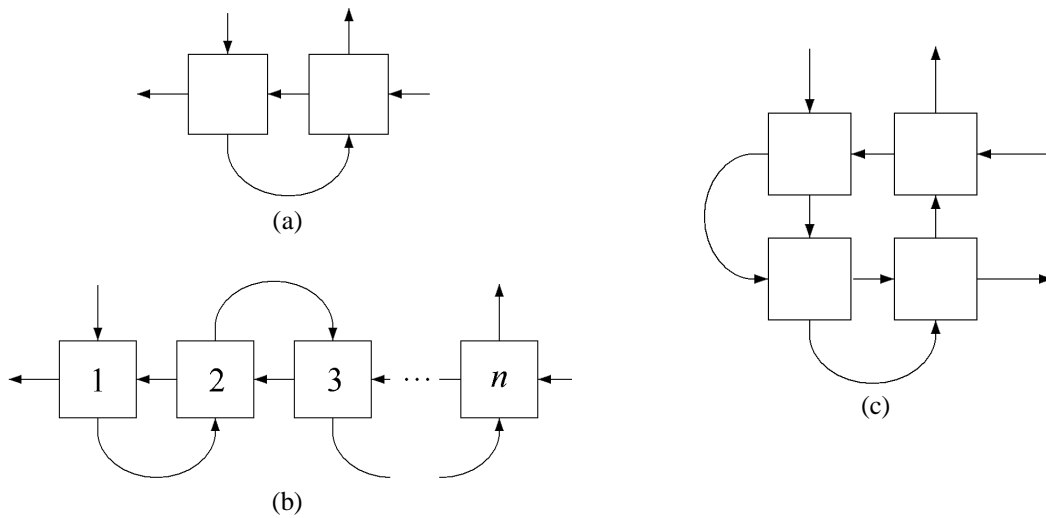


Figure 3.5. Splitting multi-pass heat exchanger into multiple 1-1 –single-pass heat exchangers for analysis: a) 1-2, b) 1-n and c) 2-2 –heat exchangers.

Finally it is naturally also possible to pass both fluids several times through a heat exchanger; an example of a 2-2 –heat exchanger broken up into a network of four individual heat exchangers is given in Fig. 3.5 c.

3.2 COMMON TYPES OF PHYSICAL CONSTRUCTION

The most critical decision when designing a heat exchanger is the selection of the basic type of heat exchanger to design. Various criteria dictate the selection of the suitable design, and some constructions (particularly the shell-and-tube) may be designed to adequately serve in a wide variety of situations. The tubular heat exchanger types are often tempting choices not only for their suitability for a given task, but also for the ease of design: the double-tube heat exchanger is probably the simplest possible construction, while the shell-and-tube exchanger has had a number of tried and tested design methods developed for it due to it being the most common heat exchanger type in process industry. The cost of finding the easiest route may be considerable however;

in those situations where other types of heat exchangers would cope, they often would provide considerably smaller and cheaper options to the tubular exchangers.

3.2.1 Tubular – double-pipe

A double-pipe heat exchanger (Figure 3.6) is perhaps the simplest type of heat exchanger possible, consisting of just two concentric tubes, and appropriate end fittings to move the fluids from one section of the exchanger to the next. If one or the other fluid has much lower heat transfer coefficient, the inner tube can be equipped with longitudinal fins on inner or, more commonly, external surface.

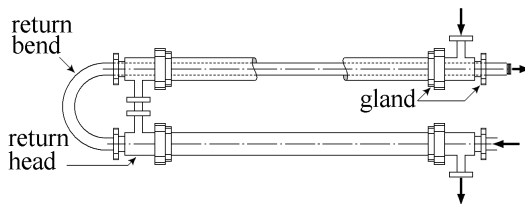


Figure 3.6. *Double-pipe heat exchanger.*

For anything but the smallest heat transfer area requirements the double-pipe construction becomes bulky and expensive compared to a shell-and-tube construction. When only a small heat transfer area is needed, the double-pipe construction does have certain advantages, however. (Guy 1983), (Bell 1983) and (Shah 2003) mention the following advantages for double-pipe heat exchangers:

- Flexibility in building, installing and if necessary altering
- Can be quickly designed and assembled from standard off-the-shelf piping components
- Pure counterflow flow arrangement easy to accomplish
- High-pressure fluids can be easily handled without excessive metal thickness
- Dismantling for cleaning is easy
- Availability of simple, well-established thermo-hydraulic calculation methods that yield accurate results.

3.2.2 Tubular – shell and tube

Shell-and-tube heat exchangers are currently the most commonly used of all the possible heat exchanger configurations: in late 1990's, the market share of shell-and-tube heat exchangers in process and petrochemical industries was over 65% of all heat exchangers (Shah 2003, pp.680).

Although particularly plate-type heat exchanger constructions often allow smaller, lighter, or cheaper heat exchangers to be constructed, shell-and-tube designs have retained their place in the industry due to their comparatively high versatility in terms

of heat exchanger size, possible pressure and temperature ranges and construction material choices, as well as a large amount of design and manufacturing knowledge.

The main components of a shell-and-tube heat exchanger are identified in Fig. 3.7, showing a 1-2 -heat exchanger: a heat exchanger with one shell-side and two tube-side passes. The tube-side fluid enters the heat exchanger from the tube fluid inlet (1) into front-end head (11), and from there into the tubes (4). The tube fluid exits the tubes of the first pass into the rear-end head (6), continues back into the second tube-side pass from which it exits back into the front-end head, and finally out of the heat exchanger from the tube fluid outlet (9). The shell-side fluid enters the heat exchanger from the shell inlet (2), flows on the shell side in a cross-parallel flow pattern in respect to the first pass, and cross-counter flow in respect to the tube pass, guided by baffle plates (8), and eventually exits from shell outlet (7). The tube bundle is held in place by the tube sheets (5), and inside the shell supported by the baffle plates.

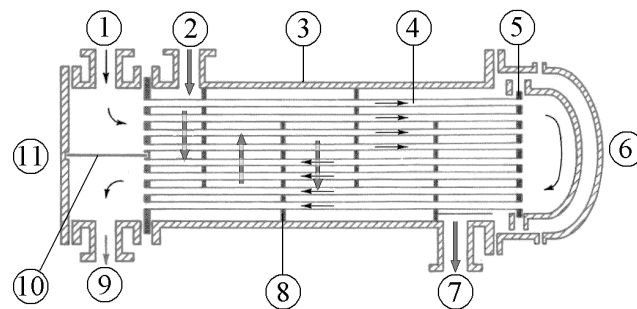


Figure 3.7 A shell-and-tube heat exchanger.

Shell-and-tube heat exchangers can have a variety of different shell, tube bundle and front- and rear-end head constructions. A commonly used standard that covers most for defining the shell and head constructions is provided by the *Tubular Exchanger Manufacturer's Association*, or TEMA. In the TEMA notation system a three-letter combination can exactly define the most common types of shell-and-tube heat exchangers: first letter defines the type of front end head, second the shell, and third the rear head, as defined in Fig 3.8. According to TEMA notation, for example a shell-and-tube heat exchanger with special high-pressure closure on the front-end head, a single-pass shell with one entry and one exit, and U-tube bundle, would be designated DEU, while the example of Fig 3.7 would be AES. In terms of fluid flow arrangement, the heat exchanger of Fig 3.7 can be identified as a 1-2 TEMA-E.

Of the different shell constructions, the single shell-side pass E type is the simplest and most common, and also provides the most effective use of heat transfer area. If there are two tube-side passes, F type shell with a longitudinal baffle to create two shell-side passes could be used to create counter-flow pattern for both tube passes and thus increase the temperature difference between the two fluids at all points of the heat exchanger (Shah 2003, pp.17). Due to several reasons such as leakage around the longitudinal baffle and difficulties with maintenance and fabrication, the F-shell is in

practice problematic however, and multiple E shells in series is often a better choice than an F shell (Shah 2003, pp.686). Split flow patterns of G, H and J shells are suitable for specific applications such as thermo-siphons, boilers or condensers, while the X shells permit lowest possible shell-side pressure drops (Shah 2003, pp.17).

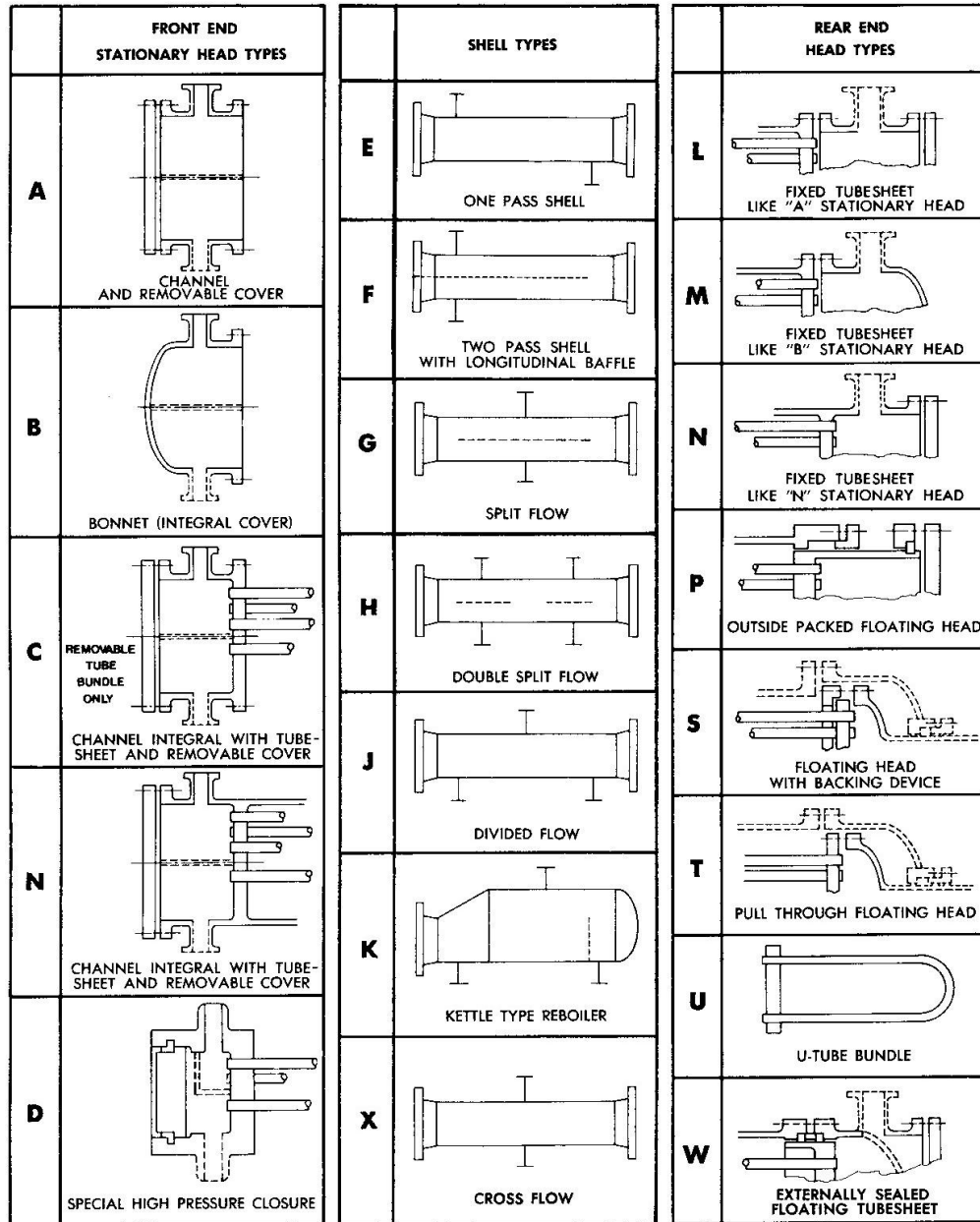


Figure 3.8. TEMA designation system of shell-and-tube heat exchanger shell and head types. (Sanders 1983, pp.4.2.2-1)

Other main components of a shell-and-tube heat exchanger are the tube bundle, and baffles. Tube bundle typically consists of standard-size tubes installed in a either square or triangular pattern, both of which can be installed in two possible angles relative to the incoming fluid flow, as shown in Fig. 3.9. The 90-degree square arrangement is the only in-line arrangement, while 30-, 45- and 60-degree arrangements are all staggered.

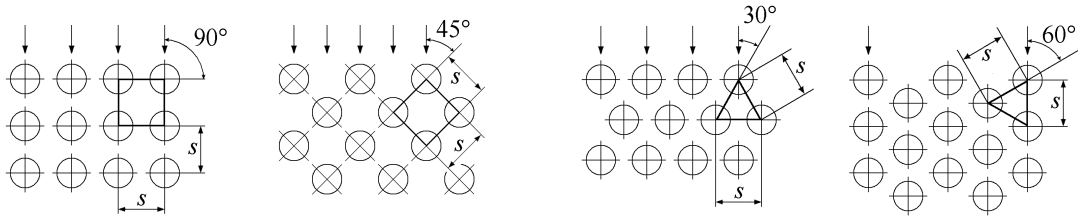


Figure 3.9. Standard tube arrangements: 90- and 45-degree square and 30- and 60-degree triangular.

The main advantages of the four tube arrangement options are as follows:

- 30-degree triangular: highest tube density for a given shell size and good heat transfer characteristics. For these reasons the 30-degree triangular arrangement is often the best choice, and should be considered as a first choice.
- 45- or 90-degree square: access for mechanical cleaning of tube outside surfaces, provided tube spacing leaves at least 6.5 mm space between the tubes.
- 90-degree square: low pressure drop for any given heat transfer coefficient in turbulent flow. Laminar flow is rare in shell-side flow and may occur only in highly viscous fluids such as oils; when laminar flow does occur, 90-degree arrangement results in highly inefficient heat transfer, however.
- 60-degree triangular has the same tube density as 30-degree triangular, but relatively higher pressure drop with a flow velocity to produce a given heat transfer coefficient, and is therefore unlikely to be the best choice.

Baffles can also be arranged in a variety of manners, and usually serve mainly two functions: to support the tubes, and to force shell-side flow into cross-flow over the tube bundle in order to increase the heat transfer coefficient.

The most common baffle configuration is the single-segmental baffle plate (Fig. 3.10a), but segmental baffles can be also double- (Fig. 3.10b), or even triple-segmental. Disk-and-doughnut baffles (Fig. 3.10c) are sometimes used to create combination of cross- and longitudinal flow, and also more complicated baffle forms can be used. If cross flow across the tube bundle is not desired, plate baffles can be replaced with rods that support the tubes without influencing the flow direction of the shell-side fluid.

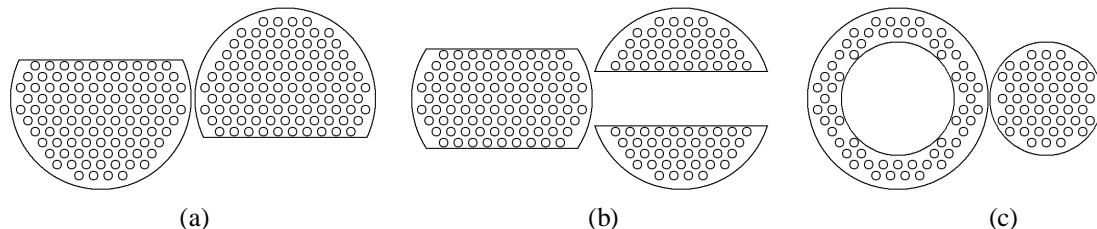


Figure 3.10. Some examples of baffle configurations: a) single-segmental baffle, b) double-segmental baffle, c) disk-and-doughnut baffle.

A summary of the main dimensions determining the shell-side geometry of a shell-and-tube heat exchanger is given in Table 3.1, with dimensions demonstrated in Fig. 3.11.

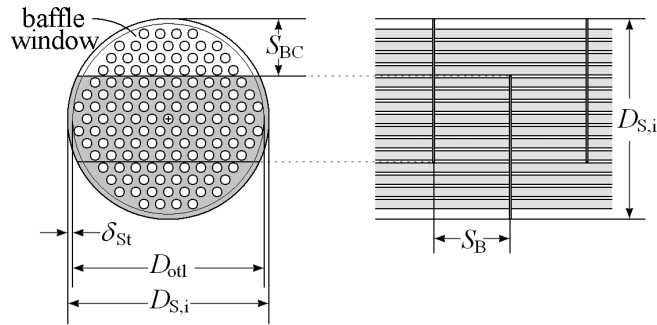


Figure 3.11. Some examples of baffle configurations: a) single-segmental baffle, b) double-segmental baffle, c) disk-and-doughnut baffle.

Table 3.1. Typical size ranges for main dimension of shell-and-tube heat exchangers.

Shell inside diameter $D_{s,i}$	<ul style="list-style-type: none"> • Standard pipes: 100 to 500mm • Rolled sheet: 300 to 2500 mm
Tube outside diameter d_o	Standard tube sizes from 5 to 55mm, typically 12.7 to 25.4mm.
Baffle cut S_{BC}	Very often 25% of shell inside diameter, but other values are also possible.
Tube spacing S	1.25 to 1.5 times tube outside diameter d_o ; <ul style="list-style-type: none"> • tighter spacing would provide insufficient rigidity of the tube plate • wider spacing results in large shell and inefficient heat transfer
Shell-to-tube clearance δ_{st}	~20mm in fixed-tubesheet designs, 80...160mm in floating-head types. <ul style="list-style-type: none"> • should be minimized to prevent excessive bypass flow on the shell side • for a detailed treatment, see (Taborek 1983b, pp.15)
Baffle plate spacing S_B	<ul style="list-style-type: none"> • Limitations due to shell-side flow conditions: 0.2 to 1.0 times $D_{s,i}$ • Limitations due to rigidity: S_{BC} should not exceed maximum unsupported tube length for given tube materials and dimensions; see for example (Taborek 1983b, pp.8) for a more detailed discussion.
Tube-side flow velocity	<ul style="list-style-type: none"> • Limitations due to erosion: < 3m/s (tubes of carbon steel or Cu-Ni alloys), < 5m/s (stainless steel), < 6m/s (Ti) • Limitations due to fouling and heat transfer: often ≥ 1m/s unless better information is available for the fluid at hand (Taborek 1983b, pp.16) • Other issues such as tube vibration may need to be considered.
Number of tube passes	Usually no more than $D_{s,i}$ in hundreds of mm e.g. a 200mm shell should have no more than two tube passes, an 800mm shell no more than eight passes.

3.2.3 Plate heat exchangers

Plate heat exchangers (PHEs) can be constructed in several ways, but mostly share certain common characteristics. As a general rule, PHEs are usually smaller, lighter and cheaper to manufacture than tubular heat exchangers for any given heat duty, but they cannot tolerate as high temperatures or pressures, which limits the possibilities of their application.

Compact heat exchangers are also frequently based on a plate-type heat transfer surface, either as primary-surface or plate-fin construction. These types of heat

exchangers are covered in more detail in the separate chapter on compact heat exchangers.

The most common type of PHE is the gasketed plate heat exchanger. A gasketed PHE is built of a stack of many thin, rectangular metal plates packed together, as shown in Figure 3.12. The flow patterns inside the heat exchanger are demonstrated in Fig. 3.13.

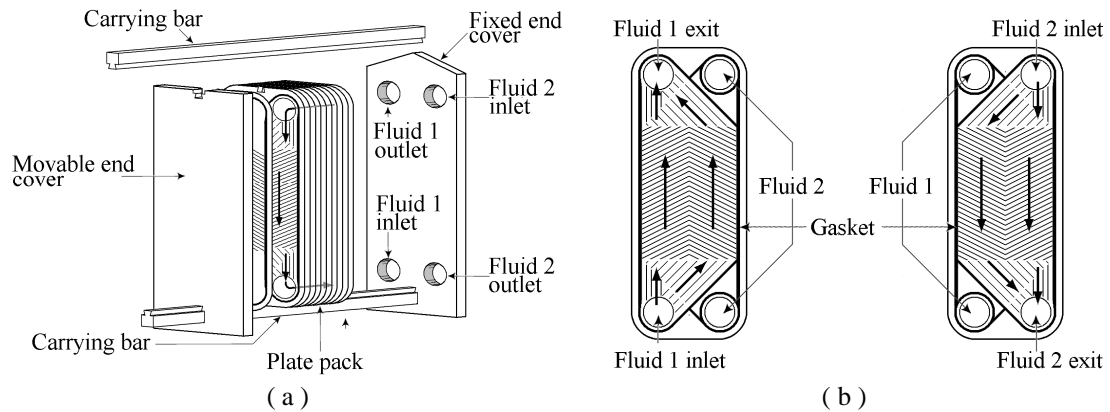


Figure 3.12. A gasketed plate heat exchanger: a) construction of the heat exchanger, b) individual plates (herringbone pattern).

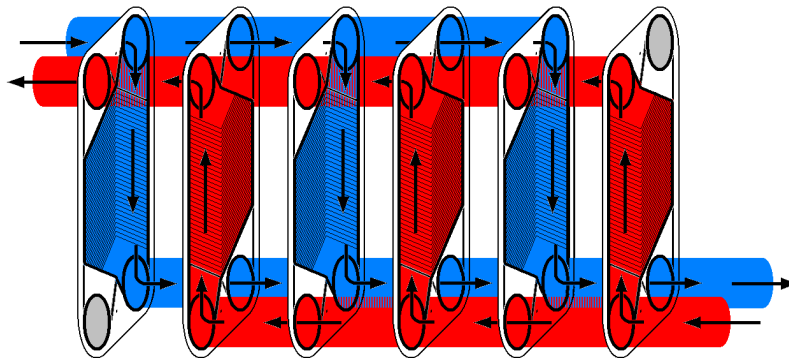


Figure 3.13. Flow pattern through a gasketed 1-1 counterflow plate heat exchanger.

Each plate has typically four flow ports, one in each corner, to provide a path for the fluid to flow through. The gaskets around the flow ports (see Fig. 3.12 b) control which fluid can flow from the port to which gap between the plates. Gaskets also seal the flow around the edges of the plates. In most plate heat exchangers the gaskets would be manufactured from a hard rubber that can compress approximately 25% when pressed tightly together in the plate pack of the heat exchanger, thus forming a tight seal and preventing leakages. (Rohsenow 1987, pp.4-109 to 4-112).

The gaskets, being typically manufactured of a suitable rubber, are the main factor limiting the temperature and pressure ranges possible to achieve with gasketed PHEs. Typical operating ranges according to (Cooper 1983), (Sarkomaa 1984) and (Shah and Sekulić 2003) are summarized in Table 3.2.

The plates can vary in size from 0.07 to 1.2 metres width and 0.4 to 5 metres in height. They are typically very thin, in the order of 0.4 to 1.4 mm. Because the plates are very thin, carbon steel is an unsuitable material due to its vulnerability to corrosion: stainless steel types such as 304 or 316, or aluminium or titanium are more typically used.

Table 3.2. *Operating range of gasketed plate heat exchangers*

Fluid pressure	0.1 to 1.0 MPa (typical construction) up to 3.0 MPa (maximum)
Fluid temperature	up to 150 °C (typical gasket material) -40 °C to 260 °C (with special high-temperature materials)
Maximum port velocity	6 m/s (for liquids)
Flow rate per channel	0.05 to 12.5 m ³ /h (typically much closer to lower end)
Maximum viscosity	5 N s / m ²

Almost always the plates are stamped to a suitable pattern; a herringbone pattern shown in Figure 3.12 is very common, but many other patterns are also possible. The pattern serves three main purposes:

- increases heat transfer rate by 1) inducing turbulence and mixing in flows with Reynolds number as low as 50...200 (Sarkomaa 1994,pp.25), thereby significantly increasing the convection heat transfer coefficient, and 2) by increasing the surface area of a plate of given dimensions.
- increases the mechanical rigidity of the thin plate
- when multiple plates are stacked together with pattern direction reversed between every other plate, the plates will come in contact at multiple points, thus dictating the plate distance as well as providing support and rigidity for the structure.

The corrugated pattern of plates creates a fluid passage path that is narrow and interrupted, and the shear stress at the surface is high. The high shear stress results in a high convection heat transfer coefficient but also high pressure drop. It also has the advantage of reducing fouling rate due to the increased ability of the fluid to “rip off” the fouling material from the surface. (Bell 1983, Shah 2003)

The flow arrangement in gasketed plate heat exchangers is typically counterflow, with either single or multiple passes per fluid: a single-pass counterflow arrangement was demonstrated in Figures 3.13 and 3.14a. Single-pass counterflow can be arranged in either U- or Z-pass (Figure 3.14a and 3.14b), of which U pass is almost always preferred, as it allows both fluid inlets and outlets to be connected to the same side, enabling disassembly for maintenance without a need to disconnect the heat exchanger from the fluid entry and exit pipes.

If pressure drop of one fluid must be kept considerably lower than in the other, or the flow rate of one fluid is much greater than that of the other, it may be necessary to arrange one fluid for multi-pass, and keep the other as single-pass; such arrangement is demonstrated in Figure 3.14c. The side effect of 1- n –multipassing in gasketed PHEs is that every other flow will be in parallel- rather than counter-flow arrangement.

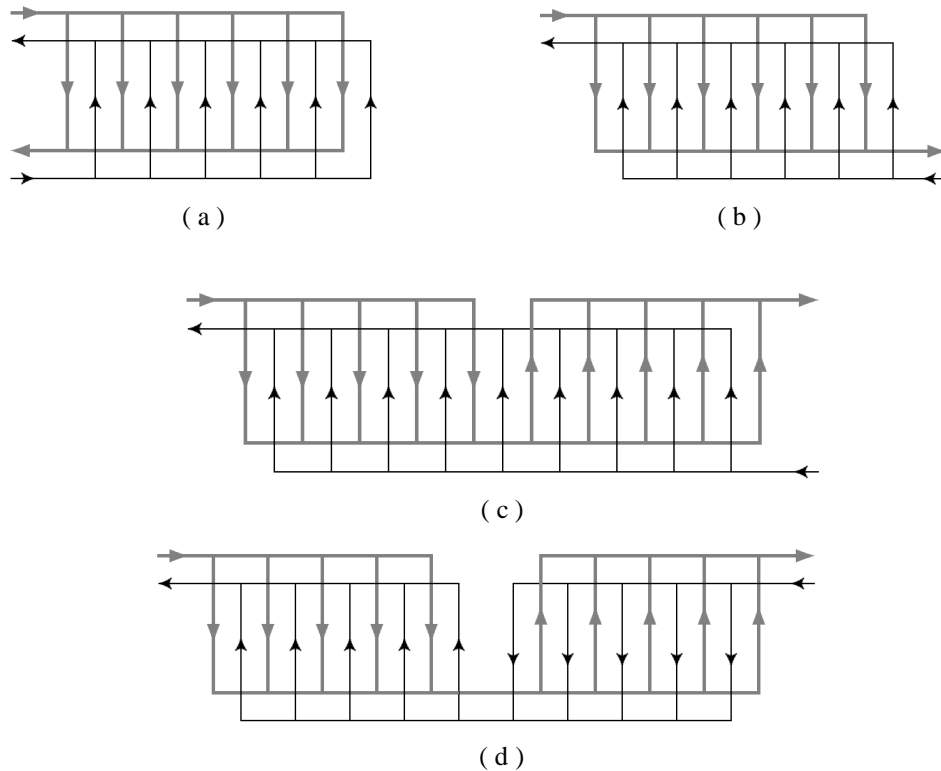


Figure 3.14. Possibilities for flow arrangements in gasketed PHEs: a) 1-1 counterflow in U arrangement; b) 1-1 counterflow in Z arrangement; c) 1-2 with counter- and parallelflow sections; d) 2-2 counterflow.

If there is a need for comparatively large heat transfer area, both fluids can be multi-passed, as shown in the example of 3.14d. Such multi-pass heat exchanger is in fact not a true multi-pass arrangement, as it is clear that the actual geometry of the flows relative to each other is in fact identical to a 1-1 counterflow arrangement with twice as long flow length.

The examples of Figure 3.14 are by no means the only options; countless different combinations can be generated. The examples are just to give the general idea of available options.

If temperatures or pressures greater than those possible with typical gasket materials are required, welding is an option for plate heat exchanger construction. Numerous plate and entry/exit head geometries, some very different from the gasketed PHEs presented above, become possible if the construction is welded rather than gasketed. Pressure ranges as high as 4.0 MPa can be achieved in simple constructions, with a pressure

shell around the exchanger this can be increased up to 20 MPa. (Shah 2003, pp.29-30). The obvious drawback is the loss of easy disassembly for maintenance and cleaning.

3.2.4 Spiral heat exchanger

A spiral heat exchanger can be considered a special case of plate-type heat exchangers. Typically a spiral heat exchanger consists of two sheets of metal formed into a spiral, as shown in Figure 3.15.

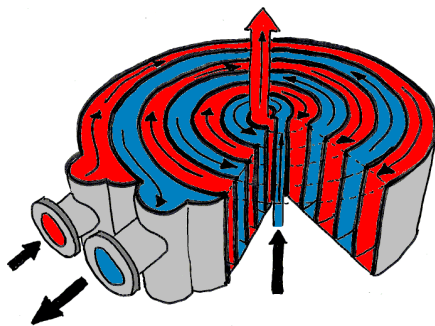


Figure 3.15. *Spiral heat exchanger.*

The fluids can either be connected to ports as shown in Fig. 3.15, or one of the fluids can be directed into the exchanger from the side of the spiral for a cross-flow arrangement. Also partly crossflow, partly counterflow arrangement where the fluid enters from side but mainly flows in a counterflow direction in the spiral is possible. (Shah 2003, pp.31)

The main advantage of a spiral heat exchanger is its self-cleaning nature if the fluids tend to foul the heat transfer surfaces quickly: because there is only single passage, a significant accumulation of fouling material in any part of the spiral will constrict the flow at that part, thus increasing flow velocity and shear stress at the surface, and increasing the tendency of the flow to clean the surface.

Being limited to a single passage also limits the spiral heat exchanger to relatively small applications. Typical passage gap width is 5 to 25 mm and spiral plate thickness 1.8 to 4 mm. Plate heights range from 100 to 1800mm. Spiral heat exchangers can be designed for fluid pressures of up to 1 MPa and temperatures of typically 200 °C, but a maximum of 500 °C is possible with suitable metal sheet and sealing material choices. (Shah 2003, pp.32), (Rohsenow 1987, pp.4-109)

3.2.5 Compact heat exchangers

The term “compact heat exchanger” refers to a wide variety of different heat exchanger constructions, which have all one thing in common: a very high density of heat transfer

area per heat exchanger core volume, usually defined as at least $700 \text{ m}^2 / \text{m}^3$. (Incropera 2002, pp.643)

When one or both fluids are gases, the heat transfer coefficient becomes poor. This must be compensated for with high heat transfer area if a high heat transfer rate is to be obtained. The actual construction can vary. Various tube-fin constructions are common particularly if the other fluid is a liquid; the liquid would flow in the tubes, while the gas would be in cross flow across the bank of finned tubes. The tubes themselves can be either normal circular tubes, or may be of for example rectangular, oval, or other more complicated shape. The non-circular tubes will typically provide better heat transfer coefficients, but at higher manufacturing cost. The fins themselves can be either circular (Figure 3.16 a), or plate-type (Figure 3.16 b).

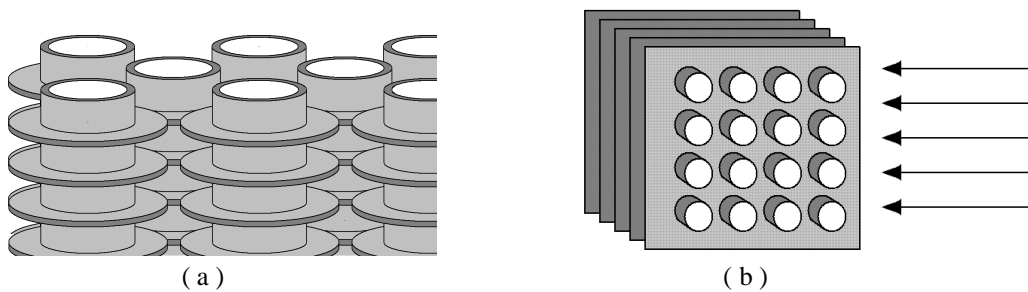


Figure 3.16. Compact tube-fin arrangements: a) circular fins, b) plate-type fins

If both fluids are gases, then a plate-type arrangement can be used. The plate arrangement can be either plate-fin (Figure 3.17 a), or a primary-surface construction (Figure 3.17 b), where no fins are used, but the primary heat transfer surface itself separates the fluids into narrow flow channels.

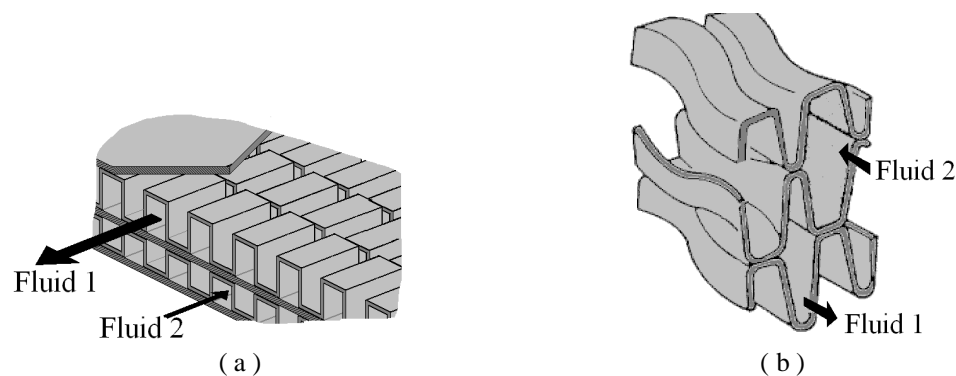


Figure 3.17. Compact plate-type surface arrangements: a) plate-fin, b) primary-surface.

Plate-fin construction requires the fins (typically made of very thin metal foil folded into the desired shape) to be brazed or soldered into the primary heat transfer surface. Laser welding makes it possible to construct primary-surface compact plate-type heat exchangers comparatively quickly and cheaply, and without the drawbacks of fin

efficiency and thermal contact resistances between the fins and the surface reducing the effectiveness of the heat transfer area.

Primary surface –type compact plate heat exchanger surfaces can in turn be constructed in a variety of ways, the two main types being cross-corrugated (similar to the herringbone structure of gasketed PHEs with plates in contact with each other), and cross-wavy (demonstrated in Fig. 13.17 b).

3.3 SELECTION OF APPROPRIATE HEAT EXCHANGER TYPE

The previous sub-chapter covered briefly the main characteristics of some of the most common types of heat exchangers, and should in itself give a preliminary understanding of their suitability for various applications. The purpose of this chapter is to summarize the information of the previous chapters for selection of appropriate heat exchanger type, and also provide additional information particularly on cost issues.

Generally the goal should be the cheapest overall solution that achieves the required thermal performance within described limits (i.e. maximum allowable pressure drop, size, weight, dimensions, etc.). To ensure reliable operation and not only low investment, but low overall operating costs, also issues such as fouling propensity and cleanability, and corrosion resistance must be considered.

In practice, various plate-type heat exchangers tend to provide lowest total costs (if not necessarily always lowest purchasing cost per heat transfer area) where conditions permit their use, while tubular exchanger types offer the most versatile applicability for more challenging operating conditions.

3.3.1 Fluid pressures and temperatures

If the fluids are liquids at less than approximately 150...200 °C temperature and 1 MPa pressure, the gasketed PHE is usually the most economical choice. Since the main limitation here is not the heat transfer surface itself, but the gasket material, somewhat higher temperature ranges can be achieved by welded or brazed construction, although this obviously comes at the expense of easy disassembly. (Shah 2003, pp.26 and 674-675)

For gas-gas heat exchangers a plate-type heat exchanger is also usually the best choice, but instead of a gasketed PHE, a compact heat exchanger of either brazed plate-fin or laser-welded primary-surface construction is often preferable. If one of the fluids is at too high pressure for plate-type heat exchangers, a finned-tube construction, with high-pressure fluid on the tube side, can be used. A tube-fin construction is also inherently

stronger and allows slightly higher temperatures to be achieved with the same materials, although at the cost of larger size, weight and cost for a given performance.

Tubular heat exchangers can be built to tolerate very high temperatures and pressures, as well as corrosive or hazardous fluids, provided that suitable materials are chosen. The high-pressure and/or high-temperature fluid should be placed into the tubes: this allows only the tubes to be constructed from expensive materials, and minimizes insulation expenses and heat losses through the shell.

For very high temperatures, regenerative instead of recuperative heat exchangers must be used - static ceramic matrices can tolerate gas temperatures of up to 2000 K.

3.3.2 Fouling

If fouling is expected to be significant on one or both fluids, both minimizing the foulant accumulation and ease of cleaning should be considered. If temperature, pressure and corrosion considerations permit, the gasketed plate heat exchanger is usually ideal from both points of view. Foulant accumulation in a plate heat exchanger tends to be much less than in a tubular exchanger for given fluids, and disassembly of the plate stack for periodic cleaning is simple and fast.

A spiral heat exchanger is also a potential candidate for applications where fouling effects are significant. If the foulant is such that it can be removed from the heat transfer surface by the increased shear stress of an accelerated fluid flow, the spiral heat exchanger tends to be self-cleaning: significant growth of foulant layer thickness in any location of the spiral channel will contract the channel, thereby locally increasing fluid velocity and shear stress. Particularly fouling by crystallization may create too strong foulant layers to be removable in this manner, however.

If a plate heat exchanger is not possible, a shell-and-tube heat exchanger allows also reasonably easy cleaning. Ideally the fluid undergoing heaviest fouling should be placed on the tube side to permit easy access for mechanical cleaning and the length of the tubes should be short enough to allow easy extraction from the shell given the physical restriction at the installation site. For ease of cleaning, straight tubes should be used instead of U-tubes. If fouling is a concern also on the shell side, the tube layout should be either 45° or 90° square pitch with at least 6 to 7 mm clearance between tubes, in order to allow cleaning lanes for mechanical cleaning. (Taborek 1983c)

(Müller-Steinhagen 1997) and (Hammo 1994) provide additional information on the topics of fouling and cleaning of shell-and-tube heat exchangers.

3.3.3 Material choices

The material chosen for the heat exchanger must be suitable for the type of physical construction, be compatible with the fluid temperature ranges expected, and not be corroded by the fluids. Cost is a significant concern as well, while thermal conductivity is rarely a significant issue.

In plate-type heat exchangers the heat transfer surfaces are currently still metallic, although ceramic materials are being developed to achieve higher temperature ranges. Aluminum is a common material in compact heat exchangers, but cannot be used or in high-temperatures applications (maximum temperature is approximately 200 °C). Also use with food fluids or highly corrosive fluids necessitates the use of other materials, often stainless steel. Aluminum is, however, useful down to very low (cryogenic) temperatures. (Shah 2003, pp.678)

Temperatures of up to approximately 650 °C are achievable with welded stainless steel plate heat exchanger constructions, most commonly Type 347 stainless steel (Aquaro and Pieve 2007). High-temperature superalloys such as Inconel can further increase the achievable temperature range up to 750...800 °C (McDonald 2003), but only at a considerably increased cost. Material and construction issues related to high-temperature gas heat exchangers are covered in more detail in for example (Aquaro and Pieve, 2007), as well as numerous publications by Colin McDonald and Ulf Sundström.

Particularly in highly corrosive use, titanium is also a common plate heat exchanger material.

Tubular heat exchangers can be constructed from a variety of materials, most commonly carbon steel unless corrosion or temperature considerations require other materials. Ordinary carbon steel can be used within a temperature range of 0 to 500 °C with non-corrosive or mildly corrosive fluids. Impact-tested carbon steel is still useful down to -45 °C, below which special steels or aluminum must be used. Refractory lining permits temperatures higher than 500 °C. (Shah 2003, pp.679)

If one of the fluids is highly corrosive, that fluid should be placed on the tube side to allow cheaper shell material to be used, and only tubes be constructed of the corrosion-resistant material. Depending on the fluid, that material could be aluminum (only mildly corrosive fluids), a suitable steel type, titanium, or a copper alloy. Also glass or carbon can be used for corrosive duties, or more conventional materials can be protected by suitable linings, for example austenitic Cr-Ni steel for general corrosion resistance, refractory materials for high-temperature applications, or lead and rubber for seawater. (Shah 2003, pp. 679)

3.3.4 Cost

Other considerations permitting, the goal is of course always to minimize the overall total cost of the heat exchanger. This total overall cost is the sum of manufacturing, installation and operating costs. The manufacturing cost is often roughly one third of total installed cost, although the ratio obviously depends much on the type, construction material and size of heat exchanger. The operating costs consist of pumping cost to overcome the pressure drop associated with the heat exchanger, maintenance, cleaning and repair costs, and often also the energy costs related to the usage of the heat exchanger.

Most heat exchanger manufacturers have their own proprietary methods for cost estimation and analysis; publically available information can be described as sketchy at best. Table 3.3, based on original cost data from 1994 in Great Britain, gives a comparison of heat transfer area cost per square meter, normalized against a 10m² shell-and-tube heat exchanger (relative cost 1.0). The costs of gasketed or welded plate heat exchangers are not available for comparison, but as a general rule, plate-type heat exchangers are the cheapest option when other considerations such as pressures and temperatures of the fluids permit.

For a rough guideline of actual costs, at the time of writing (2009) the total installed costs of large shell-and-tube heat exchangers were measured in hundreds of Euros per m², obviously depending on the exact construction and materials used.

Table 3.3. *Relative heat transfer area costs for different sizes and types of heat exchangers, 1994 (Shah 2003, pp.72)*

Heat exchanger size [m ²]	shell-and-tube	double-tube	plate-fin
2	4.0	2.5	N/A
10	1.0	0.75	3.14
60	0.29	0.31	0.52
200	0.17	0.31	0.21
2000	0.11	0.31	0.12

A more detailed treatment of costs considering materials as well as manufacturing location can be found in Appendix 3 of (Sarkomaa 1994).

4 METHODS OF HEAT EXCHANGER CALCULATION

The central variables in any heat exchanger analysis are the heat transfer rate q [W], heat transfer area A [m²], heat capacity rates \dot{C} ($= \dot{m} c_p$) [W/K], and the overall heat transfer coefficient U . On the basis of these variables and the fluid temperatures, we can write two basic equations for the heat transfer rate; first, for heat transfer rate it must hold that

$$q = U A \Delta T_m, \quad (4.1)$$

where ΔT_m is the average (mean) temperature difference of the two fluids in the heat exchanger, and the area A in equation the heat transfer area, meaning the contact area between one of the fluids, and the surface of the wall that separates the fluid. **If the areas are different on each sides of the wall, the larger area is the one to be used in equation (1) as the heat transfer area.** The areas are typically significantly different from each other in the case in tubular or extended-surface heat exchangers. Sometimes the term UA of equation (1) is written simply as G [W / K], or conductance of the heat exchanger.

Second, on the basis of 1st law of thermodynamics, the heat transfer rate q must also equal the rate of heat lost by the hot fluid stream and gained by the cold fluid stream:

$$q = \dot{C}_{hot} (T_{hot,in} - T_{hot,out}) = \dot{C}_{cold} (T_{cold,out} - T_{cold,in}). \quad (4.2)$$

For a sizing problem, where one must define the required area of a heat exchanger in order to achieve the desired outlet temperatures and/or heat transfer rate q , the main parts of the problem can in very general terms be said to consist of two parts: 1) finding the value of overall heat transfer coefficient U for the type of heat exchanger at hand, and 2) finding the correct way to get to the required heat transfer area given the U value, selected type of heat exchanger and it's flow patterns, and required heat transfer rate and/or fluid outlet temperatures.

The first part of the problem is mainly an issue of estimating the correct convection heat transfer coefficients at the heat transfer surface, and often also fouling resistances expected to develop on that surface. Determining the value of U is thus mainly a function of the exact physical geometries and flow directions and velocities in the heat exchanger, with significant impact also from fouling characteristics, and at least to some extent also the material and thickness of the heat transfer surface.

Chapter 5 will define the overall heat transfer coefficient and deal with how to determine it once the fouling resistances and convection heat transfer coefficients are known. For now the definition of U on the basis of equation (4.1) is sufficient.

Although equation (4.1) relates the overall heat transfer coefficient U to the heat transfer area A and fluid temperatures in a seemingly simple way, the matter is complicated by the various temperature distributions possible with different heat exchanger arrangements: determining the average temperature difference ΔT_m is usually not simple.

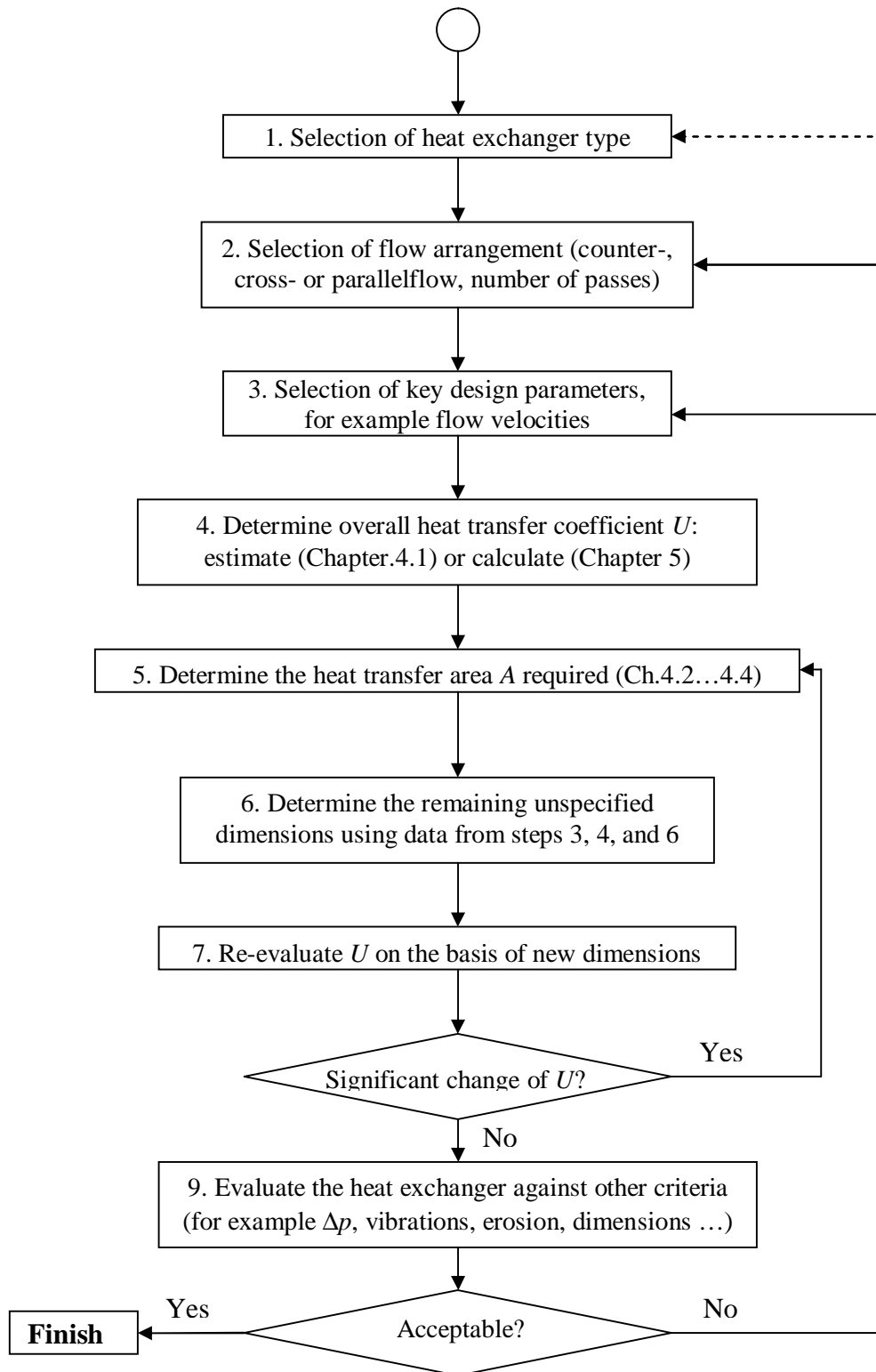
Various heat exchanger sizing methods have been developed from the basic transfer rate and conservation equations, each giving different methods for the designer to relate the overall heat transfer coefficient U and fluid temperatures and heat capacity rates \dot{C} to the required heat transfer area. All these methods are based on certain simplifying assumptions about the heat exchangers analyzed; these are:

- There is no heat transfer between the fluid streams and the outside environment
- There are no leakages from the fluid streams to each other or to the environment
- No heat is generated or lost via chemical or nuclear reactions, mechanical work, or other means
- There is no heat conduction along the length of the heat transfer surface, only in the direction of the normal of the surface
- No flow maldistribution: fluid flow rates are equally distributed throughout the whole cross-sectional areas of flow
- Where temperature distribution transverse to the flow direction is relevant, any fluid flow can be considered either completely mixed or completely unmixed
- Properties of fluids are constant inside the heat exchanger
- Overall heat transfer coefficient is a constant at all locations of the heat exchanger.

Although very different in their practical application for heat exchanger sizing, all methods derived from the same basic equations and based on the same assumptions and simplifications are essentially equivalent, and will yield the same results if correctly applied. From the several existing methods, the three most commonly used ones are dealt with in this chapter from 4.2 onwards: the very similar ϵ -NTU and P -NTU methods, as well as the traditional logarithmic mean temperature difference or LMTD method.

As can be expected from the above, no matter which of the abovementioned three methods is used, the process of sizing a heat exchanger will inevitably be an iterative one: to calculate the area one has to have at least an estimate of U , once an area is calculated on the basis of the estimate (or guess), the geometry of the heat exchanger will be known so that a better estimate of U can be calculated, leading to a better estimate of the area, therefore some change in geometry, requiring a new value of U to be calculated, and so on. The rough outline of this iteration process is demonstrated in Algorithm 4.1.

Algorithm 4.1. Heat exchanger sizing process flow chart



At step 3 in the algorithm, one usually needs to fix certain design parameters, and then evaluate the remaining dimensions at step 6 on the basis of those set at step 3, and the area calculated at step 5. For example if one is designing a shell-and-tube heat exchanger, one could assume certain diameter of tubes and number of tubes per pass,

thereby determining also a fixed value for tube-side flow velocity and by consequence the convection heat transfer coefficient of the inside flow needed in determining a good approximation for U . At step 6 the length of a tube pass would be then exactly defined with the area, number of passes, tubes per pass, and tube outer diameter known.

4.1 QUICK ESTIMATES

For a quick estimate of the required heat transfer area, one can simply take equation (4.1), and assume a “typical” value for U given the fluids and chosen heat exchanger construction. Some value ranges for U combined from (Çengel 1999), (Incropera 2002) and (Sarkomaa 1994) listed in tables 4.1 and 4.2.

Table 4.1. Typical values of U [W / m²K] for tubular, non-finned heat exchangers

Fluid 1	Fluid 2				
	gas, 1 bar	gas, ≥ 25 bar	liquid, high viscosity ¹	liquid, low viscosity ²	phase change
gas, 1 bar	5...35	10...60	15...50	20...70	20...70
gas, ≥ 25 bar	10...60	100...400	100...400	150...500	200...500
liquid, high μ	15...50	100...400	100...400	200...500	200...900
liquid, low μ	20...70	150...500	200...500	400...1700	500...2000
phase change	20...70	200...500	200...900	500...2000	700...2500

¹ for example most oils

² for example water

Table 4.2. Typical values of U [W / m²K] plate-type heat exchanger

Fluid 1	Fluid 2	
	gas, <10 bar	liquid
gas, < 10 bar	10...35	20...60
liquid	20...60	200...1200

For a rough estimate of size class of the heat exchanger one can use simply the temperature difference of the average temperatures of both fluids, or

$$\Delta T_m = \frac{1}{2}(T_{h,i} + T_{h,o}) - \frac{1}{2}(T_{c,o} + T_{c,i}) \quad (4.3)$$

and calculate an estimate for heat transfer area A from equation (1),

$$A = \frac{q}{U\Delta T_m} \quad (4.4)$$

The heat transfer rate q has to be, based on the assumption that there is no heat transfer between the heat exchanger and the surroundings, the heat lost by the hot fluid and gained by the cold fluid, or

$$q = (\dot{m} c_p)_h(T_{h,i} - T_{h,o}) = (\dot{m} c_p)_c(T_{c,o} - T_{c,i}), \quad (4.5)$$

where the product $\dot{m} c_p$ is the heat capacity rate \dot{C} of the fluid in question.

For better approximation of the required area a logarithmic mean temperature difference ΔT_{lm} can be used, which will lead to the LMTD method of heat exchanger analysis.

4.2 LOGARITHMIC MEAN TEMPERATURE DIFFERENCE (LMTD) METHOD

This chapter will describe the usage of the LMTD method for heat exchanger analysis and sizing. The first chapter 4.2.1 will define the logarithmic mean temperature difference ΔT_{lm} for simple flow geometries, followed by chapters on dealing with more complicated flow arrangements, and some special cases of fluids.

4.2.1 Definition of LMTD

As the name suggests, the LMTD method of heat exchanger analysis is based on using the equation (1) with the average temperature difference ΔT_{lm} now defined as the logarithmic mean temperature difference ΔT_{lm} .

It can be shown that although the temperature difference between the two fluids is different in every point of the heat exchanger surface, the **mean** temperature difference of the two fluids throughout the whole counterflow or parallelflow heat exchanger can be solved from

$$\Delta T_{lm} = \frac{\Delta T_1 - \Delta T_2}{\ln \frac{\Delta T_1}{\Delta T_2}}, \quad (4.6)$$

where the temperature differences ΔT_1 and ΔT_2 are the temperature differences between the inlet and outlet (Fig.4.1).

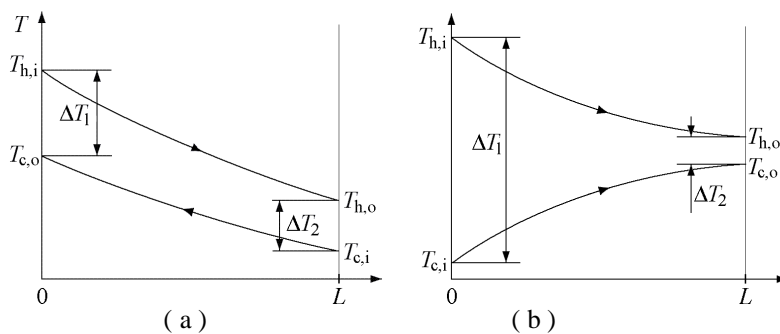


Figure 4.1 Temperature differences ΔT_1 and ΔT_2 a) counterflow and b) parallelflow arrangements.

For a counterflow arrangement the ΔT 's are therefore

$$\Delta T_1 = (T_{h,i} - T_{c,o}) \text{ and } \Delta T_2 = (T_{h,o} - T_{c,i}), \quad (4.7)$$

and for a parallelflow arrangement

$$\Delta T_1 = (T_{h,i} - T_{c,i}) \text{ and } \Delta T_2 = (T_{h,o} - T_{c,o}). \quad (4.8)$$

Once the average temperature difference is known, equation (4.4) can be used to calculate the required heat transfer area, as demonstrated in example 4.1.

EXAMPLE 4.1

PROBLEM:

A double-tube heat exchanger is used to cool hot oil from 90 °C to 40 °C temperature with cold water available at +10 °C. Mass flow rates and specific heats for oil and water are 0.60 kg/s and 2.5 kJ / kgK for oil and 0.20 kg/s and 4.2 kJ / kgK for water. With said fluid flow rates, the overall heat transfer coefficient of the heat exchanger is known to be approximately 200 W/m²K.

The exchanger is built of co-centric tubes, inner having inside and outside diameters of 26.6 mm and 33.4 mm, the outer tube diameters 52.5 mm and 60.3 mm. The exchanger is built of 1.8 metre long elements (see Figure E-4.1) The exchanger can be connected to either counter- or parallelflow; calculate the required area for both cases.

Calculate the number of elements required for both flow arrangement options.

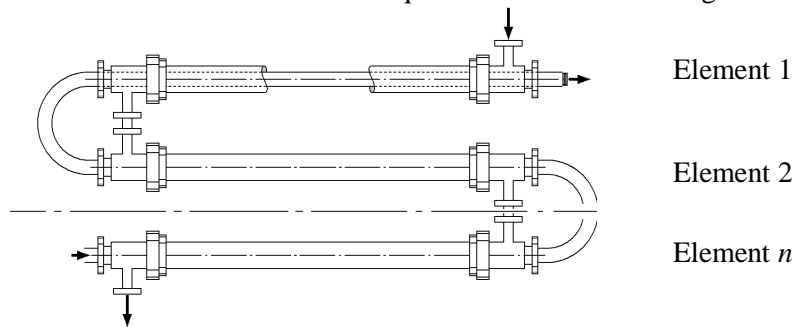


Figure E-4.1. A double-pipe heat exchanger

SOLUTION:

For this case it is irrelevant for the flow arrangement how many elements there are; throughout the whole exchanger, the arrangement is always pure counter- or parallelflow. The overall temperature distribution between the inlet and the outlet is therefore as depicted in Fig. 4.1.

We must solve the area A , and understanding that the area is the larger of the two areas, calculate then the required number of 3.6 metre elements.

First the heat transfer rate q must be found, in order to calculate the cold stream outlet temperature from equation (4.2), then ΔT_{lm} from eq. (4.6), and finally A from eq. (4.4):

Heat capacity rates of the fluids:

$$\begin{aligned}\dot{C}_h &= \dot{m}_h c_{p,h} = 0.60 \text{ kg/s} \cdot 2500 \text{ J / kgK} = 1500 \text{ W / K} \\ \dot{C}_c &= \dot{m}_c c_{p,c} = 0.30 \text{ kg/s} \cdot 4200 \text{ J / kgK} = 1260 \text{ W / K}\end{aligned}$$

Heat transfer rate, from eq. (4.2):

$$q = \dot{C}_h(T_{h,i} - T_{h,o}) = \dot{C}_c(T_{c,o} - T_{c,i}) = 1500 \text{ W/K} (90^\circ\text{C} - 40^\circ\text{C}) = 75000 \text{ W}$$

Cold fluid outlet temperature, solving $T_{c,o}$ from eq. (4.2):

$$\begin{aligned}q &= \dot{C}_c(T_{c,o} - T_{c,i}) \Rightarrow T_{c,o} = T_{c,i} + q / \dot{C}_c \\ T_{c,o} &= T_{c,i} + q / \dot{C}_c = 10^\circ\text{C} + (75000\text{W} / 1260\text{W/K}) = 69.5^\circ\text{C}\end{aligned}$$

First counterflow arrangement: Solving ΔT_{lm} by substituting from eq. (4.7) to eq. (4.6):

$$\begin{aligned}\Delta T_1 &= (T_{h,i} - T_{c,o}) = 90^\circ\text{C} - 69.5^\circ\text{C} = 20.5^\circ\text{C} \\ \Delta T_2 &= (T_{h,o} - T_{c,i}) = 40^\circ\text{C} - 10^\circ\text{C} = 30^\circ\text{C}\end{aligned}$$

$$\Delta T_{lm} = \frac{\Delta T_1 - \Delta T_2}{\ln \frac{\Delta T_1}{\Delta T_2}} = \frac{(20.5 - 30)^\circ\text{C}}{\ln \frac{20.5}{30}} = 24.95^\circ\text{C}$$

Then area from eq. (4.4):

$$A = \frac{q}{U \Delta T_{lm}} = \frac{75000\text{W}}{200 \frac{\text{W}}{\text{m}^2\text{K}} 24.95^\circ\text{C}} = 15.03\text{m}^2$$

The heat transfer area is the larger surface area separating the fluids; that is, the **outer wall area** of the **inner tube**,

$$A = \pi d_o L,$$

where L is the total length of tube in the heat exchanger that we must solve,

$$L = A / \pi d_o = 15.03 \text{ m}^2 / (\pi 0.0334\text{m}) = 143.2 \text{ m},$$

and required number of elements n therefore

$$n = \frac{143.2\text{m}}{1.8\text{m}} = 79.6 = 80.$$

Next the same procedure should be carried out for the parallelflow arrangement. Eq.(4.8) gives temperature differences at inlet and outlet

$$\begin{aligned}\Delta T_1 &= (T_{h,i} - T_{c,i}) = 90^\circ\text{C} - 10^\circ\text{C} = 80^\circ\text{C} \\ \Delta T_2 &= (T_{h,o} - T_{c,o}) = 40^\circ\text{C} - 69.5^\circ\text{C} = -29.5^\circ\text{C}\end{aligned}$$

The fact that the outlet temperature difference is negative shows what could have been concluded already from the outlet temperatures: in order to cool the oil to 40°C , water

needs to be heated a higher temperature than that. This makes it impossible to achieve the required oil outlet temperature with arrangement.

COMMENTS:

A very large number of cooling elements were needed; it is likely that another type of heat exchanger construction such as a small shell-and-tube heat exchanger with a smaller tube size would have provided a cheaper and more compact option.

4.2.2 Complex flow arrangements

If the flow geometry is more complicated than simple counter- or parallelflow, the average temperature difference can no longer be approximated with ΔT_{lm} . In such a case, equations (4.1) and (4.4) are used with the temperature difference ΔT_{lm} **defined as if the case was counterflow**, eq. (4.7), and the equation is modified with a **correction factor F** ,

$$\boxed{q = U A F \Delta T_{lm}} \quad (4.9)$$

The correction factor F is determined from charts or equations on the basis of two dimensionless parameters: temperature effectiveness P , and ratio of heat capacity rates R . **Both parameters are defined separately for each fluid flow** entering the heat exchanger, not as a single figure for the whole exchanger.

The temperature effectiveness P of one flow is the ratio of that fluid flow's temperature change to the maximum temperature difference that exists in the heat exchanger (the temperature difference between the inlets, that is):

$$P_h = \frac{T_{h,i} - T_{h,o}}{T_{h,i} - T_{c,i}} \quad \text{and} \quad P_c = \frac{T_{c,o} - T_{c,i}}{T_{h,i} - T_{c,i}} \quad (4.10)$$

The heat capacity ratio R is similarly defined separately for both fluids,

$$R_h = \frac{\dot{C}_h}{\dot{C}_c} = \frac{\dot{m}_h c_{p,h}}{\dot{m}_c c_{p,c}} \quad \text{and} \quad R_c = \frac{\dot{C}_c}{\dot{C}_h} = \frac{\dot{m}_c c_{p,c}}{\dot{m}_h c_{p,h}} \quad (4.11)$$

Because the heat capacity ratios must also represent the ratios of temperature change in the fluids (due to the definition of heat capacity and the assumption of no heat losses from the heat exchanger to surroundings), R can also be written as a ratio of temperature change in both fluids. Heat capacity rate by its definition has an inverse, linear proportionality to the temperature change given same heat transfer rate to or from the fluid, therefore

$$R_h = \frac{T_{c,o} - T_{c,i}}{T_{h,i} - T_{h,o}} \quad \text{and} \quad R_c = \frac{T_{h,i} - T_{h,o}}{T_{c,o} - T_{c,i}}. \quad (4.12)$$

Correction factors F can be then defined on the basis of these figures from either graphs or equations.

It should be noted that most flow arrangements more complex than simple counter- or parallelflow are *stream asymmetric*: the function f for $F = f(R, P)$ will become different if the fluids are switched, for example tube fluid to the shell side and vice versa in a shell-and-tube heat exchanger. For this reason the equations and graphs for F usually denote the fluids as simply 1 and 2 rather than hot and cold, because it is significant for which flow route, not whether for hot or cold, the R and P are defined.

Equations and graphs for defining F from R and P are defined for mixed-unmixed crossflow and 1-2 counter-parallelflow heat exchangers in figures 4.2 and 4.3. Graphs for more cases can be found from for example Incropera 2002.

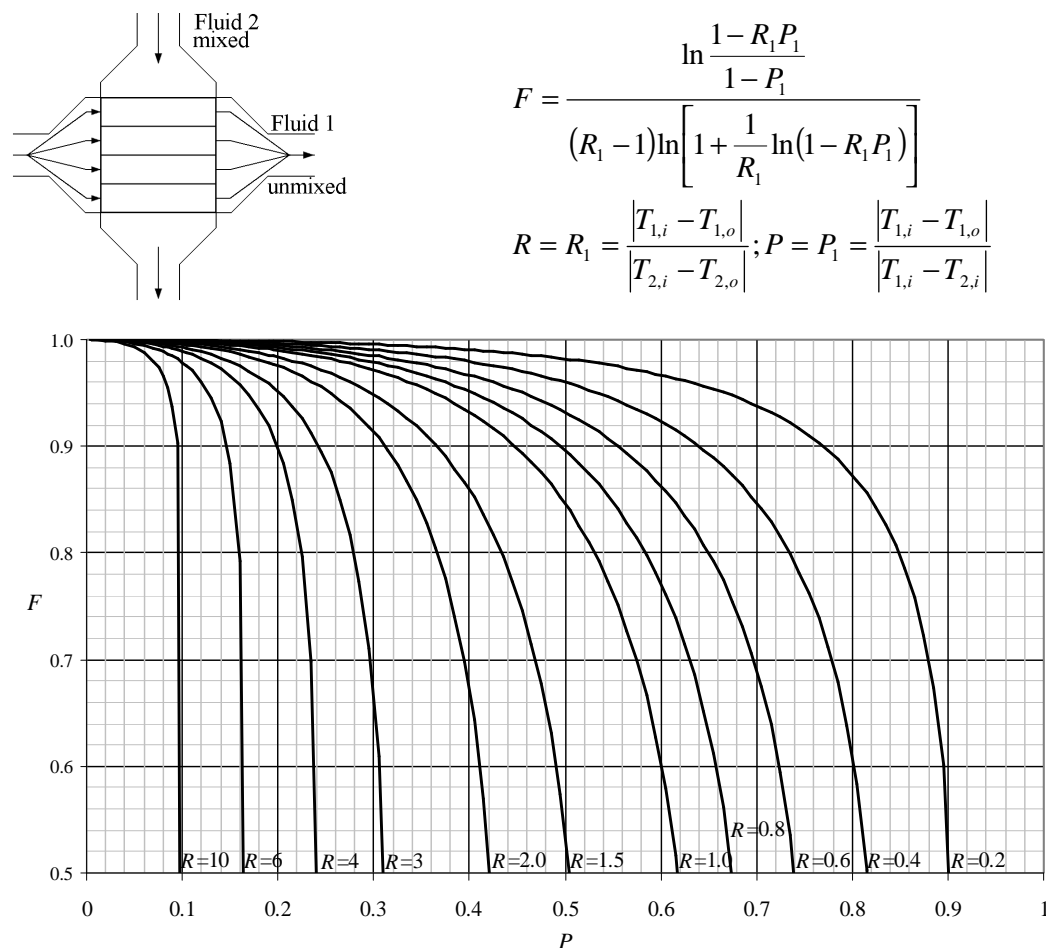


Figure 4.2 Correction factor F for a crossflow heat exchanger with fluid 1 unmixed, fluid 2 mixed.

The mixed-unmixed crossflow example of Figure 4.2 shows one example of a fluid asymmetric case. It is important that it is exactly the P and R of the unmixed stream

that are used in either the equation or in reading the graph; a different functional relationship would bind the mixed fluid's P and R to the value of F .

Although not immediately obvious from the flow geometry, it can be shown that a 1-2 parallel-counterflow arrangement is in fact stream symmetric (Shah and Sekulić 2003). An example of such a heat exchanger was the TEMA E shell-and-tube heat exchanger with two tube-side and one shell-side pass shown of Fig. 3.8. For a stream symmetric case, either of the streams can be used in determining R and P for the equation or graph; but of course not stream 1 for one and stream 2 for the other parameter.

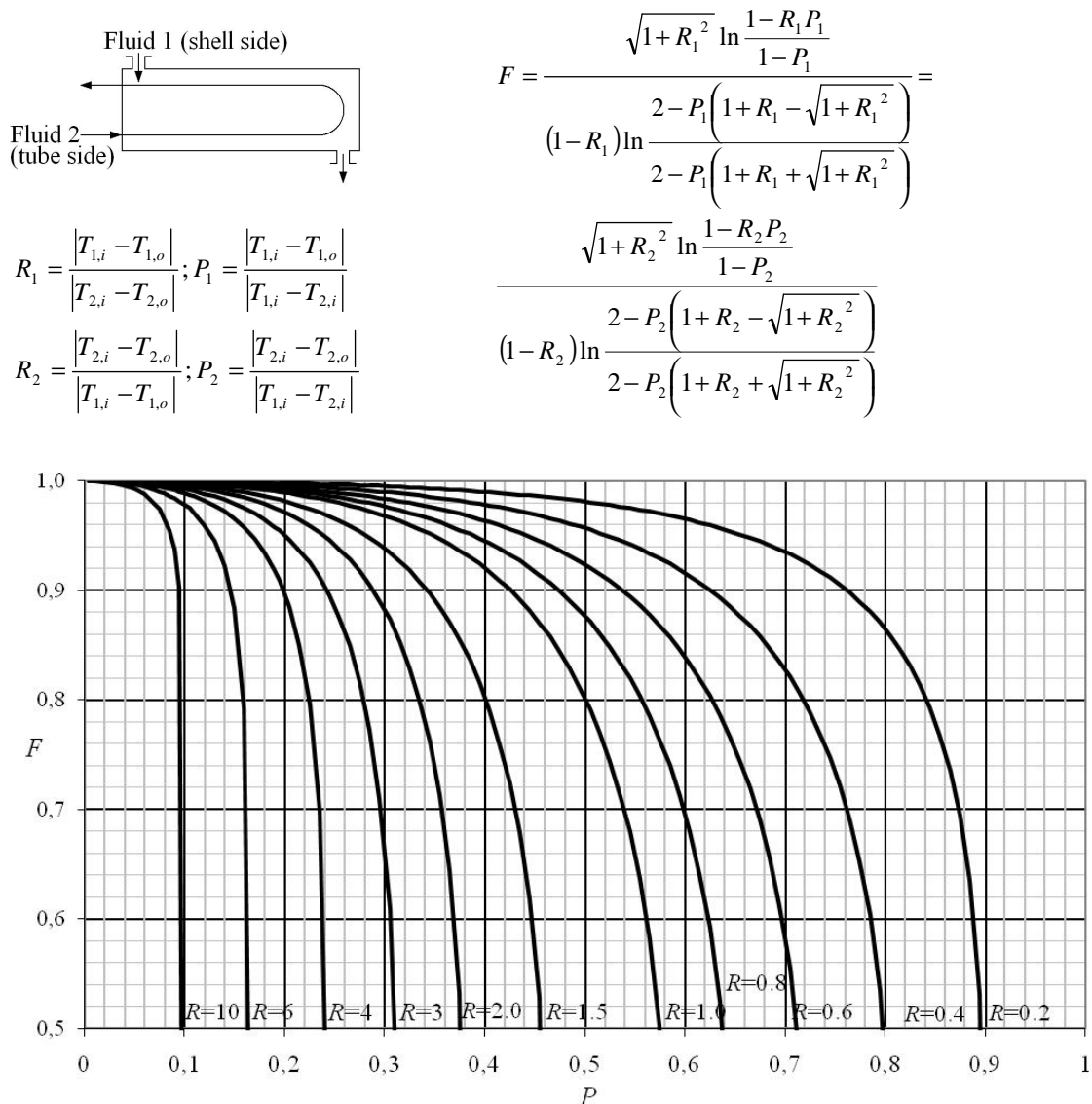


Figure 4.3 Correction factor F for a two-pass parallel-counterflow heat exchanger (for example a TEMA E with one shell-side and two tube-side passes). Case is stream symmetric; equations are the same whether determined with fluid 1 or 2.

4.2.3 Special Cases

Sometimes the heat capacity rates of the fluids may be either exactly the same, or one of the flows may have very much larger heat capacity rate than the other.

If the heat capacity rates are the same, then determining $\Delta T_{lm} = \Delta T_1 = \Delta T_2$ for all flow arrangements except parallelflow. All cases where the heat capacity rates are the same must obviously also be stream symmetric.

If the heat capacity rate of one fluid stream is very much larger than that of the other, the correction factor $F = 1$ regardless of the flow arrangement. This is also the case when the cold fluid is boiling or the hot fluid condensing, because boiling or condensation will happen at a constant temperature with the (usually safe) assumption of pressure changes not significantly affecting the saturation temperature. The specific heat of the fluid undergoing phase change can therefore be treated as $c_p = \infty$: the temperature does not change as a function of heat transferred to or from the fluid.

4.2.4 Summary

The LMTD method is convenient for sizing problems where at least one of the fluid outlet temperatures is a given parameter. It is less well suited for rating problems, where the task is to find the outlet temperatures on the basis of known heat exchanger type and fluids entering the exchanger, however.

In order to solve the outlet temperatures, one has to first make an initial guess for one of them, calculate from that q with eq. (4.2) and then from that the other outlet temperature, then ΔT_{lm} , and finally q from eq. (4.9), compare to original q , adjust outlet temperature, and continue iteratively until the values of q from equations (4.2) and (4.9) converge. This is obviously a tedious and time-consuming process, which makes the method less than ideally suited for rating problems.

The process of solving a sizing problem with LMTD method is briefly summarized in Algorithm 4.2 below; this would replace steps 4 and 5 in Algorithm 4.1 earlier. As shown in Algorithm 4.1, the resulting heat exchanger will then need to be checked against relevant limitations and design criteria (for example maximum allowable pressure drops of the fluids or maximum external dimensions), and if it violates any, appropriate changes need to be made to the fixed parameters and the process repeated.

Algorithm 4.2. *Solving a sizing problem with LMTD method.*

1. Out of heat transfer rate q and fluid outlet temperatures $T_{x,o}$, determine those that are unknown on the basis of those that are known, using equation (4.2).
2. Determine the overall heat transfer coefficient U

3. Calculate ΔT_{lm} from equation (4.6)
4. Determine F from graph or equation for the type of heat exchanger flow arrangement used
5. Calculate required heat transfer area A from equation (4.4).

4.3 ϵ -NTU -METHOD

The ϵ -NTU method of heat exchanger analysis is based on three dimensionless parameters: the heat exchanger effectiveness ϵ , ratio of heat capacity rates of the fluid streams C_R , and number of transfer units NTU. ϵ is a function of heat duty and/or outlet temperatures and NTU a function of heat transfer area. Functions correlating the three dimensionless parameters to each other exist for a variety of flow arrangements.

Use of the ϵ -NTU method starts by solving two of the dimensionless parameters from what is known about the situation, and then using the correct ϵ -NTU relationship to find the third. From that value and definition of the third dimensionless parameter one then solves what needs to be determined: for example the required heat transfer area from NTU in a sizing problem, or fluid outlet temperatures from ϵ in a rating problem. The dimensionless parameters are defined in the following chapter

4.3.1 Dimensionless parameters: ϵ , C^* and NTU

4.3.1.1 Heat capacity rate ratio C^*

As the name suggests, the parameter C^* is simply the ratio of the heat capacity rates of the fluid streams, defined as the ratio of smaller to the larger. For a heat exchanger where neither fluid experiences a phase change, C^* is therefore defined as a

$$C^* = \frac{\dot{C}_{\min}}{\dot{C}_{\max}} = \frac{(q_m c_p)_{\min}}{(q_m c_p)_{\max}}. \quad (4.13)$$

If one of the fluids of the heat exchanger does experience a phase change however, then the temperature of that fluid stream does not change, and \dot{C} of that stream is effectively infinity. Any finite \dot{C} of the other stream therefore becomes automatically the \dot{C}_{\min} , and the heat capacity rate ratio will be 0. In literature the heat capacity rate ratio is frequently noted as C^* or C_R , in older Finnish literature R without a subscript also means the ratio of smaller to larger heat capacity rate.

4.3.1.2 Heat exchanger effectiveness ε

Heat exchanger effectiveness is defined as the ratio of actual heat transfer rate q in the heat exchanger to the maximum heat transfer rate possible according to the 2nd law of thermodynamics, q_{\max} :

$$\varepsilon = \frac{q}{q_{\max}}. \quad (4.14)$$

In a heat exchanger where there is no phase change taking place in either of the fluids, the actual heat transfer rate can be expressed as a product of temperature change and heat capacity rate of either fluid, according to equation (4.2) $q = (\dot{C} \Delta T)_h = (\dot{C} \Delta T)_c$.

The maximum heat transfer rate possible is defined by the inlet temperatures of both fluid streams, and the smaller of the heat capacity rates of the two fluids, \dot{C}_{\min} : once the minimum heat capacity rate fluid (the fluid whose temperature change is fastest per given heat loss or gain) has experienced the entire temperature change $T_{h,i} - T_{c,i}$, then the entire driving potential for heat transfer is used up and further heat transfer would violate the 2nd law of thermodynamics.

With the aforementioned definitions ε can be written as

$$\varepsilon = \frac{\dot{C}_c (T_{c,o} - T_{c,i})}{\dot{C}_{\min} (T_{h,i} - T_{c,i})} = \frac{\dot{C}_h (T_{h,u} - T_{h,o})}{\dot{C}_{\min} (T_{h,i} - T_{c,i})} = \frac{|T_i - T_o| \dot{C}_{\min}}{T_{h,i} - T_{c,i}}, \quad (4.15)$$

and therefore instead of equation (4.1), the the total heat duty of the exchanger can be expressed as

$$q = \varepsilon \dot{C}_{\min} (T_{h,i} - T_{c,i}). \quad (4.16)$$

The heat exchanger effectiveness can obviously be calculated from fluid stream information for solving a sizing problem. Conversely, in a rating problem once ε is obtained from C_R and NTU , then the outlet temperatures and/or heat transfer rate can be solved.

4.3.1.3 Number of Transfer Units

Of the three dimensionless parameters NTU is the one which contains the independent design variable under the heat exchanger designer's control: overall heat transfer rate U and heat transfer surface area A . NTU is defined as

$$NTU = \frac{UA}{\dot{C}_{\min}}, \quad (4.17)$$

where UA is the conductance of the heat exchanger. In older Finnish literature the term $(UA) / \dot{C}_{\min}$ is often called the dimensionless conductance, and denoted as Z . Also various other definitions and names for the same dimensionless group exist: in plate heat exchanger design literature the NTU is sometimes referred to as the performance factor or thermal length of the heat exchanger and denoted with θ ; in case of shell-and-tube exchangers it is sometimes referred to as the reduced thermal flux.

In a sizing problem, one would first calculate ε and C_R from knowledge of the fluid streams and required heat duty; NTU can then be obtained from the relationships of the dimensionless parameters, and knowing the numerical value of NTU and U , it then becomes a simple matter to find the required heat transfer area from equation (4.17).

4.3.2 Effectiveness – NTU relationships

The core of ε - NTU method is the collection of effectiveness- NTU relationships binding the effectiveness (and thus temperatures and heat duty) to NTU (and thus heat transfer area when U and \dot{C}_{\min} are known).

As with the correction factor F with LMTD method, the relationships depend on flow arrangement: some arrangements are able to maintain on average higher local temperature differences between the streams than others, and these will have higher values of F in LMTD analysis, and give higher values of ε with any given C^* and NTU when using the ε - NTU method.

Effectiveness- NTU relationships are tabulated in both equation and graphical form in numerous heat transfer textbooks and heat exchanger design handbooks. Relationships for some common flow arrangements are given in Figures 4.4 to 4.11.

The graphs are adapted mostly the $\varepsilon = \varepsilon(NTU, C^*)$ or $P_1 = P_1(NTU, R_1)$ equations of Sekulić 2003 and Kuppan 2000 unless otherwise noted. Equations are given for solving the effectiveness ε from NTU and C^* for those flow arrangements where said equations are not excessively complicated.

Equations for solving NTU from effectiveness and C^* are given for all cases where such explicit function of $NTU = NTU(\varepsilon, C^*)$ is known. Unfortunately for many complicated flow arrangements NTU is known only as an implicit function of ε and C^* . For these cases the value of NTU must be read either from the graphs, or the equation for $\varepsilon = \varepsilon(NTU, C^*)$ must be used iteratively to find by trial and error a value of NTU that gives the correct ε with given C .

$$\varepsilon = \frac{1 - e^{-NTU(1-C^*)}}{1 - C^* e^{-NTU(1-C^*)}} \quad NTU = \frac{1}{1-C^*} \ln \frac{1-C^* \varepsilon}{1-\varepsilon}, \quad \text{if } C^* < 1$$

$$\varepsilon = \frac{NTU}{1+NTU} \quad NTU = \frac{\varepsilon}{1-\varepsilon} \quad \text{if } C^* = 1$$

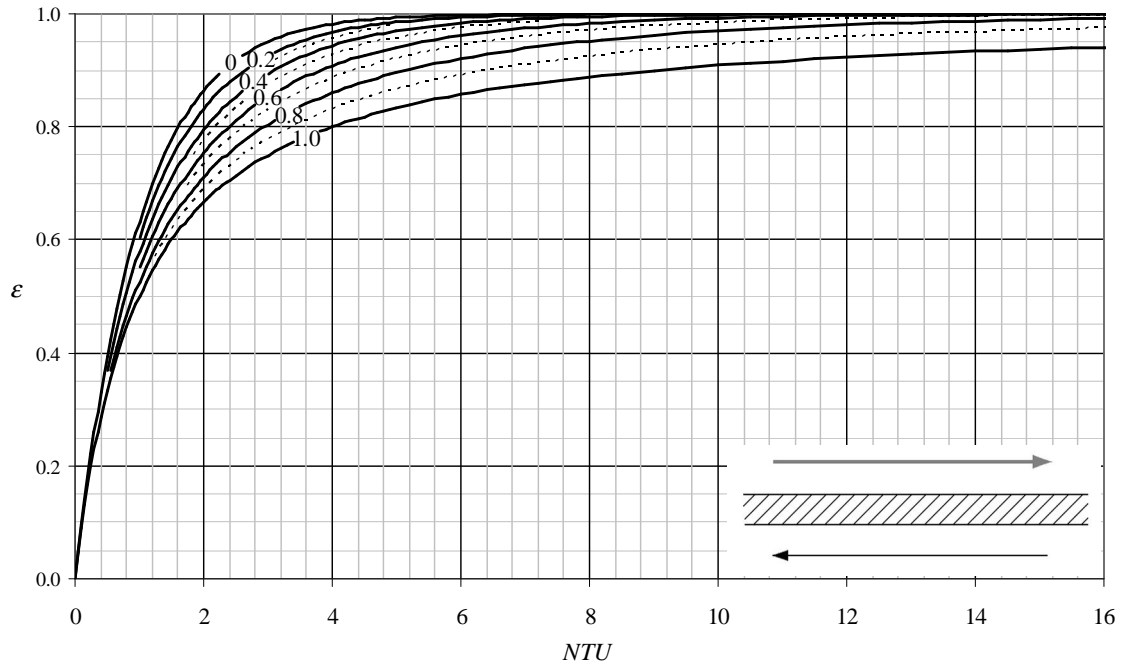


Figure 4.4. Effectiveness-NTU relationships for counterflow heat exchanger.

$$\varepsilon = \frac{1 - e^{-NTU(1+C^*)}}{1+C^*}, \quad \text{if } C^* < 1 \quad NTU = -\frac{\ln[1 - \varepsilon(1+C^*)]}{1+C^*}$$

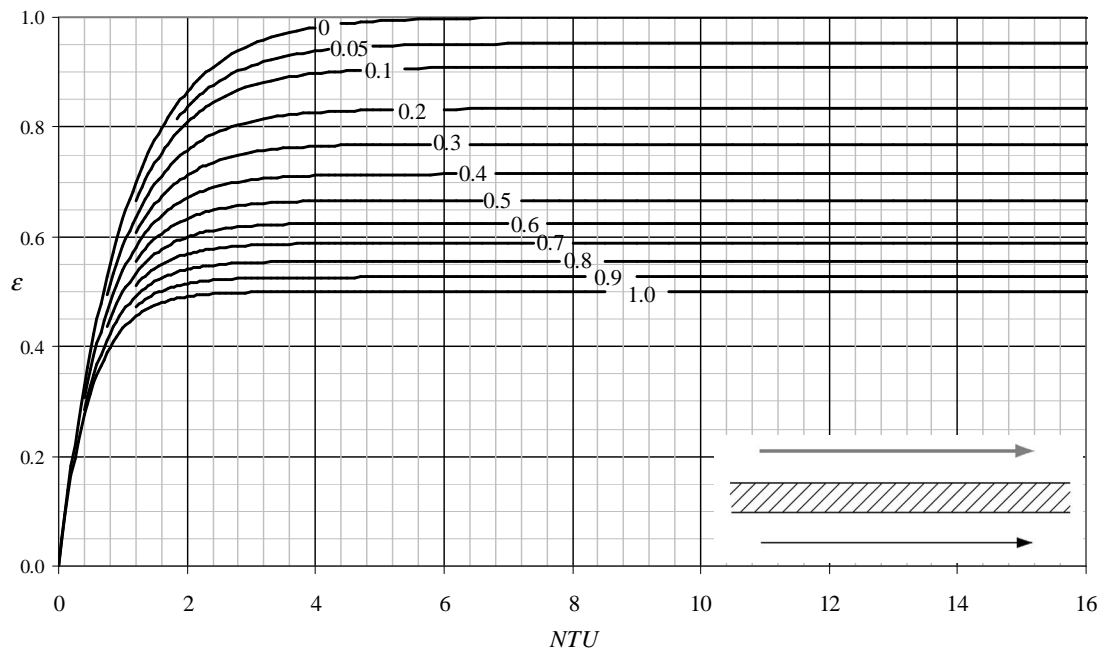


Figure 4.5. Effectiveness-NTU relationships for parallelflow heat exchanger.

$$\varepsilon = \left(\frac{1}{1 - e^{-NTU}} + \frac{C^*}{1 - e^{-C^*NTU}} - \frac{1}{NTU} \right)^{-1}$$

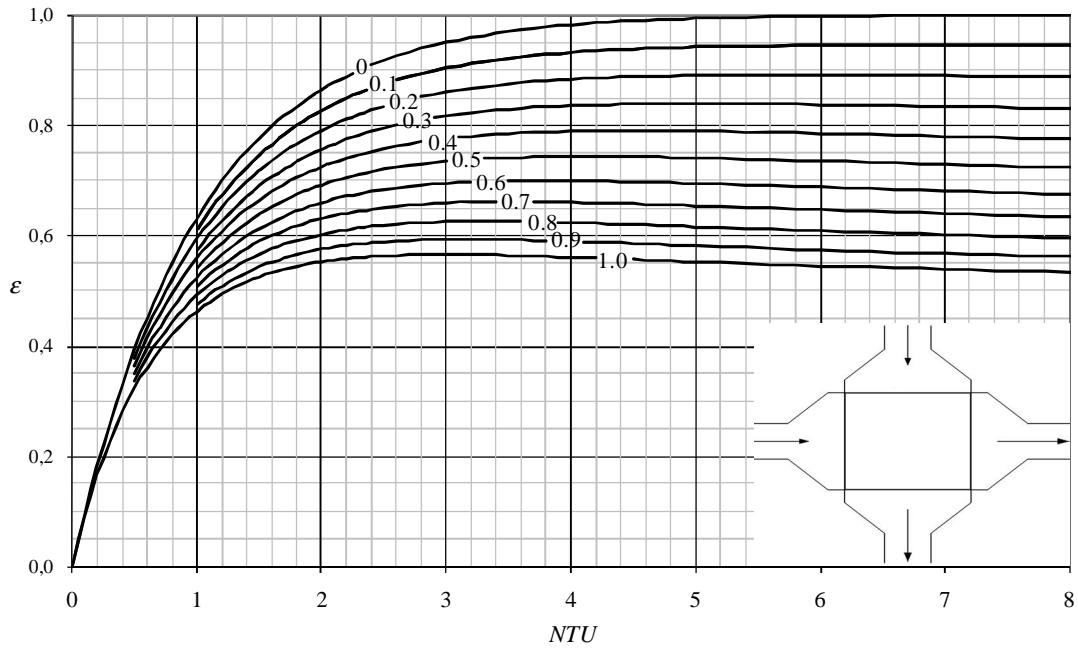


Figure 4.6. Effectiveness of crossflow heat exchanger with both fluids mixed.

$$\varepsilon = 1 - e \left(\frac{NTU^{0.22} e^{-C^*NTU^{0.78}} - 1}{C^*} \right) \text{ (Incropera 2002)}$$

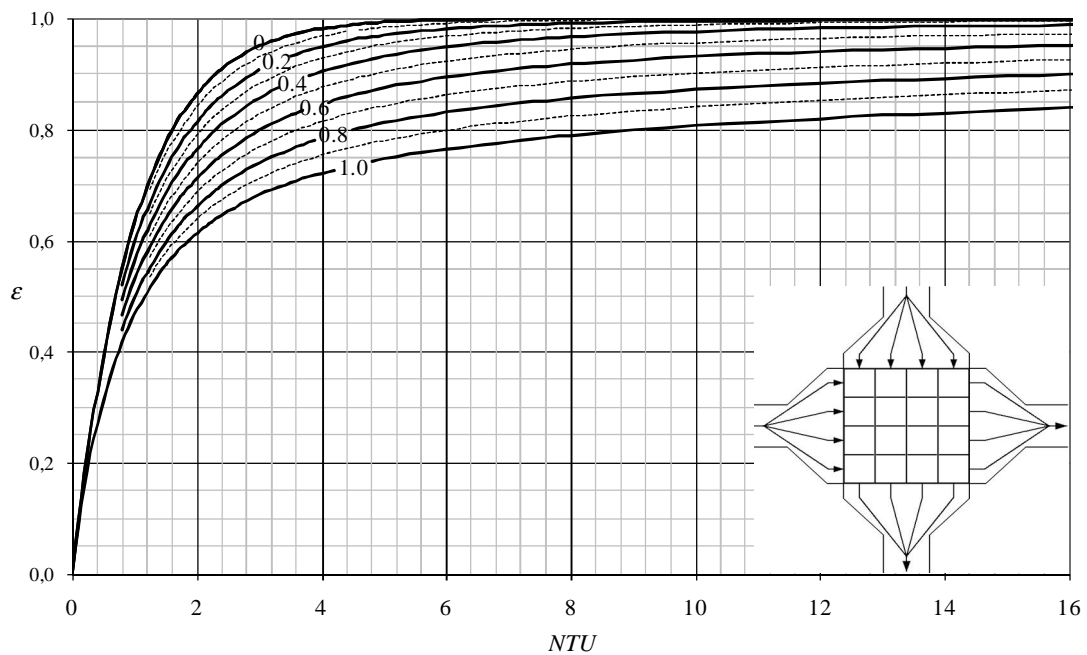


Figure 4.7. Effectiveness of crossflow heat exchanger with both fluids unmixed. Equation for ε is approximate; the considerably more complicated exact function can be found from (Kuppan, 2000).

$$\varepsilon = \frac{1}{C^*} \left\{ 1 - e^{-C^* (1 - e^{-NTU})} \right\} \qquad NTU = -\ln \left[1 + \frac{\ln(1 - C^* \varepsilon)}{C^*} \right]$$

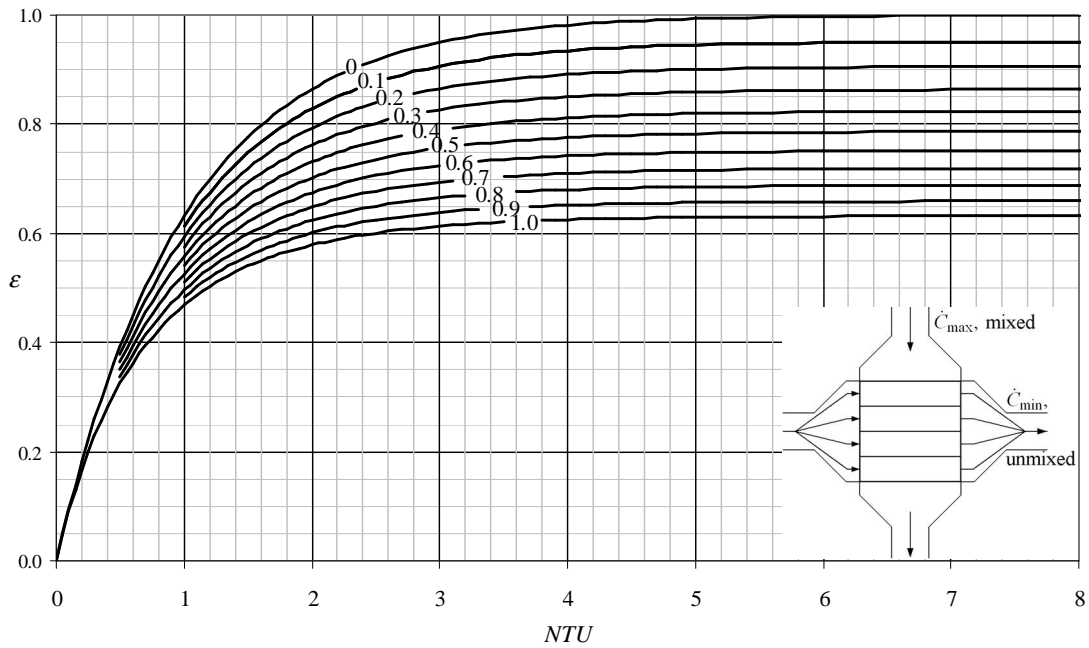


Figure 4.8. Effectiveness of crossflow heat exchanger with lower heat capacity rate stream unmixed, other stream mixed.

$$\varepsilon = 1 - e^{-\left[\frac{1 - e^{-C^* NTU}}{C^*} \right]} \qquad NTU = -\frac{1}{C^*} \ln \left[1 + C^* \ln(1 - \varepsilon) \right]$$

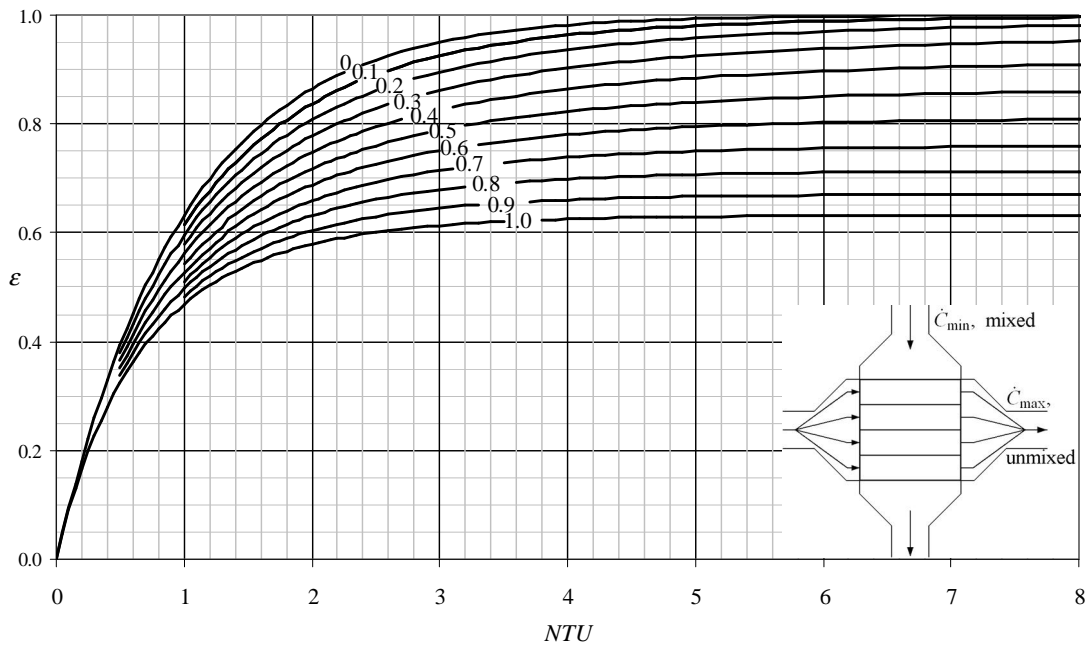


Figure 4.9. Effectiveness of crossflow heat exchanger with lower heat capacity rate stream mixed, other stream unmixed.

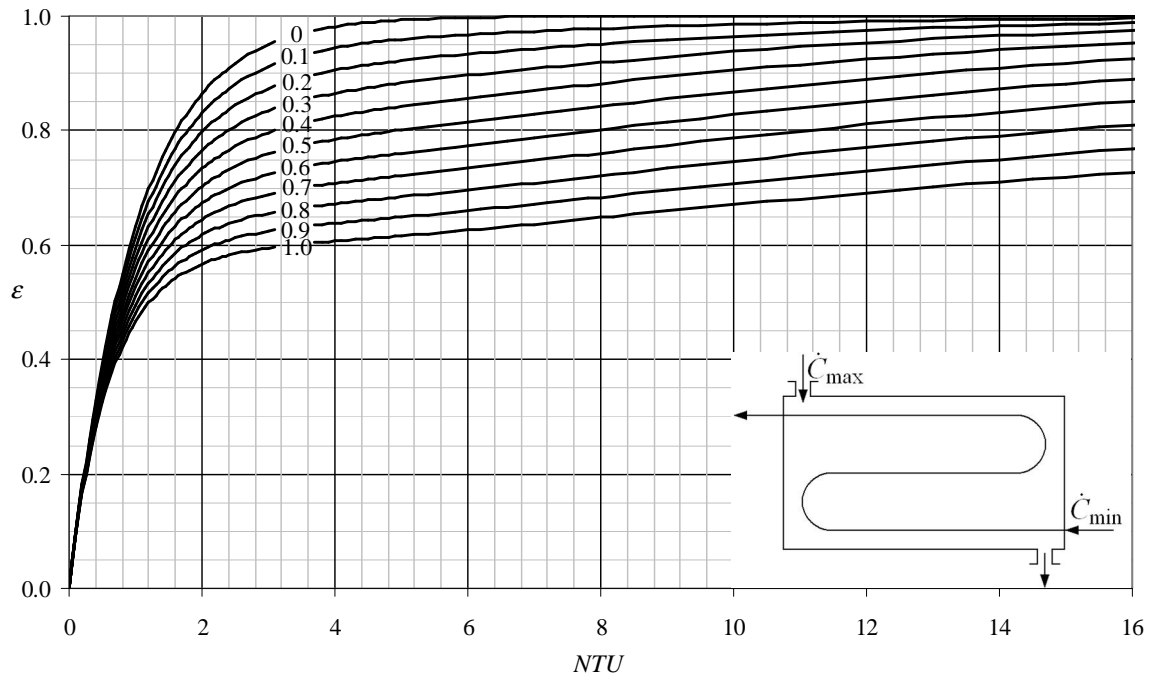


Figure 4.10. Effectiveness of an 1-3 TEMA-E shell-and-tube heat exchanger with two tube passes in counterflow, one in parallelflow arrangement, and lower heat capacity rate stream in tube side. Shell-side fluid is assumed completely mixed at any cross-section of the shell pass, and tube-side fluids become mixed between but not during each pass.

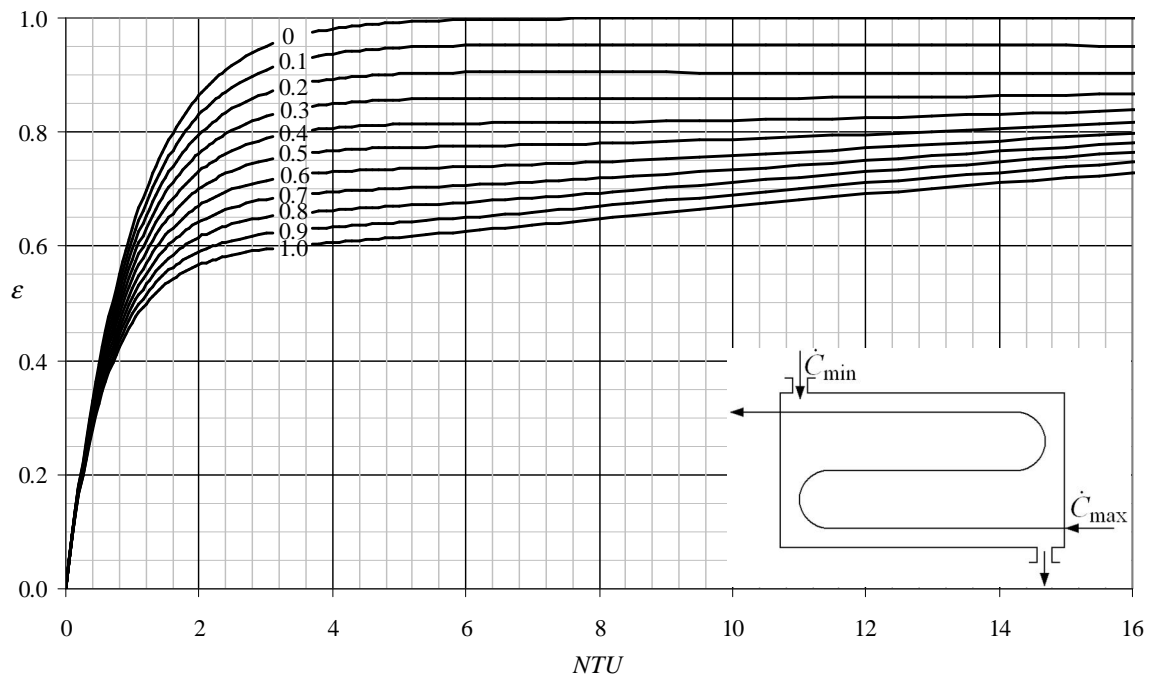


Figure 4.11. Effectiveness of an 1-3 TEMA-E shell-and-tube heat exchanger with two tube passes in counterflow, one in parallelflow arrangement, and lower heat capacity rate stream in shell side. Shell-side fluid is assumed completely mixed at any cross-section of the shell pass, and tube-side fluids become mixed between but not during each pass.

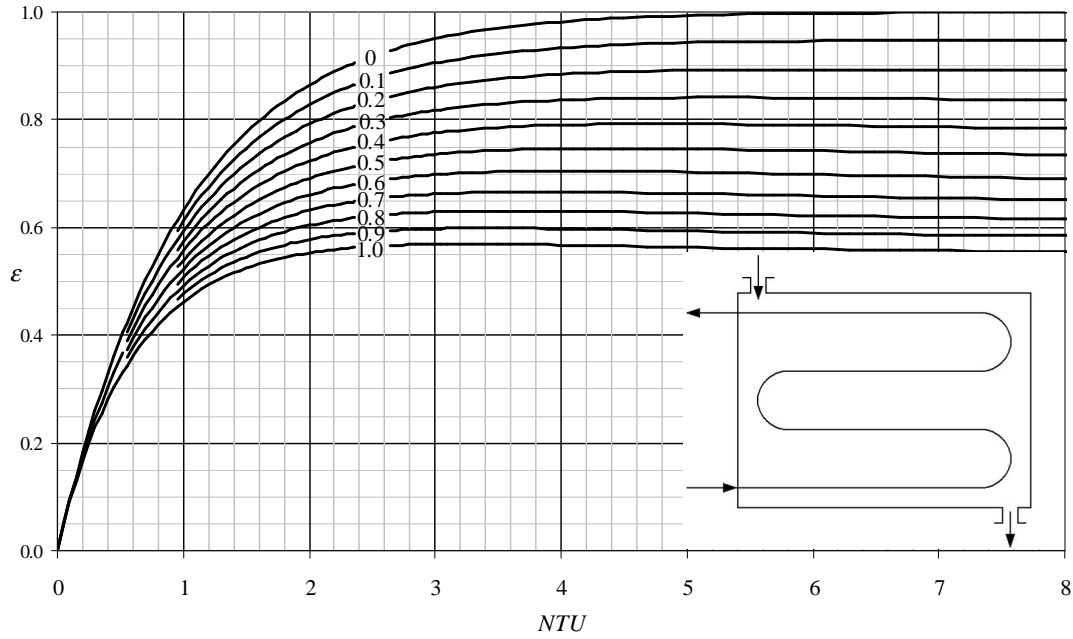


Figure 4.12. Effectiveness of a 1-4 TEMA-E shell-and-tube heat exchange. Shell-side fluid is assumed completely mixed at any cross-section of the shell pass, and tube-side fluids become mixed between but not during passes. The arrangement is not completely stream symmetric, but errors associated with assuming it to be so are negligible. The results closely approximate the case of 1 shell-side pass and an even number of tube passes that is greater than 4 (6, 8, ...).

$$\varepsilon = 2 \left[(1 + C^*) + \sqrt{1 + (C^*)^2} \coth \left(\frac{NTU \cdot \Gamma}{2} \right) \right]^{-1} \quad NTU = \frac{1}{\Gamma} \ln \left[\frac{2 - \varepsilon(1 + C^* - \Gamma)}{2 - \varepsilon(1 + C^* + \Gamma)} \right]$$

$$\Gamma = \sqrt{1 + (C^*)^2} \quad \text{in both equations}$$

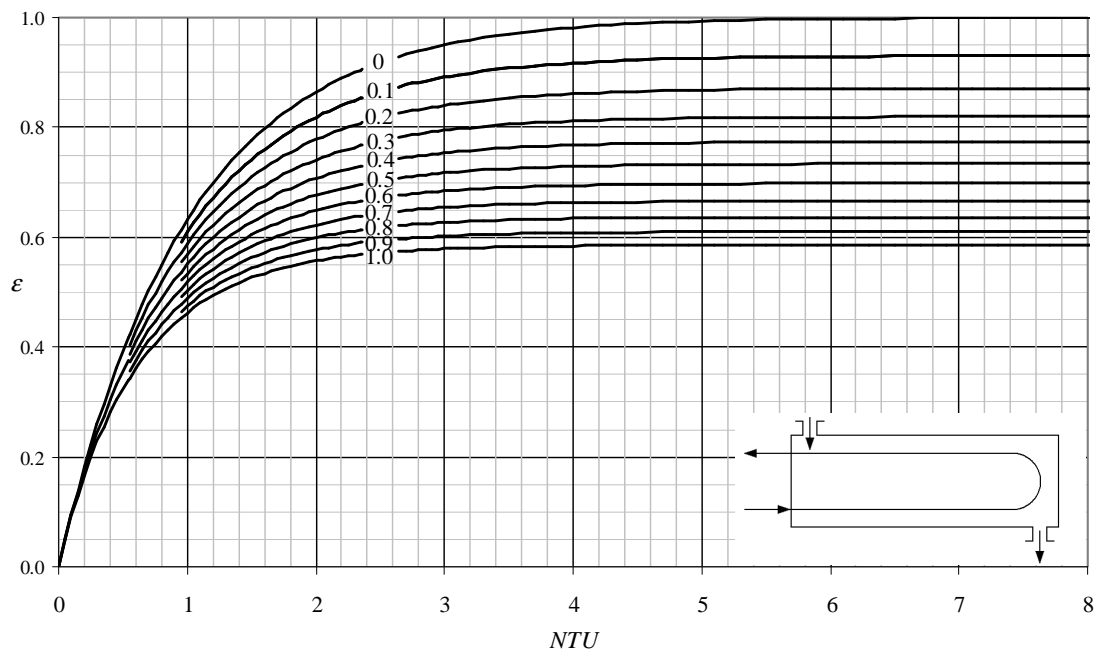


Figure 4.13. Effectiveness of a 1-2 TEMA-E shell-and-tube heat exchange. Shell-side fluid is assumed completely mixed at any cross-section of the shell pass, and tube-side fluid becomes mixed between but not during passes. The arrangement is stream symmetric.

As with the LMTD method and F factor, the case of one fluid stream having a very much larger heat capacity rate than the other (or undergoes a phase change, therefore making the heat capacity rate practically infinite for that stream) is a special case. Since the temperature change of one fluid is negligible or zero, the flow arrangement becomes irrelevant. For such case NTU and ε can be easily calculated from

$$\varepsilon = 1 - e^{-NTU} \quad (4.18)$$

and

$$NTU = -\ln(1 - \varepsilon). \quad (4.19)$$

4.3.3 Summary

Effectiveness-NTU analysis method is equally convenient for both sizing and rating problems; the basic principle is always:

- determine two of the dimensionless parameters (ε , C^* , NTU) from known data
- with the effectiveness-NTU relationships of chapter 4.3.2, determine the third dimensionless parameter from the other two, and
- from value and definitions of the third parameter, solve the problem.

The process of solving a sizing problem with the ε -NTU method is briefly summarized in Algorithm 4.3 below. This would replace step 5 in Alg. 4.1 presented earlier in the beginning of Chapter 4. As shown in Alg. 4.1, the resulting heat exchanger will then need to be checked against relevant limitations and design criteria (for example maximum allowable pressure drops of the fluids or maximum external dimensions), and if it violates any, appropriate changes need to be made to the fixed parameters and the process repeated.

Algorithm 4.3. *Solving a sizing problem with ε -NTU method.*

1. Solve C^* and ε from equations (4.13) and (4.14) or (4.15).
2. Estimate or calculate (chapters 4.1 or 5) the overall heat transfer coefficient U
3. Using ε -NTU relationships of figures 4.4 to 4.12, find NTU
4. Solve required heat transfer area A from NTU, equation (4.17).

Solving a rating problem would be similar, but one would first need to calculate U and A , and NTU from those, use the effectiveness-NTU relationships to find ε , and finally at the last step solve the heat transfer rate q and/or outlet temperatures from ε .

The following examples demonstrate the use of ε -NTU method for solving both types of problems.

EXAMPLE 4.2

PROBLEM:

The task is the same as in example 4.1: determining the number of 1.8m long elements (see Fig. E-4.1) needed to cool hot oil ($\dot{m}_h = 0.60 \text{ kg/s}$; $c_p = 2.5 \text{ kJ / kgK}$) from 90°C to 40°C temperature with $+10^\circ\text{C}$ cold water ($\dot{m}_c = 0.20 \text{ kg/s}$; $c_p = 4.2 \text{ kJ / kgK}$). The overall heat transfer coefficient of the heat exchanger is known to be approximately $200 \text{ W / m}^2\text{K}$. The tube dimensions are also the same as in E.4.1: inner tube inside and outside diameters 26.6 mm and 33.4 mm, outer tube diameters 52.5 mm and 60.3 mm, and required number of elements, when the exchanger is connected to counterflow arrangement must be solved.

SOLUTION:

As in example 4.1, the flow arrangement is counterflow regardless of number of elements. We must solve the area A , and from that then the required number of 1.8 metre elements.

Step 1. Calculate C^* and ε from equations (4.13) and (4.15):

Heat capacity rates of the fluids are

$$\begin{aligned}\dot{C}_h &= \dot{m}_h c_{p,h} = 0.60 \text{ kg/s} \cdot 2500 \text{ J / kgK} = 1500 \text{ W / K} \\ \dot{C}_c &= \dot{m}_c c_{p,c} = 0.20 \text{ kg/s} \cdot 4200 \text{ J / kgK} = 840 \text{ W / K} = \dot{C}_{\min} \\ C^* &= \frac{\dot{C}_{\min}}{\dot{C}_{\max}} = \frac{840}{1500} = 0.56\end{aligned}$$

From definition of effectiveness, equation (4.15), using the hot side for which T_o is known,

$$\varepsilon = \frac{\dot{C}_h (T_{h,u} - T_{h,o})}{\dot{C}_{\min} (T_{h,i} - T_{c,i})} = \frac{1}{C^*} \frac{(T_{h,u} - T_{h,o})}{(T_{h,i} - T_{c,i})} = \frac{1}{0.56} \frac{(90 - 40)^\circ\text{C}}{(90 - 10)^\circ\text{C}} = 0.744.$$

Step 2. $U = 200 \text{ W / m}^2\text{K}$ according to task description.

Step 3. Find NTU: arrangement is now counterflow, so we use Fig.4.4. Explicit expression of NTU is available and reasonably simple: using that that, we obtain

$$NTU = \frac{1}{1 - C^*} \ln \frac{1 - C^* \varepsilon}{1 - \varepsilon} = \frac{1}{1 - 0.56} \ln \frac{1 - 0.56 \cdot 0.744}{1 - 0.744} = 2.39.$$

Step 4. Solve required heat transfer area A from NTU, equation (4.17).

$$\begin{aligned}NTU &= \frac{UA}{\dot{C}_{\min}} \Leftrightarrow A = \frac{NTU \cdot \dot{C}_{\min}}{U} = \frac{2.39 \cdot 840 \text{ W/K}}{200 \text{ W/m}^2\text{K}} = 10.03 \text{ m}^2 \\ n &= \frac{L_{\text{total}}}{L_{\text{element}}} = \frac{A/\pi d_o}{\pi \cdot 0.0334 \text{ m} \cdot 1.8 \text{ m}} = \frac{10.03 \text{ m}^2}{\pi \cdot 0.0334 \text{ m} \cdot 1.8 \text{ m}} = 79.6 = 80.\end{aligned}$$

COMMENTS:

The result is the same as what was obtained from the LMTD calculation of E-4.1, as it should be: any other result would have indicated a mistake in one or the other solution.

EXAMPLE 4.3

PROBLEM:

A 1-2 TEMA-E shell-and-tube heat exchanger is used to heat a large mass flow rate of water from +20 °C to +60 °C with saturated steam at atmospheric pressure. Water flows on the tube side and steam condenses on the outer walls of the tubes on the shell side of the exchanger. The heat transfer surface consists of 125 steel tubes per pass, each tube being 2.00 metres long and having 25.4mm outer and 19.5mm inner diameters.

At some point water mass flow rate is reduced to only 18 t / h. Under these circumstances the heat exchanger is expected to provide an overall heat transfer coefficient of approximately 1200 W / m²K. Estimate the water outlet temperature under the changed circumstances. Specific heat of water is approximately 4200 J / kgK.

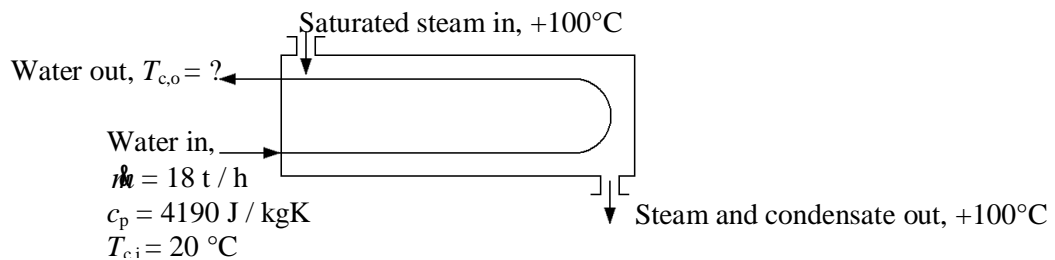


Figure E-4.2. A shell-and-tube heat exchanger with one shell-side pass and two tube-side passes.

SOLUTION:

Step 1. Calculate NTU and C^*

Since one of the fluids is condensing, its temperature does not change and heat capacity rate can therefore be considered infinite. This leads to water-side heat capacity rate being automatically the minimum one, and the heat capacity rate becomes zero:

$$\dot{C}_c = \dot{C}_{\min} = \dot{m}_c c_{p,c} = 18 \frac{t}{h} \cdot \frac{1000 \frac{kg}{t}}{3600 \frac{s}{h}} \cdot 4200 \frac{J}{kgK} = 21\,000 \text{ W / K}$$

$$C^* = \frac{\dot{C}_{\min}}{\infty} = 0$$

For NTU the area must be calculated from number and length of tubes and their outer surface area:

$$A = N_{\text{tubes per pass}} N_{\text{tube passes}} \pi d_o L_{\text{tube pass}} = 125 \cdot 2 \cdot \pi \cdot 0.0254 \text{m} \cdot 2.00 \text{m} = 39.90 \text{ m}^2,$$

and therefore for NTU

$$NTU = \frac{UA}{\dot{C}_{\min}} = \frac{1200 \frac{W}{m^2 K} \cdot 39.90 \text{m}^2}{21000 \frac{W}{K}} = 2.28$$

Step 2. Determine ε

Because $C^* = 0$, ε can be solved from equation (4.18), without Fig. 4.11 for 1-2 TEMA E:

$$\varepsilon = 1 - e^{-NTU} = 1 - e^{-2.28} = 0.8977.$$

Step 3. Determine the water outlet temperature $T_{c,o}$:

$$\varepsilon = \frac{\dot{C}_c (T_{c,o} - T_{c,i})}{\dot{C}_{\min} (T_{h,i} - T_{c,i})} = \frac{T_{c,o} - T_{c,i}}{T_{h,i} - T_{c,i}} \Leftrightarrow T_{c,o} = \varepsilon (T_{h,i} - T_{c,i}) + T_{c,i}$$

$$T_{c,o} = 0.8977(100 - 20)^\circ\text{C} + 20^\circ\text{C} = 92^\circ\text{C}$$

COMMENTS:

The above calculations were based on the assumption that the mass flow rate of steam would be sufficient to prevent complete condensation of steam and a subsequent reduction of the hot-side outlet temperature. If that were the case, the analysis would become considerably more complicated.

4.4 P-NTU -METHOD

The P -NTU method of analysis is very similar to the ε -NTU method, but has certain advantages when dealing with heat exchangers that are not stream symmetric: in other words, cases where ε -NTU yields different effectiveness at same NTU and C^* depending on which one of the streams has the lower heat capacity rate. For example mixed-unmixed crossflow (Figures 4.8 and 4.9) and 1-3 TEMA-E shell-and-tube heat exchangers (Figures 4.10 and 4.11) are examples of stream asymmetric cases.

In P -NTU method the heat exchanger effectiveness ε , defined with \dot{C}_{\min} stream in equation (14), is replaced with temperature effectiveness P , defined separately as P_1 and P_2 for streams 1 and 2 respectively,

$$P_1 = \frac{|T_{1,i} - T_{1,o}|}{|T_{1,i} - T_{2,i}|} \quad \text{and} \quad P_2 = \frac{|T_{2,i} - T_{2,o}|}{|T_{1,i} - T_{2,i}|}. \quad (4.20)$$

The heat capacity ratio C^* of ε -NTU method is similarly replaced with R defined separately for both fluids,

$$R_1 = \frac{\dot{C}_1}{\dot{C}_2} \quad \text{and} \quad R_2 = \frac{\dot{C}_2}{\dot{C}_1}, \quad (4.21)$$

and likewise NTU is defined for both streams as

$$NTU_1 = \frac{UA}{\dot{C}_1} \quad \text{and} \quad NTU_2 = \frac{UA}{\dot{C}_2} \quad (4.22)$$

With the above definitions, the expression for heat duty becomes

$$q = P_1 \dot{C}_1 |T_{1,i} - T_{2,i}| = P_2 \dot{C}_2 |T_{1,i} - T_{2,i}|. \quad (4.23)$$

The obvious advantage over ε -NTU method when dealing with stream asymmetric arrangements is that with the same heat exchanger the same P -NTU relationships remain valid with changes in fluid flow rates, or if the streams are switched. The function defining of P_1 from R_1 and NTU_1 will not change because it is always the \dot{C}_1 in the definition of NTU_1 whether or not it is the \dot{C}_{\min} , likewise R_1 remains the ratio of \dot{C}_1 to \dot{C}_2 . With ε -NTU analysis one would need to change the ε -NTU relationships if such changes would change which stream is the \dot{C}_{\min} stream.

With the above changes in the definitions of the dimensionless parameters, the P -NTU method can be used exactly in the same manner as ε -NTU method (Alg.4.3; examples 4.2 and 4.3) both in sizing and rating problems.

The P -NTU method is arguably the most commonly used analysis method particularly with shell-and-tube heat exchangers, and effectiveness-NTU relationships are readily available for a variety of flow arrangements from numerous handbooks. (Kuppan 2000), (Sekulić 2003) and VDI Heat Atlas among many others provide data for a wide variety of configurations.

Numerous other methods of heat exchanger analysis defined mostly on the basis of the same dimensionless parameters as defined for LMTD, ε -NTU and P -NTU methods also exist; for example the P_1 - P_2 method (see VDI Heat Atlas), or ψ - P method (see Shah 2003).

5 OVERALL HEAT TRANSFER COEFFICIENT

5.1 DEFINITION

Determining the correct value for the overall heat transfer coefficient U [$\text{W} / \text{m}^2\text{K}$] is a central, but often the least precise, stage in any heat exchanger design problem. From any heat transfer textbook the definition of the overall heat transfer coefficient can be found in terms of total heat transfer rate and temperature difference, as in equation (4.1).

In the case of tubular or extended-surface heat exchangers the contact area A between the fluid and the surface through which heat transfer takes place will usually be different for hot and cold fluids. As the values of temperatures and heat transfer rate q are obviously the same regardless of whether cold- or hot-side heat transfer area A is used in the above equation, it follows that U must also have different values depending on whether it is determined in terms of either hot or cold side area, so that $U_h A_h = U_c A_c$. In practice **if the areas are different on each sides of the wall, the larger area is the one used in calculating U .**

Value of U is determined from thermal circuit, using the analogy between thermal and electrical circuits. From basics of heat transfer rate it is known that if determined in terms of thermal resistance R [K / W] instead of U the heat transfer rate through any wall is

$$q = (T_h - T_c) / R_{\text{tot}}, \quad (5.1)$$

where R is the sum of surface convection resistances and the conduction resistances through the heat exchanger wall material and layers of fouling material on both sides of the surface (Fig. 5.1).

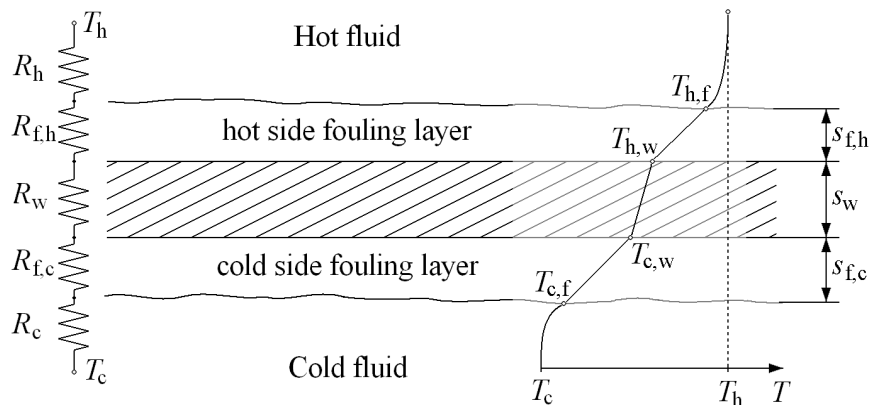


Figure 5.1. Thermal circuit for a fouled heat transfer surface.

Convection resistances R_c and R_h are calculated from the definition of convection resistance

$$R_{conv} = \frac{1}{hA}. \quad (5.2)$$

The wall conduction resistance can be calculated from

$$R_w = \frac{s_w}{k_w A} \quad (5.3)$$

for plate surfaces with same area on both sides, or, in case of a tube of length L and inner and outer diameters of d_i and d_o respectively, from

$$R_w = \frac{\ln \frac{d_o}{d_i}}{2\pi k_w L}. \quad (5.4)$$

Fouling layer resistances are in practice rarely calculated from the thickness and thermal conductivity of the fouling layers, which are rarely known precisely enough. Instead, typical values of fouling resistance per surface area R''_f [$\text{m}^2\text{K} / \text{W}$] for the type fluid and heat exchanger being considered can be looked up from handbooks, and the fouling layer resistance then obtained from

$$R_f = \frac{R''_f}{A}. \quad (5.5)$$

From the above thermal circuit analogy and equations we can now write for U

$$\frac{1}{U_h A_h} = \frac{1}{U_c A_c} = \frac{1}{h_h A_h} + \frac{R''_{f,h}}{A_h} + R_w + \frac{R''_{f,c}}{A_c} + \frac{1}{h_c A_c}, \quad (5.6)$$

and therefore the value of U can be obtained from

$$U_h = \left(\frac{1}{h_h} + R''_{f,h} + A_h R_w + \frac{A_h}{A_c} R''_{f,c} + \frac{A_h}{h_c A_c} \right)^{-1} \quad (5.7a)$$

or

$$U_c = \left(\frac{A_c}{A_h h_h} + \frac{A_c}{A_h} R''_{f,h} + A_c R_w + R''_{f,c} + \frac{1}{h_c} \right)^{-1}, \quad (5.7b)$$

depending on which of the areas is the larger one.

The assumption above is that both fluids are either liquids or non-radiating gases. If one or both of the fluids is a gas with radiating particles or gas components, the effect of radiation heat transfer between the heat transfer surface and gas must also be considered. This can be done by calculating the radiation heat transfer coefficient h_{rad} of the radiating gas, and simply using the sum of

$$h_{\text{total}} = h_{\text{convection}} + h_{\text{radiation}} \quad (5.8)$$

in place of convection heat transfer coefficient in the above equations. Instructions for finding the $h_{\text{radiation}}$ in common heat exchanger geometries can be found from for example VDI Heat Atlas.

5.2 U-VALUE OF EXTENDED-SURFACE HEAT EXCHANGERS

Particularly if one or both of the fluids is a gas, use of fins may be required in order to compensate for the low heat transfer coefficient by using larger surface area. In such a case also the fin efficiency must be considered in determining the overall heat transfer coefficient of the surface, and depending on the mechanical construction of the finned surface, also possibly a contact resistance between the fins and the plain surface. Similarly as in the simple case shown before, we start from thermal circuit description of the heat transfer surface (Fig 5.2)

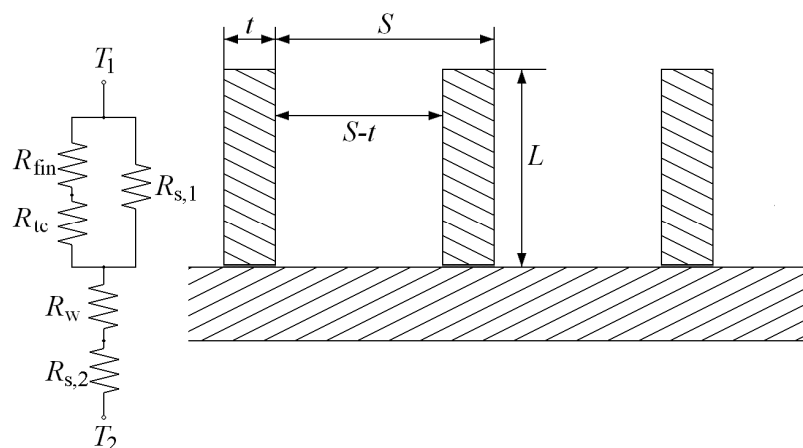


Figure 5.2. Thermal circuit for a finned surface with significant contact resistance between fins and the surface.

To find the value of U for the entire surface we must find the thermal resistance of a certain part of heat transfer area that has the length S , where S is the fin spacing. To define an exact area for calculating the thermal resistance, we can use for example a length S of a single tube in case of a circularly finned tubular heat exchanger, or area

$S \cdot B$ for a plate surface. B can be any arbitrary width, for example 1 metre for calculation convenience. Once the thermal resistance of an area (any arbitrary area will do) is known, U can then be easily solved.

In the thermal circuit of Fig 5.2 the right-side prong represents the resistance from plain surface, distance $S-t$ in the finned surface. The surface resistance R_s contains both fouling and convection resistances, which can be conveniently represented by introducing the concept of *modified convection heat transfer coefficient*, or h_m ,

$$h_m = \left(\frac{1}{h} + R''_f \right)^{-1}, \quad (5.9)$$

and according to equation (5.2) the total surface resistance becomes therefore

$$R_s = \frac{1}{h_m A_{plain}}, \quad (5.10)$$

where A_{plain} is $(S-t)B$ for a plate surface or $(S-t)2\pi d_o$ for a tubular surface.

The left-side prong represents the thermal resistance of the fin. From surface to the fluid, the first resistance is R_{tc} , which represents the thermal contact resistance between the fin and the surface, defined as

$$R_{tc} = \frac{R''_{tc}}{A_b}, \quad (5.11)$$

where R''_{tc} is the thermal contact resistance per surface area [m^2K / W] for the type of contact between the fin and surface that is used, and A_b the area of the fin base.

Second resistance is the fin resistance R_{fin} , defined as

$$R_{fin} = \frac{1}{\eta_f A_f h_m}, \quad (5.12)$$

where A_f is the external surface area of the fin, and η_f the fin efficiency. Methods for calculating the fin efficiency can be found from any heat transfer textbook. It is important to substitute the modified convection heat transfer coefficient h_m into the fin efficiency equations, however, or the result will under-predict the actual fin efficiency.

Finally, the last resistance $R_{s,f}$ is again the total surface resistance for surface area A_f , from equation (5.10) but using A_f in place of A_{plain} .

The total resistance can be obtained by reducing the thermal circuit of Fig 5.2,

$$R_{tot} = R_{s,2} + R_w + \frac{R_s(R_{tc} + R_{fin})}{R_s + R_{tc} + R_{fin}}, \quad (5.13)$$

and by marking the total surface area of $A_b + A_{plain}$ as A_{tot} , it follows from equations (4.1) and (5.1) that the overall heat transfer coefficient U defined with the finned surface area must be

$$U = \frac{1}{A_{tot} R_{tot}}. \quad (5.14)$$

If the thermal contact resistance between the fin and plain surface can be neglected, a simpler formulation of U becomes possible. Assuming fins are used on both surfaces and A_{max} being the larger of the two surface areas,

$$\begin{aligned} U &= A_{max} \left[\frac{1}{(\eta_o h A)_c} + \frac{R''_{f.c}}{(\eta_o A)_c} + R_w + \frac{R''_{f.h}}{(\eta_o A)_h} + \frac{1}{(\eta_o h A)_h} \right]^{-1}, \\ &= A_{max} \left[\frac{1}{(\eta_o h_m A)_c} + R_w + \frac{1}{(\eta_o h_m A)_h} \right]^{-1}, \end{aligned} \quad (5.15)$$

where η_o is the overall surface efficiency. η_o is defined as the relation of actual heat transfer rate from the surface to the heat transfer that would take place, if the whole surface of also the fins were at the temperature of plain surface, and can be determined on the basis of fin efficiency η_f and finned surface geometry from

$$\eta_o = 1 - \frac{N A_f}{A_t} (1 - \eta_f), \quad (5.16)$$

where N is the number of fins in any arbitrary part of the whole surface, A_f the area of a single fin, and A_t the total surface area in the same part of surface where there are N fins. In determining η_f one should use h_m , including the effect of surface fouling resistance, not the pure convection heat transfer coefficient h .

6 HEAT TRANSFER AND PRESSURE DROP CORRELATIONS

Determining the convection heat transfer coefficient h is, along with fouling estimations, the step that typically produces the greatest inaccuracies in heat exchanger analysis. This is because exact analytical solutions are available only for laminar flow situations, and in actual heat exchangers the flow is almost always turbulent. Convection heat transfer coefficient must then be solved from empirical correlations, which frequently have margins of error of 10 to 30 %, sometimes even worse.

In general terms, solving the heat transfer coefficient h can be summarized as

- 1) first determining a suitable correlation for one of two dimensionless parameters, Nusselt number Nu or the Colburn factor j_H
- 2) Solving a value for Nu or j_H
- 3) From the value found and the defining equations of Nu or j_H , solving h .

The key is to find what could be considered a “suitable correlation”: this issue is covered in chapter 6.2. Before that, chapter 6.1 briefly explains some basic concepts and terminology related to convection heat transfer (this part can be skipped by readers who are familiar with the basics of convection heat transfer), and chapters from 6.3 onwards provide a collection of correlations for a variety of flow situations.

6.1 A BRIEF INTRODUCTION ON CONVECTION HEAT TRANSFER

Convection in a heat exchanger takes places almost always by forced convection. A significant relative contribution by free convection is rare, and therefore not covered in this guide. If necessary, information on heat transfer by free convection can be found for example from VDI Heat Atlas, or Incropera 2002, chapter 9.

The differential equations governing both convection heat transfer and friction have similar forms, resulting in an **analogy of friction and heat transfer**. The theoretical backgrounds can be found in heat transfer textbooks; in this guide we limit ourselves to the practical results of this analogy. From heat exchanger analysis point of view, this analogy manifests itself in the following ways:

- 1) Similar variables and dimensionless parameters are encountered in both heat transfer and friction analysis.
- 2) If either heat transfer coefficient or friction factor is known, the analogy can be used to solve at least an approximate value for the other one as well.
- 3) A surface with a comparatively high heat transfer coefficient is bound to have also a comparatively high friction factor and thus pressure drop, and vice versa.

6.1.1 Dimensionless parameters

The following equations define a number of dimensionless parameters commonly encountered in convection heat transfer and fluid flow friction analysis. Other variables and parameters are briefly explained as they are encountered in the definitions of the dimensionless parameters.

A central parameter in all fluid flow analysis is the **Reynolds number Re** , which represents the ratio of flow inertia forces to the fluid viscous forces, and is defined as

$$Re = \frac{wL\rho}{\mu} = \frac{wL}{\nu}, \quad (6.1)$$

where w is the flow velocity [m/s], L the characteristic length [m], ρ the fluid density [kg/m³], μ the dynamic viscosity [Pa·s] and ν the kinematic viscosity [m²/s]. It is important to note that while both viscosities are relatively independent of pressure for liquids, for gases this holds only for dynamic viscosity. The kinematic viscosity ν , being defined as

$$\nu = \frac{\mu}{\rho}, \quad (6.2)$$

is obviously heavily dependent on pressure for gases. Therefore values tabulated for ν at atmospheric pressure should only be used if that is the actual pressure of the gas. The effect of density and its change and the resulting change of flow velocity in gases due to temperature change resulting from heat transfer must also be taken into account.

Reynolds number is also frequently expressed in terms of **mass velocity G** , $G = w\rho = \dot{m} / A_{ff}$, where A_{ff} is the free-flow area of flow path of the fluid. In flow geometries where the free-flow area is not constant, the area used in heat transfer and friction correlations is typically the minimum value. Using the mass velocity, equation (6.1) for the Reynolds number then becomes

$$Re = \frac{LG}{\mu}. \quad (6.1b)$$

The characteristic length L depends on geometry; for flow inside circular pipes it is the pipe inner diameter, or in non-circular channels the hydraulic diameter d_h ,

$$d_h = \frac{4A}{P}, \quad (6.4)$$

where A is the cross-sectional area of the flow channel, and P the wetted perimeter. **In various empirical correlations of Nu or j_H the characteristic length can be different, even in correlations developed for the same geometry.**

Two separate friction factors are often encountered: these are the **Fanning friction factor C_f** , sometimes also called the coefficient of friction, and the **Darcy friction factor f_D** , sometimes also called the Moody friction factor. Care must be taken in order not to confuse the two; in many textbooks the Fanning friction factor is also frequently denoted as f , which can lead to confusion. The Fanning friction factor is defined as the ratio of fluid wall shear stress τ to the dynamic pressure of the fluid flow,

$$C_f = \frac{\tau}{\frac{1}{2}\rho w^2}. \quad (6.5)$$

Darcy friction factor on the other hand is defined simply on the basis of the Darcy-Weisbach equation for friction pressure drop in a pipe flow,

$$\Delta p = \frac{\rho w^2}{2} \left(f_D \frac{L}{d} \right) \Leftrightarrow f_D = \frac{2\Delta p}{\rho w^2} \frac{d}{L}, \quad (6.6)$$

where L is the length and d the diameter of the pipe, and $\frac{1}{2}\rho w^2$ the dynamic pressure. In terms of Fanning friction factor, the Darcy friction factor is simply $4C_f$.¹

Nusselt number Nu , Stanton number St and Colburn factor j_H are central parameters in convection heat transfer analysis. The physical significance of Nu is dimensionless temperature gradient of the fluid at surface, and it is defined as

$$Nu = \frac{hL}{k_f}, \quad (6.7)$$

where L is the characteristic length and k_f the thermal conductivity of the fluid [W/mK]. Stanton number in turn is defined as a modified Nusselt number;

$$St = \frac{Nu}{Re \cdot Pr} = \frac{h}{w\rho c_p}, \quad (6.8)$$

¹ For flow in a pipe, both friction factors are typically read from a Moody's chart, which looks identical for both friction factors except for the friction factor values on the vertical axis. If the chart doesn't explicitly mention which friction factor it is for, this can be easily checked. Often the equation for friction factor for laminar flow is given: if it is $64/Re$, the chart is for Darcy, if $16/Re$, then for Fanning friction factor. If the equation is not explicitly given, then one can simply read the friction factor at $Re=10^3$: if it is 64, the chart is for Darcy, if $16/Re$, then for Fanning friction factor

and the Colburn j -factor is defined from the Stanton number as

$$j_H = StPr^{2/3} = \frac{Nu \cdot Pr^{-1/3}}{Re}. \quad (6.9)$$

Care must be taken while using the velocity w in Stanton number: different correlations may require the use of mean, maximum, or some other value for the velocity.

The **Prandtl number Pr** in equations (6.8) and (6.9) is a fluid property that represents the ratio of kinematic viscosity ν (momentum diffusivity of the fluid) to the thermal diffusivity α of the fluid. With the definitions ν and α , Prandtl number is defined as

$$Pr = \frac{\nu}{\alpha} = \frac{(\mu/\rho)}{(k_f/\rho c_p)} = \frac{\mu c_p}{k_f}. \quad (6.10)$$

In addition to the central dimensionless parameters explained above, numerous other ones are sometimes used in textbooks. Some of these are briefly listed without further explanation for reference purposes in Table 6.1 below.

Table 6.1. *Dimensionless parameters*

Parameter	Equation	Explanation
Euler number Eu	$Eu = \frac{\Delta p}{\frac{1}{2}\rho w^2}$	Pressure drop non-dimensionalized with dynamic pressure.
Graetz number Gz	$Gz = \frac{d}{x} Re Pr$	Used in entrance region calculations; x = distance from pipe entry, d = diameter of circular tube.
Peclet number Pe	$Pe = Re Pr$	Ratio of thermal energy transported to the fluid to axially conducted heat in the flow
Grashof number Gr	$Gr = \frac{g\beta\Delta TL^3}{\mu^2}$	Ratio of buoyancy to viscous forces in free convection
Rayleigh number Ra	$Ra = Gr Pr$	A modified Grashof number in free convection

6.1.2 Analogy of friction and heat transfer: practical consequences

According to Reynolds analogy, when the Prandtl number of a fluid $Pr = 1$,

$$\frac{C_f}{2} = \frac{f_D}{8} = \frac{Nu}{Re} = St, \quad (6.11)$$

which can be expanded to a range of $0.6 < Pr < 60$ with the Chilton-Colburn analogy:

$$\frac{C_f}{2} = StPr^{2/3} = \frac{Nu}{Re} Pr^{-1/3} = j_H. \quad (6.12)$$

While these analogies will yield accurate results for simple flow geometries such as flows in circular tubes or unobstructed parallel flow across a flat plate, they should not be used for more than rough estimates for more complex flow geometries.

A closer look at equations (6.11) and (6.12), and (6.5) and (6.6) reveals that both convection heat transfer coefficient (which is directly proportional to Nu , St or j_H) and friction pressure drop (directly proportional to C_f or f_D) are to some extent proportional to flow velocity. More exactly, practical experience has shown that this dependency is usually for pressure drop in turbulent flow approximately

$$\Delta p \propto w^{1.6 \dots 1.8}, \quad (6.13)$$

and for convection heat transfer coefficient in turbulent flow

$$h \propto w^{0.6 \dots 0.8}. \text{ (Sarkomaa 1994)} \quad (6.14)$$

Together from these it follows, that the proportionality of Δp and h in turbulent flow is typically approximately

$$h \propto \Delta p^{0.4}. \quad (6.15)$$

If the flow were laminar, the proportionality would be $h \sim \Delta p^{0.3}$. (Sarkomaa 1994)

6.2 SOLVING CONVECTION HEAT TRANSFER COEFFICIENT FROM EMPIRICAL CORRELATIONS

The first goal when solving the convection heat transfer coefficient is to find the correct value of Nu or j_H . Once that is done, solving h from equation (6.7) or (6.12) is simple:

$$h = Nu \frac{k_f}{L} \text{ or } h = j_H \frac{w\rho c_p}{Pr^{2/3}}. \quad (6.16)$$

Correlations for Nu and/or j_H are provided in heat transfer and heat exchanger design textbooks. In selecting a suitable correlation, the following factors must be considered:

- 1) The correlation must be for the correct surface geometry and flow direction.
- 2) Is the flow laminar or turbulent?

- 3) Does the range of validity of the correlation cover the case at hand? (check at least Reynolds and Prandtl numbers)
- 4) In the case of a flow in a tube, does the entry length make up a significant portion of the tube length?
- 5) Is the correlation for local or average heat transfer coefficient?
- 6) Are there particular characteristics such as surface roughness or highly variable fluid properties in the flow case that the correlation should take into account?
- 7) Are there different correlations for constant surface temperature T_s or constant surface heat flux q'' , and if so, which is the better approximation for the case?
- 8) At what temperature should the fluid properties be evaluated?

First point is obvious; empirical correlations for Nu and j_H for the wrong flow geometry cannot yield correct results.

Finding whether the flow is laminar or turbulent is done by calculating the Reynolds number and comparing it to the critical Reynolds number Re_{cr} of the flow geometry. If $Re < Re_{cr}$ the flow is laminar, if it is much greater than Re_{cr} , it is turbulent. For a flow in a pipe $Re_{cr} = 2300$, for parallel flow across a flat plate $Re_{cr} = 5 \cdot 10^5$.

The region where Re is only slightly greater than critical Re is problematic, as the transition to turbulence is neither an abrupt nor always predictable change: instead, turbulence begins to increase gradually as the Re increases above Re_{cr} , and this transition regime may cover a wide range of Re .

Furthermore, under favourable circumstance the flow may sometimes even remain completely laminar even if Reynolds number is noticeably above Re_{cr} . For pipe flows this unpredictable transition regime ranges from 2300 to approximately 10^4 . Results for convection heat transfer coefficient in the transition regime must be considered to have a large margin of uncertainty.

Flows in channels normally have a certain part of entry length, typically in the range of 10...60 times diameter, where the flow isn't yet fully developed, and the convection heat transfer coefficient hasn't reduced to its fully developed value. If this thermal entry length makes up a significant proportion of the total flow length, the initially higher values of h must be taken into account.

In the context of this guide, we limit ourselves to the assumption of constant values of overall heat transfer coefficient, and therefore also in solving the convection heat transfer coefficient, the goal is to find the average value \bar{h} .

Solving the average \bar{h} from a correlation for local Nusselt number correlation is relatively straightforward. If location in the flow direction is denoted with x and there is

a function that gives the local Nusselt number Nu_x as a function of some parameters, for example distance x from the beginning of the flow, Re , and Pr ,

$$Nu_x = Nu_x(x, Re, Pr), \quad (6.17)$$

then (using the definition of Nu) the local heat transfer coefficient must be

$$h_x = \frac{k_f}{L} Nu_x(x, Re, Pr). \quad (6.18)$$

Finding \bar{h} over any given range from x_1 to x_2 can then be done easily by integrating from x_1 to x_2 and dividing with distance between those points (see Fig.6.1):

$$\bar{h} = \frac{1}{x_2 - x_1} k_f \int_{x_1}^{x_2} \frac{1}{L} Nu_x(x, Re, Pr) dx \quad (6.19)$$

If characteristic length is not the distance x in flow direction, which it depending on the case and the correlation of Nu may or may not be,

$$\bar{h} = \frac{k_f}{(x_2 - x_1)L} \int_{x_1}^{x_2} Nu_x(x, Re, Pr) dx. \quad (6.20)$$

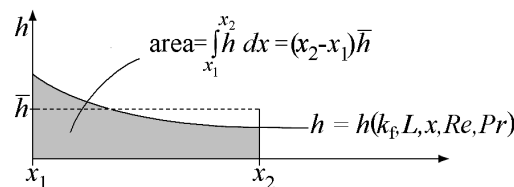


Figure 6.1. Average and local convection heat transfer coefficients

Finally, several correlations may exist for the same flow situation, some being simple but ignoring the effects of some minor effects such as surface roughness or fluid properties, some being for constant T_s approximation and some for constant surface q'' . There a judgement must be made on which is the best approximation for the case at hand, and which assumptions (such as smooth surface or constant fluid properties) are reasonable for the case.

6.3 INTERNAL FLOW IN A PIPE

The two key factors defining the behaviour of a flow in a tube are 1) whether the flow is laminar or turbulent, and 2) whether entry length constitutes a significant portion of the whole tube length. In heat exchangers the flow is almost always turbulent and the

portion of entry length is rarely significant, but also entry length and laminar flow are briefly considered at the end of the following text.

When the flow is fully developed in an internal channel, its velocity profile will be a parabola for laminar flow (assuming constant viscosity), and a somewhat blunter shape if the flow is turbulent. Typically it will take up from approximately 10 to 60 channel diameters for this profile to develop. The development of the velocity profile in the entry length is demonstrated in Figure 6.2. If the fluid is heated or cooled by the tube walls and fluid viscosity varies as a function of temperature, the actual velocity profile will be different (see Fig. 6.3.)

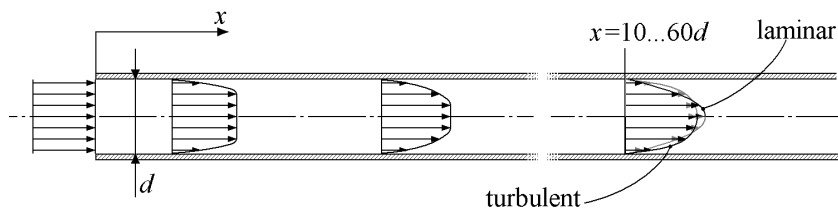


Figure 6.2. Forming of the velocity profile inside of a tube.

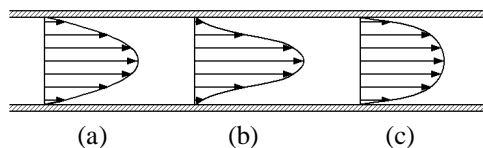


Figure 6.3. Velocity profiles in a laminar flow in a pipe: a) constant viscosity, b) cooling liquid or heating gas, c) cooling gas or heating liquid

For a turbulent flow in a tube, surface condition approximation of constant T_s or constant surface q'' has negligible effect as long as $Pr > 0.7$. This covers most but not all fluids; liquid metals in particular have much smaller Prandtl numbers.

Whether surface roughness has an effect depends not only on the absolute roughness of the tube itself, but also the flow. As can be seen in the illustration of Moody's chart in Fig. 6.4, the effect of surface roughness on friction factor becomes less at low Reynolds numbers. At low enough Reynolds number and small relative roughness the friction factor of the flow becomes almost independent of the roughness, and therefore the tube can be considered smooth.

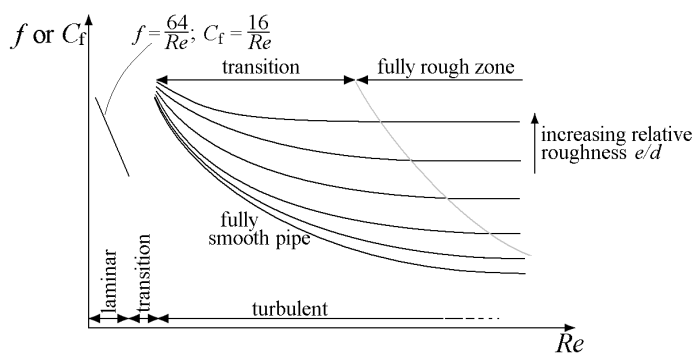


Figure 6.4. Illustration of a Moody's char; C_f is the Fanning friction factor, f the Darcy friction factor, and e the absolute surface roughness.

The characteristic length L for flows in circular tubes is the tube inner diameter d_i , both in Reynolds number and Nusselt number. Although most heat transfer correlations are for tubes of circular cross-section, these can be easily adapted to other cross-sectional shapes with little loss in accuracy by simply replacing the inner diameter d_i with the hydraulic diameter d_h , eq.(6.4).

Correlations for different cases of flow in a tube are presented in chapters 6.3.1 to 6.3.3. Typically all fluid properties in pipe flow correlations are to be evaluated at **mean bulk temperature**, or just bulk temperature,

$$T_b = \frac{1}{2}(T_i + T_o). \quad (6.21)$$

6.3.1 Fully developed turbulent flow

A simple correlation for fully developed turbulent flow in a circular tube can be obtained by simply solving Nu or j_H from the Chilton-Colburn analogy, eq.(6.12), and substituting an equation for C_f for a smooth tube as a function of Reynolds number:

$$\begin{aligned} j_H &= 0.023Re^{-0.2} \\ Nu &= 0.023Re^{0.8} Pr^{1/3}, \end{aligned} \quad (6.22)$$

where all fluid properties are to be evaluated at mean bulk temperature T_b . For a smooth tube within a range of $0.5 < Pr < 3$ and $10^4 < Re < 10^5$ the correlation is said to be accurate to within -20 ... +28 % (Shah and Sekulic 2003, pp.483).

Dittus-Boelter correlation is a slightly improved correlation for fully developed turbulent flows in smooth pipes,

$$Nu = \begin{cases} 0.024Re^{0.8} Pr^{0.4} & \text{for heating} \\ 0.026Re^{0.8} Pr^{0.3} & \text{for cooling} \end{cases} \quad (6.23)$$

Equation (6.23) is valid within $10^4 < Re < 1.2 \cdot 10^5$ and $0.7 < Pr < 120$. Within this range has errors are approximately -26...+7% for water, expanding to +10...+33 % for air ($Pr=0.7$) and -39...+21% for oils ($Pr=120$). Below $Re = 10^4$ the results are much worse. (Shah and Sekulic 2003, pp.484) It is evident that the Dittus-Boelter correlation is also suitable only for rough initial estimates but not accurate sizing calculations.

The largest errors of Dittus-Boelter correlation occur when the temperature difference between bulk temperature T_b and tube surface temperature T_s is greater than approximately 6 °C for liquids, or 60 °C for gases (Chapman pp.281). A further improved version for cases where greater temperature differences are present has been

proposed by Sieder and Tate, taking into account the effect of fluid properties varying as a function of temperature with a correction factor ϕ :

$$Nu = a Re^{0.8} Pr^{0.33} \phi, \quad (6.24)$$

where the constant a is in various sources given values ranging from 0.019 to 0.027. The function ϕ taking into account variable fluid properties also has different forms in different textbooks; according (Perry 1988, pp.894) it depends on the type of flow:

$$\phi = \begin{cases} \left(\frac{\mu}{\mu_s}\right)^{0.14} & \text{for liquids, all cases} \\ 1 & \text{for gases, cooling} \\ \left(\frac{T_b}{T_s}\right)^{0.50} & \text{for gases, heating} \end{cases} \quad (6.24b)$$

As with the Colburn and Dittus-Boelter correlations, also in Sieder-Tate correlation all properties should be evaluated at bulk temperature T_b , except those with subscript s , which are to be evaluated at the estimated average surface temperature. Equation (5.1) can be used for estimating the surface temperatures of heat exchanger tubing.

Although equation (6.24) improves the accuracy over the Dittus-Boelter correlation, errors as large as $\pm 20\%$ are still possible (Chapman 2002, pp.282). More accurate correlations also exist, but they inevitably lose the simplicity of the aforementioned three correlations which are easy to use, but also too inaccurate to be used in final sizing calculations.

A correlation by Petukhov and Popov for fully developed rough tubes gives results accurate to within $\pm 5\%$ (Shah and Sekulic 2002, pp.482):

$$Nu = \frac{\frac{C_f}{2} Re \cdot Pr}{a + 12.7 \sqrt{\frac{C_f}{2}} (Pr^{2/3} - 1)}, \quad (6.25)$$

where all properties are evaluated at bulk temperature T_b , and the parameter a is calculated from Re and Pr :

$$a = 1.07 + \frac{900}{Re} + \frac{0.63}{1 + 10Pr}. \quad (6.25b)$$

The correlation is valid within $4000 < Re < 5 \cdot 10^6$ and $0.5 < Pr < 2000$. Gnielinski has proposed a slightly simpler version accurate to within $\pm 10\%$ for otherwise similar range of parameters, but down to $Re = 3000$, and with properties evaluated at T_b :

$$Nu = \frac{\frac{C_f}{2}(Re - 1000)Pr}{1 + 12.7\sqrt{\frac{C_f}{2}}(Pr^{2/3} - 1)}. \quad (6.26)$$

Although the Gnielinski correlation is useful down to smaller Reynolds numbers than most turbulent flow correlations, it still tends to over-predict Nu at the transition regime. An improvement to transition regime can be achieved by simply taking a weighed mean value between the laminar and fully turbulent values of Nu (Shah 2003, pp.481)

$$Nu = \gamma Nu_{\text{lam}} + (\gamma - 1) Nu_{\text{turb}}, \quad (6.27)$$

$$\gamma = 1.33 - (Re/6000).$$

6.3.2 Fully developed laminar flow

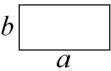
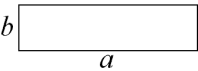
Laminar flow is rarely experienced in heat exchangers due to the very poor convection heat transfer coefficients that are an inevitable result of the flow remaining laminar.

If the flow is laminar, it can be shown that Nu has a constant value that is independent of the friction factor, Re , Pr and axial location along the pipe (provided that location is outside of the entry length into the tube). For circular tube Nu is then

$$Nu = \begin{cases} 4.36 & \text{if } q'' \text{ is constant} \\ 3.66 & \text{if } T_s \text{ is constant} \end{cases} \quad (6.28)$$

Values of Nu for some non-circular tube geometries are listed in Table 6.2 below.

Table 6.2. Nusselt numbers for fully developed laminar flow in some non-circular tube geometries (Holman 1989).

Geometry	a/b	Nu (constant T_s)	Nu (constant q'')	$C_f Re$
	1	3.09	3.00	14.2
	2	3.01	3.39	15.6
	8	2.90	5.60	20.6

	1.1	2.93	4.44	18.2
	$\frac{2}{\sqrt{3}}$	1.89	2.47	13.3

6.3.3 Entry length

In turbulent flow in a channel, particularly in circular tubes, the thermal entry length where the convection heat transfer coefficient is higher than the fully developed value is generally quite short, and can frequently be neglected without significant loss of accuracy in predicting U . In non-circular, angular tubes the entry length can be noticeably longer due to areas of laminar flow in the corner regions (Shah 2003, pp.502). The smaller the values of Re and Pr , the longer the thermal entry length will be.

Regardless of the boundary conditions (constant heat flux or constant surface temperature), the ratio of average Nusselt number up to a distance x from tube entry, Nu_{avg} , to the fully developed Nusselt number Nu_{∞} , can be calculated from

$$\frac{Nu_{avg}}{Nu_{\infty}} = 1 + \frac{Pr^{1/6} \left(0.68 + \frac{3000}{Re^{0.81}} \right)}{(x/d_h)^{0.9}} \quad (6.29)$$

The correlation is valid within $3500 < Re < 10^5$, $0.7 < Pr < 75$, and $(x/d_h) < 3$. With $Pr = 0.7$, the results agree within $\pm 12\%$ of data from experimental measurements. (Shah 2003, pp.505-6)

In laminar flow the entry length is frequently longer than in turbulent flow. Correlations for Nusselt number or Colburn factor j_H are typically expressed as a function of a dimensionless group Graetz number Gz ,

$$Gz = \frac{x}{d_h} Re \cdot Pr, \quad (6.30)$$

Where the characteristic length in Re is the hydraulic diameter d_h . For constant surface temperature Sieder and Tate have presented a correlation for local Nusselt number Nu_x ,

$$Nu_x = 1.86 \cdot Gz^{1/3} \cdot \left(\frac{\mu}{\mu_s} \right)^{0.14}, \quad (\text{Incropera 2002, pp.490}) \quad (6.31)$$

where all properties are evaluated at the mean bulk temperature T_b , except μ_s , which is evaluated at the surface temperature T_s . For cases where the Fanning friction factor C_f of the fully developed flow is known, a correlation by Bhatti and Shah exists for Nu ,

$$Nu = C(C_f Re)^{1/3} Gz^{1/3}, \text{ (Shah 2003, pp.503)} \quad (6.32)$$

where C is a constant, depending on the surface condition (constant heat flux or constant surface temperature), and whether the correlation is to provide the local value of h at distance x from entry, or the average between distance x and entry. Values for C can be read from Table 6.3 below.

Table 6.3. Values of constant C for equation (69).

	constant T_s at all locations along the tube surface	constant q' , with a constant T_s throughout perimeter at any x
For local Nu_x	0.427	0.517
For average Nu_{avg}	0.517	0.775

6.4 FLOW ACROSS TUBE BUNDLES

Flows across bundles (or banks) of tubes are frequently encountered in cross-flow and shell-and-tube heat exchangers. The tube arrangement can be either staggered or aligned, as depicted in Figure 6.5. The main parameters defining the tube bundle are tube spacing, S_L in the longitudinal and S_T in the transverse direction and the tube outside diameter d_o , and number of rows in the flow (longitudinal) direction N_L .

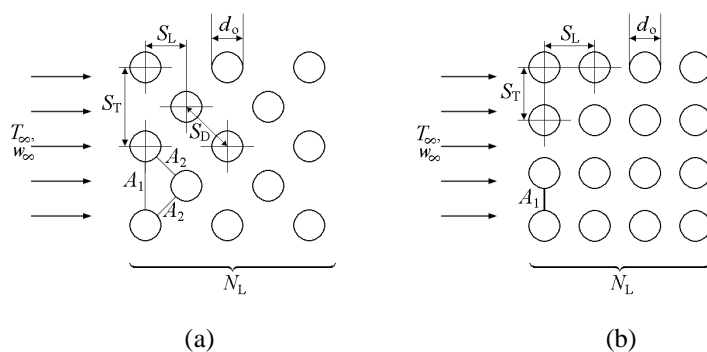


Figure 6.5. Tube bank arrangements: a) staggered, b) in-line

The flow patterns in a tube bundle are generally rather complicated, and a number of phenomena have varying levels of effect depending on the bank geometry and flow velocity.

6.4.1 Plain tubes

If there is only a **single row of tubes** in the longitudinal direction ($N_L=1$), the convection heat transfer coefficient can be predicted relatively accurately by treating the situation as a single isolated tube in cross-flow. For this case Bernstein has developed a correlation for average Nu along the tube surface,

$$Nu = 0.3 + \frac{0.62 Re^{1/2} Pr^{1/3}}{\left[1 + \left(\frac{0.4}{Pr}\right)^{2/3}\right]^{1/4}} \left[1 + \left(\frac{Re}{2.82 \cdot 10^5}\right)^{5/8}\right]^{4/5} \cdot \text{(Incropera 2002)} \quad (6.33)$$

The characteristic dimension for Re and Nu is the tube outside diameter d_o , and all properties should be evaluated at the film temperature, $T_f = 1/2(T_s + T_\infty)$. The correlation is valid throughout the range of Re and Pr , as long as the product $Re Pr > 0.2$. Errors may be up to 20%. (Incropera 2002, pp.411)

As the number of rows increases, the turbulence at the wake of each individual tube tends to increase the Nusselt number of each increasing row of tubes up to approximately fourth or fifth tube (Incropera 2002), while on the other hand parts of the tubes may be shielded from most of the flow, with the opposite effect. Depending on the geometry of the tube bank and the flow velocity, the magnitude of these effects can vary, but generally the Nusselt number is somewhat larger for tube banks than isolated tubes, except for aligned tube banks with large transverse but small longitudinal spacing.

Zhukauskas has suggested a correlation accurate to within approximately 25% (Holman 1989, pp.302), of the form

$$Nu = C_1 C_2 Re_{\max}^m Pr^{0.36} \left(\frac{Pr}{Pr_s}\right)^{0.25}, \quad (6.34)$$

where constants C_1 , C_2 and m can be read from Table 6.4 and Figure 6.6. The correlation is valid for $10 < Re_{\max} < 10^6$ and $0.7 < Pr < 500$. All properties are to be evaluated at the mean bulk temperature T_b (average of entry and exit temperatures to and from the tube bundle), except for Pr_s which is evaluated at the average temperature of the outer surfaces of the tubes T_s .

Reynolds number Re_{\max} should be evaluated with using the maximum fluid velocity w_{\max} (i.e. the fluid velocity at the smallest cross-sectional flow area between tubes in the bank). If the tubes are in an aligned arrangement it is clear this velocity will have to take place in the gap between tubes marked as A_1 in Fig. 6.5 b, where the velocity will be

$$w_{\max} = w_{A1} = w_{\infty} \frac{S_T}{S_T - d_o} \quad (6.35)$$

In a staggered arrangement the maximum velocity may also take place in the gap marked as A_2 in Fig. 6.5 a, where the velocity will be

$$w_{A2} = w_{\infty} \frac{S_T}{2 \left[\sqrt{S_L^2 + \left(\frac{S_T}{2} \right)^2} - d_o \right]} \quad (6.36)$$

Table 6.3. Values of constants C_2 and m for equation (71).

Arrangement	Re	S_T/S_L	C_2	m
Aligned	$10 \dots 10^2$	any	0.80	0.40
	$10^2 \dots 10^3$	any	Treat as a single tubes, eq.(6.33)	
	$10^3 \dots 2 \cdot 10^5$	≥ 0.7	0.27	0.63
	$10^3 \dots 2 \cdot 10^5$	< 0.7	Heat transfer inefficient, other arrangements should be used.	
	$2 \cdot 10^5 \dots 10^6$	any	0.021	0.84
Staggered	$10 \dots 10^2$	any	0.90	0.40
	$10^2 \dots 10^3$	any	Treat as a single tubes, eq.(6.33)	
	$10^3 \dots 2 \cdot 10^5$	> 2	0.40	0.60
	$10^3 \dots 2 \cdot 10^5$	< 2	$0.35 \left(\frac{S_T}{S_L} \right)^{0.2}$	0.60
	$2 \cdot 10^5 \dots 10^6$	any	0.022	0.84

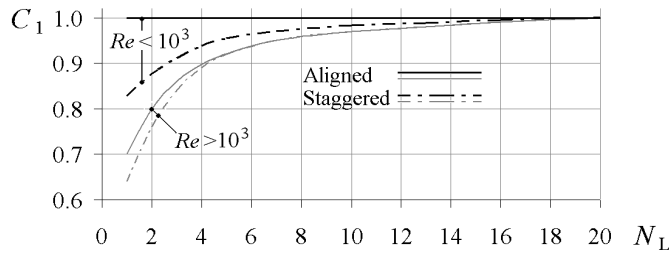


Figure 6.6. Correction factor for longitudinal tube row counts $N_L < 20$ for equation (71). Adapted from (Chapman 2002) and (Incropera 2002).

A re-formulation by Gaddis and Gnielinski and then Martin based on more recent graphical data from Zhukauskas provides slightly better accuracy of $\pm 14\%$ for staggered and $\pm 20\%$ for aligned banks, but at the cost of considerably more complicated calculations (Shah 2003, pp.512-514). Also other correlations exist, including an older, relatively simple experimental correlation by Grimson (Incropera 2002, pp.419), and the results from obtained by Gnielinski by treating the flow across a tube analogously to parallel flow across a flat plate, including laminar and turbulent parts of the flow (VDI Heat Atlas, part Gd, 1993).

6.4.2 Finned tube banks

Particularly in heat exchangers which have a gas flowing outside across tubes with a liquid as the tube-side flow it is often desirable to augment the gas-side heat transfer with additional area in the form of fins. Many different fin geometries are possible; for example (Rohsenow 1987) or (Shah 2003) provide general correlations for a variety of fin types, while (Kays 1984) has a collection of graphical data for numerous finned surfaces. Here only one of the most common types, and one for which some reasonably simple yet general correlations exist, is considered: individually finned tubes, depicted in Figure 6.7.

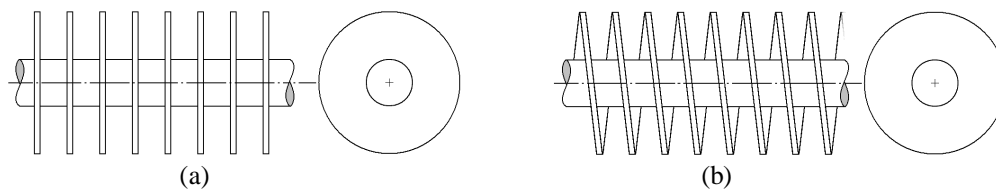


Figure 6.7. Common types of individually finned tubes: a) disc fins c) helical coil.

As flow patterns are very similar whether the fins consist of separate discs or a helical coil, same correlations can be used for both cases.

Banks of individually finned tubes are almost always in a staggered arrangement; this is due to the fact that in an in-line setting the flow resistance of the fins would force too much of flow into the bypass stream between the longitudinal rows of tubes, resulting in poor heat transfer characteristics. In a staggered arrangement the stream leaving the gap between two tubes will be headed straight towards a tube of the following vertical row, thus alleviating the problem of bypass streams to a large extent. The central geometrical variables for an individually finned tube are shown in Figure 6.8 below.

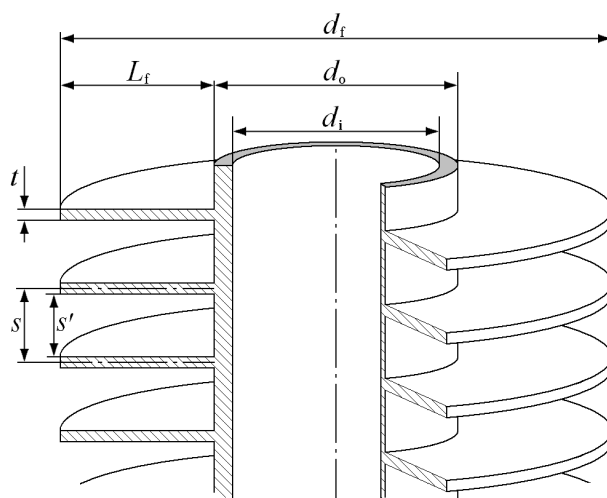


Figure 6.8. Dimensions of a tube with circular fins.

$$\text{Fin density } \gamma = \frac{1}{s} \text{ [1/m]}$$

A frequently quoted correlation by Briggs and Young exists for staggered banks of at least six rows of tubes in flow direction ($N_L \geq 6$):

$$Nu = 0.134 Re_{\max}^{0.681} Pr^{1/3} \left(\frac{s-t}{L_f} \right)^{0.20} \left(\frac{s-t}{t} \right)^{0.113} \quad (\text{Bejan 2003}). \quad (6.37)$$

In the Reynolds number Re_{\max} in equation the characteristic length L is the tube outside diameter d_o , while velocity is the maximum velocity in the smallest cross-sectional area. The correlation is made on the basis of experimental data from staggered tube banks with equilateral triangular staggered arrangement of tubes (see Fig.6.8), where $N_L \geq 6$, $11.1\text{mm} < d_o < 40.9\text{mm}$, $11.42\text{mm} < L_f < 16.57\text{mm}$, $0.33\text{mm} < t < 20.0\text{mm}$, $1.30\text{mm} < (s-t) < 4.06\text{mm}$, $25\text{mm} < S_T < 111\text{mm}$, fin density of $246 < \gamma < 768$ fins per metre, and $1100 < Re_{\max} < 1.8 \cdot 10^4$. Standard deviation within this range is 5.1% (Rohsenow 1987, pp.4-237)

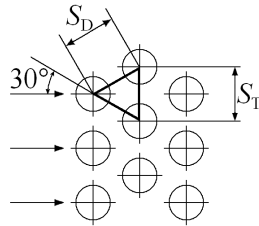


Figure 6.9. Tube bank of equilateral triangular arrangement: $S_T = S_D$.

The maximum velocity w_{\max} within the tube occurs in the smallest free-flow area, which for equilateral triangular tube pitch is the transverse gap between a row of tubes (A_1 in Fig. 6.5). The minimum free-flow area is therefore

$$A_{ff} = \left\{ N_T \left[(S_T - d_o) - (d_f - d_o) \frac{L}{s} \right] + (S_T - d_o) - (d_f - d_o) \frac{L}{s} \right\} L, \quad (6.38)$$

where L is the tube length. The maximum velocity is therefore

$$w_{\max} = \frac{\dot{m}}{A_{ff} \rho}. \quad (6.39)$$

For staggered tube banks with $S_L \leq S_T$ and high number of very low fins ($L_f / d_o \approx 0.1$), a better empirical correlation by Rabas et.al. gives the Colburn factor j_H as

$$j_H = 0.292 Re_d^{-0.415 + 0.0346 \ln \frac{d_f}{s}} \left(\frac{s}{d_o} \right)^{1.115} \left(\frac{s}{L_f} \right)^{0.257} \left(\frac{s}{t} \right)^{-0.666} \left(\frac{d_f}{d_o} \right)^{0.473} \left(\frac{d_f}{t} \right)^{0.772} \quad (6.40)$$

(Rohsenow 1985, pp.4-237).

The correlation is based on data from cases where $N_L \geq 6$, $1000 < Re < 2.5 \cdot 10^4$, $L_f < 6.35\text{mm}$, $4.76\text{mm} < d_o < 31.8\text{mm}$, $11.42\text{mm} < L_f < 16.57\text{mm}$, $0.33\text{mm} < t < 20.0\text{mm}$, $1.30\text{mm} < (s-t) < 4.06\text{mm}$, $15\text{mm} < S_T < 111\text{mm}$, $10.3\text{mm} < S_L < 111\text{mm}$, fin density

of $246 < \gamma < 1181$ fins per metre, and $1100 < Re_{\max} < 18000$. For 94% of the experiments by Rabas et.al., the predictions of equation (6.40) are within $\pm 15\%$ of measured data.

6.4.3 Shell-side flow in a shell-and-tube exchanger

The shell-side flow pattern of a baffled shell-and-tube heat exchanger is complicated, characterized by a multitude of leakage paths in addition to the main flow path, which in itself is not a straightforward simple case but involves parts where the flow direction is mainly axial, perpendicular, and oblique relative to the tubes. The main flow paths are depicted in the diagram of Figure 6.8 below.

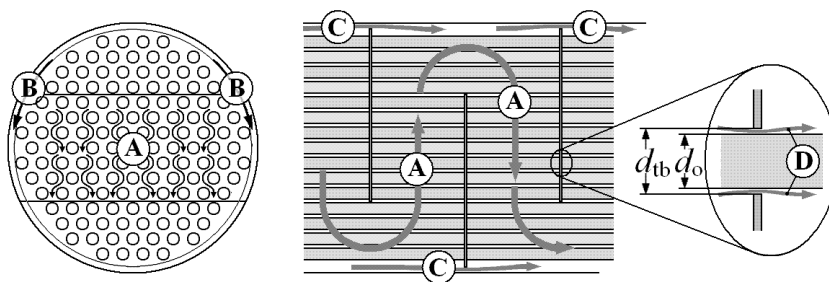


Figure 6.10. Main flow paths of shell-side flow in a baffled shell-and-tube heat exchanger: main flow (A), leakage past between the outer tubes and shell (B), leakage between baffle plates and shell (C), tube-to-baffle clearance hole leakage (D).

While the main stream A is always the largest of the streams, the sum of all leakage streams represents a significant fraction of the whole stream, typically at least 35% but in some cases up to 70% (Shah 2003, pp.295). Particularly the shell-to-baffle leakage (stream C in Fig.6.10) and bundle-to-shell leakage (stream B) are detrimental to the performance, as they tend to remove the shell-side flow from proper contact with the tube-side flow.

It is evident from the complexity of the flow that developing a single all-encompassing correlation that would cover all possible shell-side geometries would be challenging to say the least. There are two publicly available methods for analyzing the flow behaviour in shell side of a shell-and-tube heat exchanger: the Bell and Kern methods. Kern method is simpler, but limited in applicability and accuracy, whereas the Bell method covers practically all segmented-baffle shell-and-tube geometries possible, taking into account a wider range of parameters.

The Bell method is based on determining first the dimensionless parameter for convection heat transfer (either Nu or j_H , depending on the formulation) for the centre row of tubes at the middle of the shell, and applying a variety of correction factors to account for the leakages, baffle dimensions, and various clearances in the design. Due to the method's relative complexity it is omitted here; the equations for calculating the correction factors are presented for example in (VDI Heat Atlas 1993), (Shah and

Sekulic 2003) and (Bell 1983), while a somewhat easier-to-use but less precise and more restricted graphical presentation can be found in for example (Rohsenow 1987) and (Perry 1988).

Within this text, the simpler Kern method is presented. The main variables determining the geometry are presented in Figure 6.11.

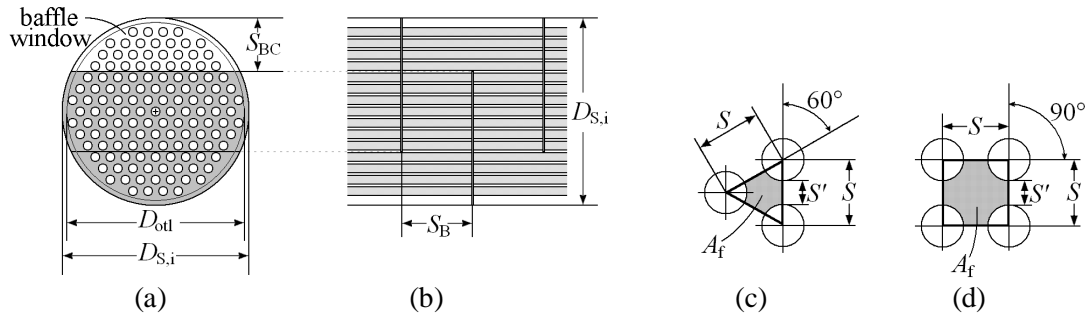


Figure 6.11. Geometrical parameters defining the shell side of a segmentally baffled shell-and-tube heat exchanger.

Kern in (Kern 1950) presented a graphical correlation for j_H made on the basis of industrial data that ranging from Reynolds number $Re = 10$ to $Re = 10^6$, and a wide variety of shell-side fluids. Within $2000 < Re < 10^6$ a relatively simple equation of Nu represented the same data well.

The data used was from exchangers built according to baffle-to-shell and baffle-to-tube clearances as defined in TEMA Standards of 1949, with a baffle cut BC ,

$$BC = \frac{S_{BC}}{D_{S,i}},$$

of 25%, and ratio of baffle spacing to shell inside diameter of $0.20 < S_B / D_{S,i} < 1.00$.

A curve was drawn as a “safe” curve along the lowest data points, and would thus frequently under-predict but hopefully never over-predict the j_H . The definition of Reynolds number used was

$$Re = \frac{D_e G}{\mu}, \quad (6.42)$$

where D_e is an equivalent diameter, defined as

$$D_e = \frac{4A_f}{P}. \quad (6.43)$$

Although the so-called equivalent diameter is defined very similarly to the previously encountered hydraulic diameter, it is in fact not quite the same. The hydraulic diameter as defined by eq.(6.4) would in fact change constantly as the flow direction, free-flow area and wetted perimeter all change constantly throughout the fluid's path through the exchanger. The A_f is defined as free area between the tubes (again not to be confused with the free-flow area A_{ff} which it is not), shown as shaded gray in Fig.6.11 c) and d), and the wetted perimeter P is the total tube perimeter bordering on the free area A_f .

The free area A_f for square and triangular tube arrangements is therefore obtained from

$$A_{f,s} = S^2 - \frac{\pi d_o^2}{4} \quad (6.44a)$$

and

$$A_{f,t} = \frac{1}{2} \cdot S^2 \cos 30^\circ - \frac{1}{2} \cdot \frac{\pi d_o^2}{4} \quad (6.44b)$$

It is evident from geometry that for 90° square pitch the wetted perimeter is the tube outside perimeter πd_o , and for equilateral triangular pitch half tube perimeter, $\frac{1}{2}\pi d_o$.

The mass velocity G also requires further explanation, as again both free-flow area and velocity change constantly throughout the flow path. For the correlations presented by Kern, the mass velocity was defined according to the free-flow area at the centre of the shell:

$$G = \frac{\dot{m}}{A_{ff}} = \frac{\dot{m}}{D_{S,i} S_B \frac{S'}{S}} = \frac{\dot{m} S}{D_{S,i} S_B (S - d_o)}. \quad (6.45)$$

The dimensions are defined in Fig. 6.9. With the aforementioned definitions and test data, the following correlation was developed for Nusselt number:

$$Nu = 0.36 Re^{0.55} Pr^{1/3} \left(\frac{\mu}{\mu_s} \right)^{0.14} \quad (\text{Kern 1950, pp.137}), \quad (6.46)$$

where all properties should be evaluated at the mean bulk temperature $T_b = \frac{1}{2}(T_i + T_o)$, except for μ_s , which should be evaluated at the estimated average temperature at the tube outer surface T_s .

It is evident that the correlation takes in no way into account the relative magnitudes of the leakage streams (Fig.6.10) or obliquity of the main stream across the tube bank. The correlation is useful for an initial estimate, but for final sizing calculations the more

accurate Bell method should be used. The correlation presented by Bell is also not limited to a baffle cut of 25%, which while common, is by no means exclusively used.

Other reasonably simple-to-use correlations also exist; see for example (Sarkomaa 1994, pp.24), or (McCabe et.al. 2005, pp.450). Note that although the geometry is the same, the definition of Re is different in different correlations for shell-side flow in a shell-and-tube heat exchanger.

6.5 PLATE HEAT EXCHANGER SURFACES

6.5.1 Gasketed plate heat exchangers

Gasketed plate heat exchanger design is typically almost always done not by designing and manufacturing the surface from scratch, but obtaining the plates from a manufacturer. The designer is then free to choose the number of plates and flow arrangement, as depicted for example in Fig.3.14 earlier.

The plate manufacturer typically provides computer software with experimental heat transfer and pressure drop data built in as a “black box”, and for accurate results these software packages should be used for design of plate heat exchangers.

For very rough estimates, a correlation of the type

$$j_H = CRe^{-m} \left(\frac{\mu}{\mu_s} \right)^{0.14} \quad (6.46)$$

may be used; m can range from approximately 0.17...0.62, while C ranges from 0.03...2.0, typical values being approximately $C = 0.5...0.8$ and $m \approx 0.6$ according to (Rohsenow 1987, pp. 4-111) and (Sarkomaa 1994, pp. 26). Reynolds number in the above equation is defined in terms of average velocity in the passage between gaps, and the characteristic length is the equivalent diameter $D_e = 2\delta$.

A more accurate but considerably more complicated method of estimating convection heat transfer coefficient of chevron plates with angle of corrugations between 10 and 80 degrees was recently developed by Martin et.al; however, there too errors in Nusselt number can be up to 30%, and in fact several times larger for pressure drop. It is therefore clear that accurate data from manufacturer is essential for design of typical plate heat exchangers. (Shah 2003, pp.514)

As a general rule, plate-type heat exchangers come with lower total lifetime costs than equivalent shell-and-tube heat exchangers if the pressure, temperature and chemical composition of both fluids are compatible with the gasket material and the thin plates; unfortunately this is often not the case, hence the widespread use of shell-and-tube exchangers.

6.5.2 Spiral heat exchangers

The flow geometry in a spiral heat exchanger is very simple, and considering the passage simply a straight rectangular tube with characteristic length in Nu and Re being the hydraulic diameter gives useful results for an initial estimate. For more accurate sizing calculations, the following correlation is recommended (Rohsenow 1987, pp.4-109) for $Re > 100$:

$$Nu = Pr^{0.25} \left(\frac{\mu}{\mu_s} \right)^{0.17} \left[0.0315 Re^{0.8} - 6.5 \cdot 10^{-7} \cdot \left(\frac{L}{\delta} \right)^{1.8} \right], \quad (6.47)$$

where L is the total length of the spiral plate, and d the flow channel width (i.e. the spacing between consecutive rounds of the spiral plate). The velocity is the average flow velocity in the channel, all properties should be evaluated at mean bulk temperature $T_b = \frac{1}{2}(T_i + T_o)$, and the characteristic length is the channel hydraulic diameter d_h .

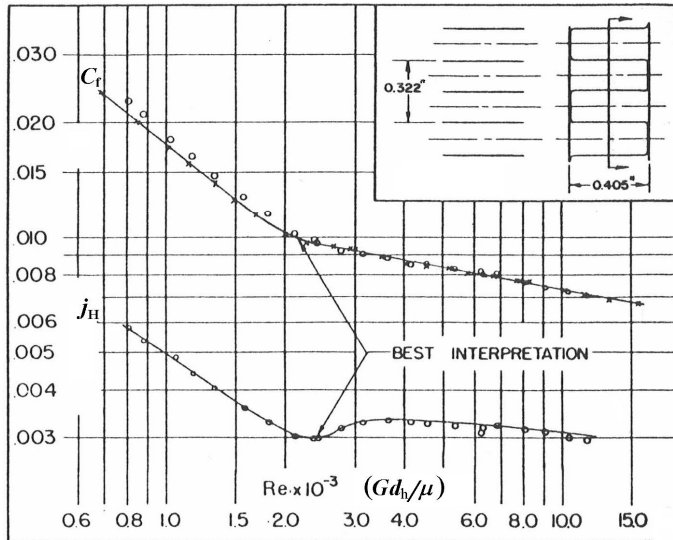
6.6 COMPACT HEAT EXCHANGER SURFACES

Compact heat exchangers may have a large number of different surface configurations, including plate-fin and tubular, and in the latter case frequently also having non-circular tubes. Rather than attempting to model the flows using the correlations of the previous chapters, it is advisable to use empirical heat transfer and friction data available from *Compact Heat Exchangers* by Kays and London, which lists data for almost one hundred different types of heat transfer surfaces in terms of Fanning friction factor C_f and Colburn factor j_H . One such example, of a plate-fin surface similar to the one shown in Fig. 3.17 a) earlier, is shown in Figure 6.12.

In Fig.6.12 the mass velocity G in Reynolds number defined in terms of minimum free-flow area A_{ff} , and all properties should be evaluated at the mean bulk temperature. Parameter β gives the compactness of the surface; in the example, a rather modest 670 square metres of heat transfer area cubic metre. Such plate-fin surfaces are usually assembled by brazing the fin plates between the plates separating the fluids, resulting in very low contact thermal resistance R''_{tc} at the fin base.

Neglecting the contact resistance, the last parameter of Fin area / total area allows convenient use of equations (5.16) to obtain the overall finned surface efficiency for determining U from equation (5.15) without the need for geometrical calculations to determine the ratio of $N \cdot A_f$ to total heat transfer area.

Plain plate-fin surface 6.2.



Fin pitch = 6.2 per in = 244.1 per m
 Plate spacing, $b = 0.405$ in = 10.29×10^{-3} m
 Flow passage hydraulic diameter, $d_h = 0.0182$ ft = 5.54×10^{-3} m
 Fin metal thickness = 0.010 in, aluminum = 0.254×10^{-3} m
 Total transfer area/volume between plates, $\beta = 204$ ft²/ft³ = 669.3 m²/m³
 Fin area/total area = 0.728

Figure 6.12. Example of empirical heat transfer and friction data for a plate-fin surface (Kays and London, 1984).

7 PRESSURE DROP

Fluid must usually be pumped through the heat exchanger, and the pumping power can contribute a significant fraction of the total lifecycle costs of a heat exchanger. The pumping power P [W] is directly proportional to the pressure drop Δp [Pa] through the heat exchanger,

$$P = \Delta p \frac{q_m}{\rho \eta_p}, \quad (7.1)$$

where ρ is the fluid density and η_p the efficiency of the pump or fan. Pressure drop increases as fluid flow velocity through the heat exchanger is increased, as does the convection heat transfer coefficient; a good design is therefore always a compromise of sufficiently heat transfer characteristics with acceptable pressure drop.

If a maximum allowable pressure drop is defined by for example customer, **achieving the smallest possible heat transfer area (i.e. cheapest possible heat exchanger of the selected type) means maximizing pressure drop within the allowed limits.** If no maximum pressure drop is defined, the optimum design is that which minimizes the life cycle cost consisting of 1) investment and cleaning costs roughly proportional to the heat transfer area, and 2) fluid pumping cost roughly proportional to the pressure drop.

The proportionalities of fluid velocity w to both convection heat transfer coefficient h and the pressure drop Δp were presented earlier in equations (6.13), (6.14) and (6.15) in chapter 6.1. From these it follows that the proportionality of pressure drop to heat transfer coefficient h in a turbulent flow is usually approximately

$$\Delta p \propto h^{2.5}. \quad (7.2)$$

The causes of pressure drop can be roughly divided into two by their location: the pressure drop in the core of the heat exchanger (the part of heat exchanger where flow is in contact with the heat transfer surface), and pressure drops caused by the devices needed to distribute the flow into the core, and collect it when it exits from it: the inlet and outlet headers, manifolds, ducting, etc.

Ideally the pressure drop in parts other than the core should be very small compared to the core pressure drop: this allows maximum usage of allowable pressure drop to be used to enhance heat transfer and thus reduce the heat transfer area. Particularly in plate-type heat exchangers this may be difficult to achieve in practice, however.

The causes of pressure drops can be divided in four:

1. pressure drop caused by flow entry to the core: acceleration and irreversibilities of sudden flow channel contraction
2. friction (including form drag) on the heat transfer surface
3. momentum effects due to change of density and therefore velocity in the core due to change of temperature and sometimes also pressure
4. pressure drop caused by flow exit from the core: deceleration and irreversibilities of sudden flow channel expansion

Additionally if the fluid is a liquid, also height difference between fluid entry and exit ports will contribute significantly to the total pressure difference over the heat exchanger. As this is a function of not only the heat exchanger but how it is installed on the site, the following approach considers only the pressure drops caused by the listed four items. Chapter 7.1 will explain how to calculate the individual pressure drop components and presents the final equation for total pressure drop, while chapter 7.2 will provide information on determining the parameters specific to the heat exchanger and heat transfer surface type, particularly the friction factor.

7.1 PRESSURE DROP CALCULATION – GENERAL PRINCIPLE

Pressure changes take place in 1) entrance to the heat exchanger core (between 1 and 2 in Fig.7.1), where the flow area is contracted from core frontal area A_e to the free-flow area in the core A_{ff} , 2) in the core due to form drag, skin friction and fluid density change (between 2 and 3 in Fig.7.1), and 3) the sudden expansion on exit from the core (between 3 and 4 in Fig.7.1).

The ratio of free-flow area (minimum free-flow area if it varies inside the core) A_{ff} to core frontal area A_e (usually $A_e = A_o$) is denoted as σ .

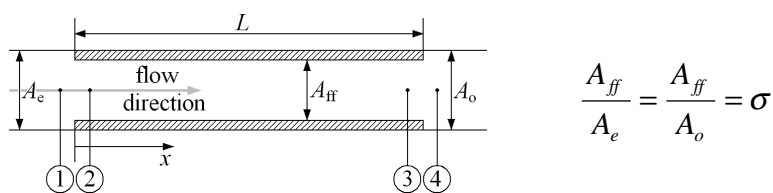


Figure 7.1. Locations and dimensions used in the following pressure drop analysis.

The individual elements of pressure drop are first explained in chapters 7.1.1 to 7.1.3, and on the basis of these, a generic equation for total pressure drop is presented in chapter 7.1.4.

7.1.1 Core entrance pressure drop

Pressure change at core entrance (1 in Fig.7.1) has two components: the (reversible) pressure drop caused by flow acceleration due to reduction of flow area, and the irreversibilities caused by the entrance. Assuming negligible effects of fluid density

change, friction, and gravitational potential energy on the entrance, and a flow velocity much less than speed of sound, the Bernoulli equation for incompressible flow dictates the pressure drop on entrance as a result of flow acceleration as

$$\Delta p_{e,acc} = \frac{\rho w_2^2}{2} \left[1 - \left(\frac{w_1}{w_2} \right)^2 \right] = \frac{\rho w_2^2}{2} (1 - \sigma^2), \quad (7.3)$$

where σ is the ratio of (minimum) free-flow area to the core frontal area (see Fig.7.1), and subscripts 1 and 2 refer to the states on entrance just before the core, and just inside the core, respectively (Fig.7.1).

The irreversible pressure drop component is a result of a number of phenomena present in sudden flow contractions, and can be taken into account with a single loss coefficient K_c . Loss coefficients for a variety of entrance configurations can be found from a number of handbooks, including VDI Heat Atlas, *Compact Heat Exchanger* by Kays and London, and many others. When the loss coefficient K_c is defined relative to the core velocity after the contraction w_2 (which it usually is in most, but not necessarily all handbooks), irreversible pressure drop on entrance is defined as

$$\Delta p_{e,irr} = \frac{\rho w_2^2}{2} K_e, \quad (7.4)$$

resulting in a total entrance pressure drop Δp_e of

$$\Delta p_e = \frac{\rho_2 w_2^2}{2} (1 - \sigma^2 + K_e) = \frac{G^2}{2\rho_2} (1 - \sigma^2 + K_e), \quad (7.5)$$

where G is the flow mass velocity, defined as

$$G = \frac{\dot{m}}{A_{ff}} = \rho_2 w_2 = \rho_n w_n. \quad (7.6)$$

Unless the pressure drop on entrance is very high (which is usually unacceptable in a heat exchanger design), $\rho_1 = \rho_2$ can usually be assumed even if the fluid is a gas.

7.1.2 Core pressure drop

Pressure drop within the core consists of two components: 1) the pressure drop due to skin friction and form drag, and 2) the pressure drop due to momentum change, which in turn is a result of the fluid density change.

The friction pressure drop from friction and form drag is defined relative to the average core velocity in the minimum free-flow area A_{ff} as

$$\Delta p_{core} = \frac{\rho w_m^2}{2} \left(f_D \frac{L}{d_h} + \sum K \right) = \frac{G^2}{2\rho_m} \left(C_f \frac{4L}{d_h} + \sum K \right), \quad (7.7)$$

where f_D is the Darcy (Moody) friction factor (equation 6.6), C_f the Fanning friction factor (eq.6.5), L the flow channel length, d_h the channel hydraulic diameter (eq.6.4; $d_h = d_i$ for a circular tube), and $\sum K$ the sum of loss coefficients K . Subscript m refers to the mean values within the heat exchanger core.

For flows in tubes the friction factor can be read from a Moody's chart (depicted earlier in Fig.6.4. and available from numerous handbooks). Care must be taken to ensure which friction factor the chart is made for; Moody's charts exist for both Fanning and Darcy friction factors, and both friction factors are frequently denoted with f in literature.

In case of more complex heat transfer surface geometries, equations or graphs for the type of surface at hand should be used; some are presented later in chapter 7.2. These are typically based on experimental data. Experimental friction factor correlations often include the effects of loss coefficients caused by surface features, in which case the $\sum K$ of Δp_{core} is zero.

It is also important to realize that **experimental friction factors can only be used with that equation of Δp and definition of Re for and with which the correlation is made.** For a single heat transfer surface geometry there sometimes exist different correlations of friction factor based on different definitions of characteristic length and velocity in Reynolds number or different definition of density and/or velocity in the dynamic pressure than in eq. (7.7) above.

The change of fluid density in the heat exchanger is negligibly small if the fluid is a liquid, but in gas flows the density change resulting from temperature change is usually too large to be neglected. The change of density causes a change in flow velocity and therefore momentum rate, with a resulting pressure change Δp_{mom} of

$$\Delta p_{mom} = \frac{q_m(w_3 - w_2)}{A_{ff}} = \frac{G^2}{\rho_2} \left(\frac{\rho_2}{\rho_3} - 1 \right), \quad (7.8)$$

where subscripts 2 and 3 refer to the entrance and exit from the heat exchanger core, as defined in Fig.7.1.

7.1.3 Core exit pressure drop

Pressure effects on exit of incompressible fluid flow from the core include two factors; a **pressure increase** due to the **deceleration** of flow velocity as the flow area increases $\Delta p_{o,dec}$, and a **reduction of pressure** due to the **irreversibilities** present at the exit $\Delta p_{o,irr}$. These are calculated similarly to the core entry pressure drop described earlier, the pressure loss being

$$\Delta p_{o,irr} = \frac{\rho_3 w_3^2}{2} K_o \quad (7.9)$$

and pressure increase due to flow deceleration

$$\Delta p_{o,dec} = \frac{G^2}{2\rho_3} (1 - \sigma^2), \quad (7.10)$$

for a total **pressure loss on exit** (with a negative value in the common situation where overall effect is an increase of pressure) Δp_o of

$$\Delta p_o = \frac{G^2}{2\rho_3} (\sigma^2 - 1 + K_o). \quad (7.11)$$

7.1.4 Total pressure drop

Assuming that $\rho_1 = \rho_2$ and $\rho_3 = \rho_4$ (an assumption almost always reasonable), the pressure drops of equations (7.5), (7.7), (7.8) and (7.11) can be combined into a single expression for the total pressure drop throughout the heat exchanger

$$\Delta p_{tot} = \frac{G^2}{2\rho_1} \left[\underbrace{1}_{entry} \underbrace{\sigma^2 + K_o}_{243} + 2 \underbrace{\left(\frac{\rho_1}{\rho_2} - 1 \right)}_{4243} + \frac{\rho_1}{\rho_m} \underbrace{\left(C_f \frac{4L}{d} + \sum K \right)}_{44424443} + \frac{\rho_1}{\rho_4} \underbrace{(K_o + \sigma^2 - 1)}_{4442443} \right]. \quad (7.12)$$

The above correlation is suitable as such for calculating pressure drops on plate-type compact heat exchangers and tube side flow of tubular heat exchangers once the friction factor is known.

Some heat exchanger geometries require additional considerations or may allow for some terms to be neglected, either because of negligible effect, or because of being accounted for by an experimentally created correlation for the friction factor. The important issue of values from experimental correlations of C_f being specific to certain

definitions of velocity, density and also dimensions L and d_h when these are not unambiguous (for example tube banks or shell-side flow in a shell-and-tube heat exchanger) must also be kept in mind. These issues are explained in more detail for certain specific heat exchanger types in the following chapter.

7.2 PRESSURE DROP IN SPECIFIC TYPES OF HEAT EXCHANGER

7.2.1 Tubular heat exchangers, outside flow

7.2.1.1 Banks of plain tubes

When calculating the pressure drop of a fluid flowing across a bank of plain or individually finned tubes, the friction factors already include the effect of loss coefficients due to the tubes, removing the ΣK term from Δp_{core} in equation (7.12).

The pressure effects on the entrance to the first row of tubes and exit from the last row of tubes are also clearly of similar magnitude to those on any row of tubes within the core, and therefore accounted for in the friction factor: therefore the entrance and exit pressure drops Δp_e and Δp_o are also accounted for in the friction factor.

Numerous experimental correlations exist for friction factor in a tube bank. One of the earliest was provided by Jakob in 1938 (Holman 1983, pp.301). When used in equation (7.7) or (7.12) the mass velocity G is determined according to the minimum free-flow area (or maximum velocity) as specified in (7.6), and the term (L/d_h) should be replaced by the number of rows in the longitudinal direction N_L . For said equations the correlation for C_f takes then form of

$$C_f = \left[1 + \frac{0.472}{\left(\frac{S_T - d_o}{d_o} \right)^{1.08}} \right] \cdot Re^{-0.16} \quad (\text{Holman 1983, pp.301}) \quad (7.13)$$

for staggered equilateral triangular arrangement, with dimensions S_T and d_o as defined in Fig.6.5. The correlation is frequently presented in the form giving a modified Darcy friction factor with the constant multipliers of the terms of the sum are $\frac{1}{4}$ of those in eq.(7.13); this value of friction factor should obviously not be used in eq.s (7.7) or (7.12). The Reynolds number Re is calculated from maximum velocity as defined by minimum free-flow area A_{ff} , mean density ρ_m and mass flow rate q_m , and d_o as the characteristic length, with all properties determined at bulk temperature T_b .

Similarly an estimate of C_f for aligned tube banks can be obtained from

$$C_f = \left[0.176 + \frac{0.32 \frac{S_L}{d_o}}{\left(\frac{S_T - d_o}{d_o} \right)^{0.43 + 1.13(d_o/S_L)}} \right] \cdot Re^{-0.15} \quad (\text{Holman 1983, pp.301}), \quad (7.14)$$

where dimensions are similarly as in Fig.6.5 and Re calculated from w_{\max} and d_o . If viscosity varies significantly as a function of temperature or the temperature difference between hot and cold flows is particularly high, the core friction pressure drop should be calculated taking this into account; for this equation (7.7) becomes

$$\Delta p_{core} = \frac{G^2}{2\rho_m} C_f N_L \left(\frac{\mu_s}{\mu} \right)^{0.14} \quad (\text{Holman 1983, pp.301}), \quad (7.15)$$

where μ and μ_s are the fluid dynamic viscosities evaluated at mean bulk temperature T_b and (estimated) tube outside surface temperature T_s respectively.

7.2.1.2 Finned tube banks

Several correlations have been developed for banks of tubes individually finned with circular fins, either as individual discs or in the form of a helical coil. The following correlations give results that can be used directly in equations (7.7) or (7.12), with the term (L/d_h) replaced by the number of rows in the longitudinal direction N_L .

Using the same notation for geometrical variables as earlier (see Fig.6.7.), and Reynolds number Re_{\max} defined with the outside diameter d_o and maximum velocity in the smallest cross-sectional area, a correlation by Robinson and Briggs for staggered bundles is written as

$$C_f = 9.465 \cdot Re_{\max}^{-0.316} \cdot \left(\frac{S_T}{d_o} \right)^{-0.937} \quad (\text{Rohsenow 1987, pp. 4-237}). \quad (7.16)$$

The correlation predicts C_f with a standard deviation of 7.8 % (Rohsenow 1987, pp.4-237), and is based on data covering the following range of dimensions:

$$\begin{array}{ll} 2 \cdot 10^3 < Re_{\max} < 5 \cdot 10^4 & 0.15 < (s'/L_f) < 0.19 \\ 18.6\text{mm} < d_o < 40.9\text{mm} & 3.75 < (s'/\delta) < 6.03 \\ 0.35 < (L_f/d_o) < 0.56 & 1.86 < (S_T/d_o) < 4.60 \\ 0.011 < (\delta/d_o) < 0.025 & 311\text{m}^{-1} < s^{-1} < 431\text{m}^{-1}. \end{array}$$

For tubes with high density of low fins Rabas et.al. suggest the following correlation

$$C_f = 3.805 Re_d^{-0.234} \left(\frac{s}{d_f} \right)^{0.251} \left(\frac{s}{L_f} \right)^{-0.759} \left(\frac{d_f}{d_o} \right)^{-0.729} \left(\frac{d_o}{S_T} \right)^{0.709} \left(\frac{S_T}{S_L} \right)^{-0.379} \quad (7.17)$$

(Rohsenow 1985, pp.4-237),

valid within the following range:

$$\begin{array}{ll} 10^3 < Re_{\max} < 2.5 \cdot 10^4 & L_f < 6.35 \text{ mm} \\ 4.66 \text{ mm} < d_o < 31.75 \text{ mm} & S_L < S_T \\ 15.08 \text{ mm} < S_T < 111 \text{ mm} & 10.32 \text{ mm} < S_L < 96.11 \text{ mm} \\ S_L < S_T & 246 \text{ m}^{-1} < s^{-1} < 1181 \text{ m}^{-1}. \end{array}$$

According to (Rohsenow 1985, pp.4-238) the correlation of equation (7.17) predicts 90% of experimental data on which it is based within $\pm 15\%$ accuracy.

7.2.1.3 Shell-side flow in a shell-and-tube heat exchanger

Accurate calculation of shell-side pressure drop in a shell-and-tube heat exchanger is complicated by the same leakage and bypass stream that complicate the heat transfer analysis of shell-side flow (see chapter 6.4.3).

The method proposed by Bell is based on first evaluating the pressure drops for ideal cross-flow and window flow sections, and then applying various correction factors to account for the bypass and leakage streams.

Various formulations of the method exist; equations for calculating the correction factors are presented in (VDI Heat Atlas 1993), (Shah and Sekulic 2003) and (Bell 1983), while graphical presentation can be found in for example (Rohsenow 1987) and (Perry 1988).

A simpler method proposed by Kern in (Kern, 1950) provides a single equation for the core pressure drop term, accounting for all flow paths and loss coefficients with a single friction factor C_f . An adaptation of Kern's original correlation of C_f as a function of Reynolds number¹ (Kern 1953, pp.839) into SI units is shown in Figure 7.2. The correlation is based on a large amount of experimental data from heat exchangers built according to 1949 TEMA standards and 25% baffle cut (BC) (Kern 1950).

For Reynolds number values of $Re > 500$, the curve of Fig.7.2 follows the equation

$$C_f = 1.733 Re^{-0.1891}. \quad (7.18)$$

When calculating the core pressure drop with friction factor determined from Kern's correlation, the flow path length L of equations (7.7) and (7.12) should be shell inner

¹ Reynolds number is defined in terms of equivalent diameter D_e of equation (6.43), and mass velocity G defined on the basis of free-flow area in the centre of the shell, equation (6.45): $Re = D_e G / \mu$.

diameter multiplied with number of times the fluid flow across the shell (N_B+1 for a shell with N_B baffle plates), and instead of hydraulic diameter d_h , the equivalent diameter D_e (see equation 6.43) should be used. If also variable fluid properties must be accounted for, equation (7.7) then finally becomes

$$\Delta p_{shell} = \frac{G^2}{2\rho_m} C_f \frac{D_s (N_B + 1)}{D_e} \left(\frac{\mu_s}{\mu} \right)^{0.14} \quad (\text{Kern 1950, pp.839}), \quad (7.19)$$

where μ and μ_s are the fluid dynamic viscosities evaluated at mean bulk temperature T_b and (estimated) tube outside surface temperature T_s respectively.

The resulting values represent not average, probable results but a “safe” curve with a safety margin of 0 to 20% for a heat exchanger under typical fouling conditions. For shell-side flow of a segmentally baffled shell-and-tube heat exchanger fouling has an effect on pressure drop by partially plugging the gap between the tube outer diameter d_o and baffle plate tube hole d_{tb} , thereby reducing the leakage stream D of Figure 6.8. (Gupta 1990, pp.92)

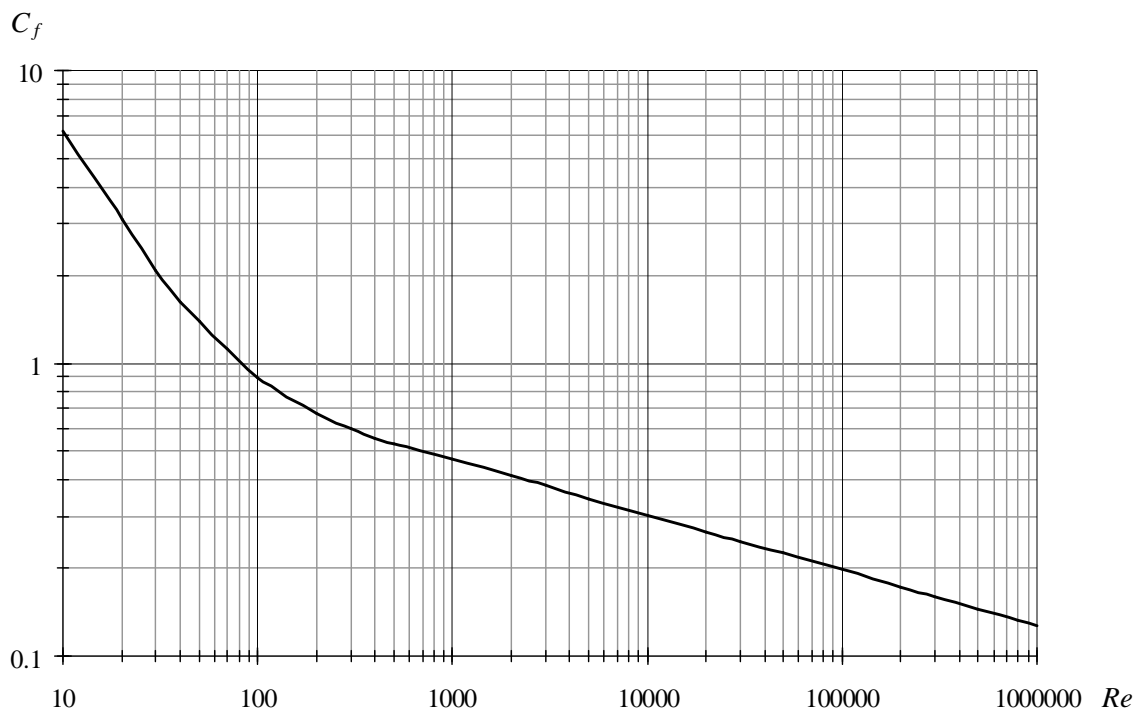


Figure 7.2. Kern’s correlation of (Kern 1950, pp.893) for friction factor C_f in the shell side flow of a shell-and-tube heat exchanger with 25% baffle cut and built to 1949 TEMA standards. Use in equation (7.19) to obtain shell-side pressure drop. Re definition according to equation (6.42).

Entry and exit effects of the shell-side flow of a segmented-baffle shell-and-tube heat exchanger are usually negligibly small compared to the core pressure drop.

7.2.2 Gasketed plate heat exchangers

Pressure drop in a gasketed plate heat exchanger is characterized by the relatively large fraction of port pressure drop from the total pressure drop (Gupta 1990). Due to the way how gasketed PHEs are constructed, flow velocities at the inlet and outlet manifolds are constricted by the port size and cannot be reduced by adding more plates; this can be problematic particularly with a gas flow with strict pressure drop restrictions.

An empirical equation gives the total pressure drop of both inlet and outlet manifolds of a gasketed PHE as 1.5 times the dynamic pressure at the beginning of inlet manifold per pass (Shah 2003, pp.397). Re-writing equation (7.12) with inlet and outlet manifold losses as a single term, the pressure drop of one fluid in a heat exchanger is obtained from

$$\Delta p_{tot} = \frac{G^2}{2\rho_1} \left[1.5\sigma^2 n_p + 2 \left(\frac{\rho_1}{\rho_4} - 1 \right) + \frac{\rho_1}{\rho_m} C_f \frac{4L}{d_h} \right], \quad (7.20)$$

where n_p is the number of passes for the fluid, σ the ratio of port flow area to total free-flow area between the plates, L the plate height, and the hydraulic diameter d_h is often defined as twice the plate spacing. The middle one of the sum terms represents the pressure drop due to momentum change; since the port pressure drop characteristic make the gasketed PHE rarely practical for gas-gas heat exchangers and liquid density changes due to temperature change are negligible, the term can usually be omitted as negligibly small.

The ratio of flow areas σ can be obtained from

$$\sigma = \frac{N_p b w}{\left(\frac{\pi D_p}{4} \right)}, \quad (7.21)$$

where N_p is the number of flow passages of for the fluid in question, b the plate spacing and w the plate width, and D_p the port diameter. Typically the flow are between the plates is much larger than the flow are in the ports, and therefore $\sigma > 1$.

The Fanning friction factor C_f in equation (7.20) is a function of Reynolds number. Exact function will obviously depend on the type of plate surface used, but are often of the form

$$C_f = a Re^{-b}, \quad (7.21)$$

where a can range from 0.25 up to 3 and b is typically between 0.25 and 0.3 (Cooper, 1983b), (Rohsenow 1987), (Shah 2003). A more general method for determining the friction factor of chevron-type plates taking into account geometrical variables defining the surface pattern is provided in (Martin 1996).

Finally, it should be remembered that the change of hydrodynamic pressure due to the height difference between inlet and outlet ports, $\Delta p_H = \rho g \Delta H$, can make a significant contribution to the total pressure difference over a PHE with large plate size.

8 FOULING

Fouling means the undesirable accumulation of solid layers on heat transfer surface. The effect of fouling on heat exchanger performance is to reduce heat transfer due to the added thermal resistance, and sometimes also to increase pressure drop due to the constriction of the free-flow area. From economical point of view, heat exchanger fouling causes additional costs due to the following (Shah 2003 pp.864, Müller-Steinhagen 1997 pp.2):

- 1) Heat exchangers must be over-sized to account for the reduction of overall heat transfer coefficient due to the expected fouling layers
- 2) Maintenance costs due to cleaning and possibly treatment of fluids to reduce fouling rates
- 3) Energy losses due to increased pressure drops and therefore pumping power requirements
- 4) Loss of production due to maintenance activities

In the following chapter 8.1 introduces the mechanisms of fouling, and resulting fouling rates, and effects of heat exchanger operating parameters on fouling rates. Chapter 8.2 describes the effects of fouling on heat exchanger thermo-hydraulic performance, and how to take those effects into account in the design.

8.1 FOULING PROCESS

Fouling can happen with a number of mechanisms, depending on the fluids, surfaces and temperatures (Rohsenow 1987 pp.864, Müller-Steinhagen 1997 pp.2):

- 1) Crystallization (precipitation) fouling: a solution becomes oversaturated with salts, resulting in precipitation of dissolved substance on the heat transfer surface
- 2) Particulate fouling: finely divided solids suspended on the fluid are gradually deposited on the surface
- 3) Chemical reaction fouling: a chemical reaction not involving the surface material results in solid material deposited on the surface
- 4) Corrosion fouling: heat transfer surface becomes oxidized, creating an additional thermal resistance but more importantly provides a roughened surface suitable for other foulants to attach to.
- 5) Biological fouling: algae, bacteria, or other micro- or macro-organisms may start to grow on the heat transfer surface
- 6) Freezing fouling: The hot-side fluid or some of its components may solidify on the heat transfer surface.

As a general rule, fouling rates tend to be higher on liquid than on gas side, and higher on hot than on cold fluid side.

8.1.1 Rate of fouling

While foulant material is being attached to the heat transfer surface, a process of removal from the surface back into the stream by the shear forces or some other mechanism may simultaneously take place. As an increasingly thick layer of foulant builds up, the removal mechanisms often become more effective through increased shear force due to the increase of velocity in a plugged flow channel, and possibly weakening of the foulant attachment to the surface.

The net rate of foulant accumulation is then the difference between attachment and removal rates. Both deposition and removal rates may change over time, depending on a number of variables including the type of fouling layer being accumulated, type of surface, and flow velocity. The net fouling rate may therefore change also, and three different fouling rate scenarios are usually identified on the basis of change of fouling rate as a function of time; these are represented in Figure 8.1 below.

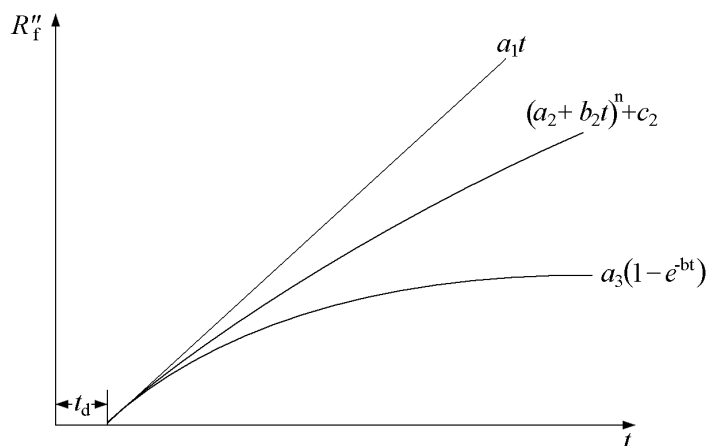


Figure 8.1. Three main time models of fouling rate. (Sarkomaa 1994, pp.17), (Shah and Sekulic, 2003)

The time t_d in Fig.8.1 represents an initial period during which no reduction of overall heat transfer coefficient is seen, or even a very slight increase could appear. This is due to the small conduction resistance of a very thin layer of fouling material being compensated for by the increase of convection heat transfer coefficient h due to the increased surface roughness. (Müller-Steinhagen 1997, pp. 3)

Fouling by the crystallization of a single salt and chemical reaction fouling are mechanisms which frequently create a strong layer of foulant on which removal processes are ineffective, resulting in a linearly increasing fouling resistance. (Shah 2003, pp. 878).

A weaker fouling layer of particulate fouling, or crystallization fouling combining different salts with different sizes and shapes of crystals and/or particulate and crystallization fouling may result in weaker bonds in the foulant layer. This allows an increasingly effective removal as flow velocity increases due to plugging of the channel (Shah 2003, pp. 878). The rate of foulant attachment may also decrease over time due to the accumulation of foulant material itself, which may sometimes be the case in the crystallization fouling (Müller-Steinhagen 1997, pp. 5).

The rate of deposition may remain always greater than the rate of removal, or the removal and deposition rates may eventually reach a balance: in the last case an asymptotic curve approaching some value of fouling resistance will result. Sometimes a reducing curve may also have a saw-tooth pattern where increasing fouling resistance is repeatedly interrupted by an abrupt reduction. Such pattern is typical for such processes where foulant aging contributes significantly to its removal, as is frequently the case in corrosion fouling (Shah 2003, pp. 878).

Due to the complexity of foulant deposition and removal processes and their dependency on a number of variables related to both the fluids, fouling rate models can in most situations give only rough indications on the development of the fouling layers. If necessary, more detailed treatment of fouling rate models can be found for example in references (Müller-Steinhagen 1997) or (Shah 2003).

8.1.2 Effects of operating parameters on fouling

Methods of accurate prediction of heat exchanger fouling, and mitigation thereof, is beyond the scope of this guide. The following is intended to be only a brief and general treatment of issues related to the topic covering some of the main the issues that may need to be considered and some general trends, but not means of prediction.

Knowledge of the type of fouling process is vital if the fouling rate is to be minimized by finding suitable operating parameters. Increasing the flow velocity will increase the shear stress on the heat transfer surface; if the foulant layer is susceptible to removal, this will increase the removal rate and reduce the rate of fouling resistance growth, and the asymptotic value of the foulant layer. Maximizing flow velocity within allowable pressure drop limits will frequently minimize the fouling resistance if the foulant layer is easily removable. This is typically the case for particulate fouling.

If the fouling process is controlled by mass transfer rather than adhesion of particles, and the foulant deposit adheres strongly enough to the surface to make removal rate negligible, the opposite will be true, however. The fouling rate will be proportional to the mass transfer coefficient, which in turn will be proportional to the heat transfer coefficient; in other words, in turbulent flow fouling rate can be expected to increase roughly in proportion to $w^{0.8}$.

The temperature of the heat transfer surface may also be an important factor determining the fouling rate. Crystallization and chemical reaction are often heavily influenced by the temperature of the heat transfer surface. Even if the fluid temperatures present are dictated by the needs of the process, the heat transfer surface temperatures can still be influenced to some extent by the choice of flow geometry, which may allow avoiding the most unfavourable temperature conditions in the heat exchanger.

A more detailed treatment of fouling processes, as well as further sources for dealing with particular fouling situations, can be found in (Müller-Steinhagen 1997, pp. 4...6).

8.2 ACCOUNTING FOR THE EFFECTS OF FOULING

Although fouling and the resulting thermal resistance are clearly time-dependant phenomena and the fouling rates are frequently dependant on variables at least partly under the designer's control, predicting the fouling rates accurately is difficult at best. Although particularly in heavily fouling applications such as crude oil preheat train applications increasing efforts are aimed at fouling rate prediction and minimization, the most common design approach for the majority of applications is still to simply assume a certain fouling resistance, calculate the overall heat transfer coefficient U accordingly (see chapter 5), and thereby find the appropriately over-designed heat transfer area A that accounts for fouling resistances to achieve the required thermal performance. Pressure drop increase due to flow channel contraction and increase of surface roughness caused by the accumulation of a foulant layer on the heat transfer surface is usually not significant enough to require consideration.

Fouling thermal resistances for various liquids are readily available from literature. Any heat transfer textbook lists values for most common fluids, while for example (Sarkomaa 1994), (Müller-Steinhagen 1997) and (Shah 2003) provide resistance for far more comprehensive lists of fluids. The obvious problem with most sources is the absence of data on the type of surface, flow conditions, temperatures, and most importantly the time at which the resistance is reached.

Ideally, if the cleaning/maintenance schedule of the application is known, a value applicable for the chosen heat exchanger construction at the end of the period of usage should be used, but such data is often not readily available. The available resistance values then need to be used without exact knowledge on the conditions for which they apply, and therefore with the understanding that they will contain a considerable degree of uncertainty.

Table 8.1 lists some fouling resistances available from literature. Values originating from TEMA (Tubular Exchanger Manufacturer's Association) apply for tubular heat exchangers, while Weiermann's values are for finned surfaces. As a general rule of

thumb, plate heat exchangers tend to experience noticeably less fouling than tubular exchangers due to the greater shear stresses on the surface, as can be clearly seen by comparing values for same fluid when data is available for both. Footnotes indicate further information (when available) on the conditions for which the resistance values apply.

Table 8.1. Typical values of R''_{tf} [10^{-4} m² K / W] from literature. (See footnotes for conditions for which the values apply, if available)

Fluid	TEMA, 1978 (Incropera 2006)	TEMA, latest (Müller- Steinhagen 1997)	Various sources (Shah 2003)	Weiermann: design of heat transfer equipment for gas- side fouling service (Müller- Steinhagen 1997)
Distilled water	-	0.9 to 1.8	-	-
Treated boiler feedwater	1 ¹ 2 ²	-	0.9	-
Seawater	1 ¹ 2 ²	1.8 to 3.5 ³	1.8 to 3.5 ⁴ 0.18 ⁵	-
Brackish water	-	3.5 to 5.3 ³	-	-
River/lake water	2 to 10 ¹	3.5 to 5.3	1.8 to 3.5 ⁴ 0.44 ⁵	-
Fuel oil	9	3.5 ⁶ 8.8 ⁷	3.5 ⁶ 9 ⁷ 5.3 to 12.3 ⁸	-
Ammonia, vapour	-	1.8 ⁹ 5.3 ¹⁰	-	-
Refrigerant, liquid	2	1.8	-	-
Refrigerant, vapour	-	3.5 ¹⁰	-	-
Water vapour	1 ⁹	0.9 ⁹ 2.6 to 3.5 ¹⁰	1.8 ^{5,10} 0.09 ^{4,10}	-
Compressed air	-	1.8	-	-
Flue gas / nat. gas	-	8.8	0.9 to 5.3; 1.76	0.9 to 5.3 ¹¹
Flue gas / Diesel	-	-	-	5.3 ¹²
Flue gas / crude oil	-	-	-	7 to 27 ¹²
Flue gas / coal	-	17.6	8.81 to 88.1	8.9 to 88.5 ¹³

1 below 50 °C

2 above 50 °C

3 below 44 °C

4 tubular heat exchanger

5 plate heat exchanger

6 No. 2 fuel oil (kevyt polttoöljy in Finnish terminology)

7 No. 6 fuel oil

8 Heavy fuel oil (raskas polttoöljy)

9 Oil-free

10 Contains oil

11 Finned surface, 30 to 40 m/s flow velocity

12 Finned surface

13 Finned surface, 15 to 21 m/s flow velocity

REFERENCES

Aquaro, Pieve, 2007

High temperature heat exchangers for power plants: Performance of advanced metallic recuperators. Journal of Applied Thermal Engineering, Vol 27, Feb 2007, pp.389-400.

Bejan, Kraus, 2003

Heat Transfer Handbook

Bell, Kenneth J, 1983

Heat Exchanger Design Handbook, Part 3, 3.1.2 Types of Heat Exchangers. VDI-Verlag, Hemisphere Publishing Ltd, 1983.

Chapman, Alan J.

Heat Transfer. 4th edition. Macmillan Publishing Company, New York, 2002.

Cooper, Anthony D., Usher, J. Dennis, 1983a

Heat Exchanger Design Handbook, Part 3, 3.7.10. Methods of Surface Area Calculation. VDI-Verlag, Hemisphere Publishing Ltd, 1983.

Cooper, Anthony D., Usher, J. Dennis, 1983b

Heat Exchanger Design Handbook, Part 3, 3.7.4. Friction Factor correlations. VDI-Verlag, Hemisphere Publishing Ltd, 1983.

Gupta, J.P., 1990

Working with heat exchangers : questions and answers. Hemisphere Publishing, cop., New York, 1990.

Guy, A.R., 1983

Heat Exchanger Design Handbook, Part 3, 3.2.2 Applications of Double-Pipe Heat Exchangers. VDI-Verlag, Hemisphere Publishing Ltd, 1983.

Hammo Simo, 1994

Lämmönsiirtimien likaantuminen : lämpö- ja virtaustekniikan jatkokurssi. Lappeenrannan Teknillinen Korkeakoulu, ENTE julkaisu D-33, 1994.

Holman, J.P., 1989

Heat Transfer. 6th edition, McGraw-Hill Book Company – Singapore. Singapore, 1989.

Incropera Frank P, DeWitt David, 2002

Fundamentals of Heat and Mass Transfer. 5th edition. John Wiley & Sons, Inc. United States, 2002.

- Kays, W.M., London, A.L., 1984
Compact Heat Exchangers. 3rd edition. McGraw-Hill Book Company.
- Kern, Donald Q, 1950
Process Heat Transfer, International Student Edition. McGraw-Hill Kogakusha Ltd, Tokyo, Japan.
- Kuppan T, 2000
Heat Exchanger Design Handbook. 1st edition. CRC Press, 2000.
- Martin, Holger, 1996
A theoretical approach to predict the performance of chevron-type plate heat exchangers, Chemical Engineering and Processing, Volume 35, Issue 4, Pages 301-310.
- McCabe W.L., Smith J.C., Harriott, P., 2005
Unit Operations of Chemical Engineering, McGraw-Hill Inc., 6th Ed.
- McDonald, Colin F., 2003
Recuperator considerations for future higher efficiency microturbines Journal of Applied Thermal Engineering, Vol 23, Aug 2003, pp.1463-1487.
- Perry R.E., 1988
Perry's Chemical Engineers' Handbook, International Edition, 4th Ed., McGraw-Hill Book Co.
- Rohsenow W., Hartnett J.P., Ganic E., 1987
Handbook of Heat Transfer Applications, 2nd Edition. McGraw-Hill Inc., USA
- Sarkomaa Pertti, 1994
Lämmönsiirtimien Suunnittelumenetelmät ja Lämpötekkinen Mitoitus. LTKK, Opetusmoniste C-65, Lappeenranta, May 1994.
- Saunders E.A.D, 1983
Heat Exchanger Design Handbook, Part 4, 4.2.2 Design and construction codes. VDI-Verlag, Hemisphere Publishing Ltd, 1982.
- Shah R.K., Sekulić D.P., 2003
Fundamentals of Heat Exchanger Design and Manufacture, xyz Inc., xth Ed.
- Taborek J., 1983a
Heat Exchanger Design Handbook, Part 3, 3.1.3 Introduction to Heat Exchanger Design, Logic of the Design Process. VDI-Verlag, Hemisphere Publishing Ltd, 1983.

Taborek J., 1983b

Heat Exchanger Design Handbook, Part 3, 3.3.5 Shell-and-tube Heat Exchangers, Input Data and Recommended Practices. VDI-Verlag, Hemisphere Publishing Ltd, 1983.

Taborek J., 1983c

Heat Exchanger Design Handbook, Part 3, 3.3.10 Shell-and-tube Heat Exchangers, Design Procedures. VDI-Verlag, Hemisphere Publishing Ltd, 1982.

VDI, 1993a

VDI Heat Atlas, part Gd. VDI-Verlag, 1993.

VDI, 1993b

VDI Heat Atlas, part Oc.:. VDI-Verlag, 1993.